

DESIGN AND ANALYSIS OF A RESISTIVELY
HEATED SURGICAL PROBE

Jon Philip Groff

United States Naval Postgraduate School



THESIS

Design and Analysis of a
Resistively Heated Surgical Probe

by

Jon Philip Groff
Lieutenant Commander, United States Navy
B.S., Juniata College, 1961

Thesis Advisor:

Thomas E. Cooper

December 1971

Approved for public release; distribution unlimited.

Design and Analysis of a
Resistively Heated Surgical Probe

by

Jon Philip Groff
Lieutenant Commander, United States Navy
B. S., Juniata College, 1961

Submitted in partial fulfillment of
the requirements for the degree of

MASTER OF SCIENCE IN MECHANICAL ENGINEERING

from the

NAVAL POSTGRADUATE SCHOOL
December 1971

ABSTRACT

This thesis examines the use of heat for producing clinical lesions in tissue and presents the design and analysis of a resistively heated surgical probe. The probe temperature is accurately maintained and measured by using a Wheatstone bridge. The probe was embedded in an agar-water test medium and the temperature field emanating from the probe was measured using liquid crystal tapes. The experimental results compare within approximately 10% of a two-dimensional numerical solution. A one-dimensional theoretical model is developed and results are presented to show the relative effects of metabolism and blood flow on the temperature field.

TABLE OF CONTENTS

I.	INTRODUCTION -----	11
II.	SUMMARY OF HEATING TECHNIQUES -----	13
	A. DIRECT CURRENT (dc) METHOD -----	13
	B. RADIO-FREQUENCY (rf) METHOD -----	14
	C. HIGH RESISTANCE HEATING METHOD -----	15
III.	HIGH RESISTANCE HEATING PROBE -----	18
	A. THEORY -----	18
	B. DESIGN -----	19
	C. TEMPERATURE CONTROL -----	21
IV.	EXPERIMENTAL APPARATUS -----	29
	A. TEST MEDIUM -----	29
	B. LIQUID CRYSTALS AND TEMPERATURE MEASUREMENT -----	30
	C. TEST CELLS -----	33
V.	EXPERIMENTAL PROCEDURE -----	37
VI.	THEORETICAL ANALYSIS -----	41
	A. ONE-DIMENSIONAL MODEL -----	41
	1. Metabolic and Blood Flow Effects Neglected ----	41
	2. Metabolic and Blood Flow Effects Included -----	43
	B. TWO-DIMENSIONAL MODEL -----	45
VII.	RESULTS -----	47
	A. EXPERIMENTAL RESULTS -----	47
	B. ONE-DIMENSIONAL MODEL -----	62
	1. Effect of Blood Flow on the Temperature Field -----	62
	2. Effect of Increased Time on the Temperature Field -----	62

C. TWO-DIMENSIONAL MODEL -----	66
VIII. CONCLUSIONS AND RECOMMENDATIONS -----	68
A. CONCLUSIONS -----	68
B. RECOMMENDATIONS -----	69
APPENDIX A: ONE-DIMENSIONAL MODEL SOLUTION -----	70
APPENDIX B: ERROR ANALYSIS OF EXPERIMENTAL RESULTS -----	74
COMPUTER PROGRAM 1 -----	94
COMPUTER PROGRAM 2 -----	105
COMPUTER PROGRAM 3 -----	108
COMPUTER PROGRAM 4 -----	111
COMPUTER PROGRAM 5 -----	114
COMPUTER PROGRAM 6 -----	117
BIBLIOGRAPHY -----	120
INITIAL DISTRIBUTION LIST -----	122
FORM DD 1473 -----	123

LIST OF TABLES

I.	Resistivity and the temperature coefficient of resistivity for various metals -----	20
II.	Theoretical values for θ for various values of nondimensional location (R) and values of τ between 0.1 and 0.9: one-dimensional solution, $\beta = 0.0$ -----	76
III.	Theoretical values for θ for various values of nondimensional locations (R) and values of τ between 1.0 and 9.0: one-dimensional solution, $\beta = 0.0$ -----	77
IV.	Theoretical values for θ for various values of nondimensional location (R) and values of τ between 10.0 and 100.0: one-dimensional solution, $\beta = 0.0$ -----	78
V.	Theoretical values for θ for various values of nondimensional locations (R) and values of τ between 0.1 and 0.9: one-dimensional solution, $\beta = 0.1$ -----	79
VI.	Theoretical Values for θ for various values of nondimensional location (R) and values of τ between 1.0 and 9.0: one-dimensional solution, $\beta = 0.1$ -----	80
VII.	Theoretical values for θ for various values of nondimensional locations (R) and values of τ between 10.0 and 100.0: one-dimensional solution, $\beta = 0.1$ -----	81
VIII.	Theoretical values for θ for various values of nondimensional location (R) and values of τ between 0.1 and 0.9: one-dimensional solution, $\beta = 0.5$ -----	82
IX.	Theoretical values for θ for various values of nondimensional locations (R) and values of τ between 1.0 and 9.0: one-dimensional solution, $\beta = 0.5$ -----	83
X.	Theoretical values for θ for various values of nondimensional location (R) and values of τ between 0.1 and 0.9: one-dimensional solution, $\beta = 1.0$ -----	84

XI.	Theoretical values for θ for various values of nondimensional locations (R) and values of τ between 1.0 and 9.0: one-dimensional solution, $\beta = 1.0$ -----	85
XII.	Theoretical values of θ for various values of nondimensional time (τ) and nondimensional location (R): two-dimensional solution, $\beta = 0.0$, $X=1R$ -----	86
XIII.	Theoretical values of θ for various values of nondimensional time (τ) and nondimensional location (R): two-dimensional solution, $\beta = 0.0$, $X=5R$ -----	87
XIV.	Theoretical values of θ for various values of nondimensional time (τ) and nondimensional location (R): two-dimensional solution, $\beta = 0.0$, $X=8.5$ -----	88
XV.	Theoretical values of θ for various values of nondimensional time (τ) and nondimensional location (R): two-dimensional solution, $\beta = 0.0$, $X=11.5$ -----	89
XVI.	Theoretical values of θ for various values of nondimensional time (τ) and nondimensional location (R): two-dimensional solution, $\beta = 0.0$, $X=13.5R$ -----	90
XVII.	Experimental data -----	91

LIST OF ILLUSTRATIONS

1.	Construction of probe -----	22
2.	Completed probe -----	23
3.	Wheatstone bridge -----	24
4.	Temperature control circuit -----	26
5.	Probe calibration curve -----	27
6.	Test cells -----	34
7.	Removable support rings for liquid crystal tape -----	35
8.	Top view of circular test cell -----	38
9.	Overall view of apparatus -----	40
10.	Mathematical model of probe -----	42
11.	TRUMP nodal network -----	46
12.	Radial temperature field for $\tau = 0.0$ -----	48
13.	Radial temperature field for $\tau = 1.0$ -----	49
14.	Radial temperature field for $\tau = 3.0$ -----	50
15.	Radial temperature field for $\tau = 5.0$ -----	51
16.	Radial temperature field for $\tau = 10.0$ -----	52
17.	Axial temperature field for $\tau = 0.0$ -----	53
18.	Axial temperature field for $\tau = 1.0$ -----	54
19.	Axial temperature field for $\tau = 3.0$ -----	55
20.	Axial temperature field for $\tau = 5.0$ -----	56
21.	Axial temperature field for $\tau = 10.0$ -----	57
22.	R_c vs. τ for $\theta_c = 0.200$ and $\beta = 0.0$ -----	59
23.	R_c vs. τ for $\theta_c = 0.235$ and $\beta = 0.0$ -----	60
24.	Axial position (X) vs. R_c for various values of τ and $\theta_c = 0.285$ -----	61

25.	θ vs. R for $\tau = 5.0$ and $\beta = 0.0, 0.1, 0.5$ and 1.0 ----	63
26.	θ vs. τ for various values of R and $\beta = 0.0$ -----	64
27.	θ vs. τ for various values of β and $R = 2.5$ -----	65
28.	Axial position (X) vs. R for various values of τ and $\theta = 0.300$ -----	67

NOTATION

<u>Symbol</u>	<u>Description</u>	<u>Typical Units</u>
α	Tissue thermal diffusivity	cm^2/sec
α'	Temperature coefficient of resistance	$\text{ohm}/\text{ohm}/^\circ\text{C}$
c	Tissue specific heat	$\text{cal}/\text{gm}/^\circ\text{C}$
c_b	Blood specific heat	$\text{cal}/\text{gm}/^\circ\text{C}$
I	Current	amps
k	Tissue thermal conductivity	$\text{cal}/\text{cm}/^\circ\text{C}/\text{sec}$
m_b	Volumetric blood flowrate	$\text{gm}/\text{cm}^3/\text{sec}$
Q	Heating rate	watts
r	Radial location in tissue	cm
r_o	Probe radius	cm
R	Resistance	ohms
S_m	Matabolic heat generation rate	$\text{cal}/\text{cm}^3/\text{sec}$
t	Time	sec
T	Tissue temperature	$^\circ\text{C}$
T_b	Arterial temperature	$^\circ\text{C}$
T_c	Critical temperature	$^\circ\text{C}$
T_o	Initial tissue temperature	$^\circ\text{C}$
T_p	Probe temperature	$^\circ\text{C}$
V	Voltage	volts
ρ	Tissue density	gm/cm^3
ρ'	Resistivity	ohm-cm

Non-dimensional Groups

$$R = \frac{r}{r_o}$$

$$\beta = \frac{m_b c_b r_o^2}{k}$$

$$\theta = \frac{T - T_o}{T_p - T_o}$$

$$\tau = \frac{\alpha t}{r_o^2}$$

ACKNOWLEDGEMENTS

I wish to express my sincere appreciation to my advisor, Professor Thomas E. Cooper, for his willing assistance and continued encouragement throughout this project. I also wish to thank Mr. James W. Crossin of Hoffman-LaRoche Inc. for supplying the liquid crystal tapes and Mr. Dale Schauer of Lawrence Livermore Laboratory for providing the TRUMP computer program solutions.

Finally, I wish to express my appreciation to my wife Nola for her patience and understanding while I worked on this thesis.

I. INTRODUCTION

A variety of surgical techniques are presently used to produce clinical lesions. In addition to the familiar mechanical or "scalpel" method, surgical procedures employing chemical, ultrasonic, focused x-rays, radiation, and cooling and heating agencies are used to destroy discrete regions of tissue, normally nervous tissue. The choice of methods depends largely on the nature of the clinical problem. Ideally, the surgeon desires a technique that possesses the following characteristics: 1) Safety, 2) Reversibility, 3) Reproducibility, 4) Sharp delimitation, 5) Hemostasis, 6) Flexibility, 7) Simplicity, and 8) Speed of application. At times, it is not possible to meet all of the above surgical ideals. In such cases, the choice of procedures is based largely on an optimization of the ideals, with safety being of paramount importance. Gengler [10] presents a summary of the various methods, complete with the advantages and disadvantages of each.

In this thesis, the use of heat for producing lesions is investigated. In particular, the design of a resistively heated surgical electrode, henceforth referred to as a probe, is presented. Tissue destruction is accomplished by using the probe as a heating element to raise the temperature of a predetermined region of tissue above a critical level, normally taken to be 55°C [2].

The unique feature of this probe is that its surface temperature can be accurately measured and controlled by using a Wheatstone bridge. As a result, the temperature field in the medium surrounding the probe can be analytically predicted by solving the heat equation prior to applying the probe. This is quite significant when one considers that

the volume of tissue destroyed depends solely on the local tissue temperature.

Temperature fields determined experimentally with the probe embedded in a 0.30% agar - 99.7% water test medium compare within an accuracy of 13% of those predicted using the analytical model. A novel, relatively new, temperature sensing device was used in the experimental phase of the study. Liquid Crystals [12], a material that changes color over a known and well defined temperature range, were employed to obtain a two-dimensional, visual display of the transient temperature field which developed around the probe. By using two separate orientations of the liquid crystals, a three-dimensional picture of the temperature field was inferred. In addition to the highly desirable visual aspect of the liquid crystal material, it also produces a minimum disturbance in the test medium.

The effects of blood flow and metabolism on the size of the lesions produced were also investigated using an analytical model.

II. SUMMARY OF HEATING TECHNIQUES

A. DIRECT CURRENT (dc) METHOD

Localized lesions have been produced in tissue by applying a direct current between two electrodes. An active electrode is inserted into a predetermined location in the tissue, and an inactive electrode, or ground, is placed on some other part of the body. The resistivity of the tissue causes electrical energy to be converted into heat, thus increasing the local tissue temperature. When the tissue temperature is raised above 55°C [2], the tissue is destroyed.

Although small and discrete lesions can be produced by the dc method, it has several disadvantages. Direct current follows the path of least resistivity and tends to have preferred paths in tissue, thus causing irregular lesions. Gas bubbles, a result of electrolysis, form around the active electrode and block the flow of current. In addition, dc devices suffer from polarization which can produce transients that stimulate muscle and nervous tissue [23].

Nerve stimulation does have one advantage. The probe placement can be checked by observing the patient's reaction to the stimulating effect of the current. However, other nerves, as well as those in the lesion, could also be stimulated.

Herrero [14] states another disadvantage of the dc method: "Animals with dc lesions usually had extensive scar tissue both around and infiltrated with the tissue".

It should also be noted that the dc method depends on both the thermal and electrical properties of the tissue. The thermal properties are known within an accuracy of approximately 5% [7] and are relatively

constant throughout the tissue. However, the electrical properties are not well known, are anisotropic and tend to vary with location.

One advantage of the dc method is that the electrodes are small; approximately two millimeters in diameter. Therefore the probes can be painlessly inserted and removed, and cause little damage to the surrounding tissue.

In summary, although the dc method can produce localized lesions, the irregularity of the lesions, control difficulties, and possible side effects of the current, greatly diminish its usefulness.

B. RADIO-FREQUENCY (rf) CURRENT METHOD

The radio-frequency technique produces lesions in much the same way as the direct current method. A long, thin, needle-like probe emits low power continuous wave radio-frequency current. An indifferent electrode is placed on some other part of the body and acts as a ground. As current is passed between the electrodes, the resistivity of the tissue causes electrical energy to be converted to tissue internal energy, thus increasing the local tissue temperature. As in the dc method, lesions are a function of the tissue's thermal and electrical properties.

Gengler [10] presents a detailed analysis of the rf technique. In his summary of the method he states: "The radio-frequency method allows controlled and predictable lesions to be produced within safe limits for physiological and clinical applications."

Unlike direct current, rf current has no preferred path in tissue and no stimulating effect. However, low-frequency alternating current does have a stimulating effect in tissue. Therefore, the probe location can be checked by passing low-frequency current between the electrodes and observing the patient's response.

Brodkey and others [3] discuss another way of assuring proper probe location. They found that a temperature range of 40-49°C reversibly blocks nervous function. Thus, after positioning the probe, and raising the local tissue temperature to the reversible range, the patient's response can indicate if the probe is positioned correctly.

Like the dc electrode, the radio-frequency probe is small, can be painlessly inserted and removed, and causes little damage to the surrounding tissue.

The rf method does have several disadvantages. The local tissue temperature may exceed 100°C causing boiling, gas formation, carbonization of the tissue, and adherence of coagulum to the probe [2]. Also, defects in the probe insulation have been known to cause irregular lesions along the probe tract. However, these difficulties can be avoided by carefully controlling the various physical parameters used in the rf technique.

In summary, the radio-frequency method can be used to produce well-circumscribed lesions and the probe location can be checked by two methods. However, as in the dc method, lesions are still a function of both the thermal and electrical properties of the tissue.

C. HIGH RESISTANCE HEATING PROBE METHOD

In this method, a high resistance electrode is inserted into the tissue. Current is passed through the electrode and the resistance of the electrode causes the probe temperature to increase. Heat is conducted away from the probe into the surrounding tissue. A region of destroyed tissue is formed when the local tissue temperature is raised above approximately 55°C [2].

Theoretically, there is less uncertainty in producing lesions purely by heating than there is in the direct current or radio-frequency techniques. The dc method produces both thermal and electrolytic tissue destruction. As the lesion forms, it offers an increased resistance to the passage of current. Thus, the parameters are changing as the lesion forms. The rf method minimizes electrolysis but still depends on the electrical and thermal properties of the tissue. On the other hand, the high resistance probe depends only on the tissue's thermal properties.

Carpenter and Whittier [4] attempted to produce lesions in animals by using a heating electrode. Although their results were poor, they concluded that it was due to the crude instruments employed. They stated: "It would seem profitable to explore this technique with a more finely perfected thermocautery."

Gildenberg [11] conducted studies with a high resistance heating electrode and a rf probe and found that the heating probe produced less variable lesions than the rf probe. In addition, the rf lesions had significantly more lesions along the puncture canal than lesions formed by the heating probe.

As discussed earlier, a temperature range of 40-49°C can reversibly block nervous function. This technique can be used to check the position of the heating electrode.

Since lesions formed using the resistance heating method depend only on the temperature field surrounding the probe, the surface temperature of the probe must be accurately measured and controlled. This has been one of the difficulties of previous resistance probe designs. Watkins [23] used a probe with a thermocouple placed in the tip. He found that the actual temperature of the probe could exceed the recorded temperature by several degrees if the thermocouple was not

positioned carefully. Thermocouples placed in the surrounding tissue to record the temperature can distort the temperature field and give erroneous readings. Gildenberg [11] inserted a thermocouple one millimeter from the heating electrode to record the tissue temperature. He determined that controlling the current to maintain a constant temperature at the thermocouple was no more accurate than maintaining a constant current.

It should also be noted, that since the lesions produced by the heating probe depend only on thermal destruction of the tissue, the lesions are smaller than those produced by the direct current or radio-frequency current method.

In summary, a properly designed high resistance heating probe can produce small, safe and predictable lesions. The uncertainty is less than the radio-frequency or direct current method since tissue destruction depends only on the thermal properties of the tissue.

III. HIGH RESISTANCE HEATING PROBE

A. THEORY

It is well known that the flow of electric current against any resistance is accompanied by a dissipation of electrical energy in the form of heat. The amount of heat generated is expressed by Joule's law:

$$Q = IV = I^2R \quad (1)$$

Q = heating rate

V = voltage

I = current

R = resistance

The resistance of a conductor at ordinary temperature is a function of the length and the cross-section of the conductor, varying directly with the length and inversely with the cross-section according to the following relationship:

$$R = \rho' \frac{l}{A} \quad (2)$$

R = resistance observed

l = length of sample

A = cross-section area of sample

The proportionality constant ρ' is called the resistivity of the material. Therefore, all other factors remaining equal, the material having the highest resistivity will generate the most heat.

All metals exhibit some change in resistance with temperature. For pure metals, there is a definite and constant relationship between the temperature and the resistance of the metal. This characteristic is used in electrical-resistance thermometers where temperature is

indicated by measuring the change of resistance. Since electrical resistance measurements can be made with high accuracy on bridge circuits, this type of instrument can give precise temperature measurements.

The theory of the resistance thermometer was applied to the design of the high resistance heating probe. From the above discussion, a given metal will have a particular resistance at a particular temperature. The inverse of this was used in designing the probe. That is, imposing a particular resistance on a metal should cause the metal to come to the corresponding temperature for that resistance. The resistance can easily be controlled by regulating the voltage and current. Thus, the temperature of the probe can be measured and controlled accurately without the use of any external measuring devices.

The change in resistance with temperature of a metal is given by the following expression:

$$R_2 = R_1 [1 + \alpha' (T_2 - T_1)] \quad (3)$$

R_1 = resistance at temperature T_1

R_2 = resistance at temperature T_2 .

The constant α' , is the temperature coefficient of resistivity and is expressed as ohms per ohm per degree. It should be noted that, in general, α' is a function of temperature.

B. DESIGN

Equations (1), (2) and (3) express several factors that were considered in designing the high resistance probe. From equations (1) and (2) it can be seen that resistivity should be high to generate the most heat. Equation (3) shows that the temperature coefficient of resistivity should also be high so that the change in resistance with

temperature will be large and therefore easier to measure and control. Ideally, α' should be constant over the range of temperatures to be measured.

Several metals were investigated. Their properties are listed in Table I. In addition, the properties of thermistors were also investigated. Although they are small, rugged, can be made in any shape and have a long life, their change in resistance with temperature is extremely nonlinear. Since this makes temperature control difficult, thermistors were not considered further.

TABLE I

<u>Metal</u>	<u>Resistivity (at 20°C)</u>	<u>Coefficient of Resistivity</u>	<u>Constant</u>
Platinum	10 microhm/cm	.0038 ohm/ohm/°C	
Nickel	7.8	.006	
Nichrome	100	.0004	
Copper	1.72	.0038	
Aluminum	2.8	.0039	
Balco	19.9	.0045	25-100°C
Iron	10	.005	

After comparing the properties of the metals in Table I, Balco was chosen. Balco is the commercial name of an alloy, consisting of 70% nickel and 30% iron, that has the properties that are desirable in a heating electrode. Its temperature coefficient of resistivity is large ($\alpha' = 19.9$ microhm/cm) and nearly constant between 25°C and 100°C [24].

Electrode insulation was an important consideration in the probe design, since a voltage leak in the probe can cause tissue electrolysis. Balco is available with a standard enamel insulation. The enamel is

made from an oil modified expoxy based resin and has a continuous duty operating temperature of 150°C [24].

Various shaped heating probes were considered. However, to facilitate the construction of the probe, a cylindrical shape was chosen. A probe length to diameter ratio (L/D) of ten to one was used to reduce end effects and to ensure good experimental data.

In order to increase the extent of the temperature field in the test medium, thus increasing the accuracy of the experimental data, the probe was made approximately four times larger than an actual surgical probe.

The heating electrode (see Figures 1 and 2) consists of a skeleton of 0.3894 centimeter (cm) diameter glass tubing. Two 0.038 cm copper wires were inserted in the tubing. One wire was passed out the tip and high resistance 0.0068 cm Balco wire was attached. The Balco wire was tightly wound back along the glass tubing for approximately 3.9 cm. It was then led back into the tubing through a small hole and attached to the second copper wire. The holes at the tip and side of the glass tubing were closed with expoxy. The probe was then given a thin coating of General Electric No. 7031 Adhesive and Insultating Varnish thinned with Xylene to ensure against any insulation defects in the Balco wire. The outside diameter of the completed probe was 0.4145 cm.

C. TEMPERATURE CONTROL

Precision resistance measurements can be made by using a Wheatstone bridge. The bridge (see Figure 3) consists of four resistance arms, a voltage source and a detector. When A is to B, as X is to the standard, there will be no potential difference bewteen points d and b. Therefore, whenever the detector reads zero voltage from point d to b, the bridge

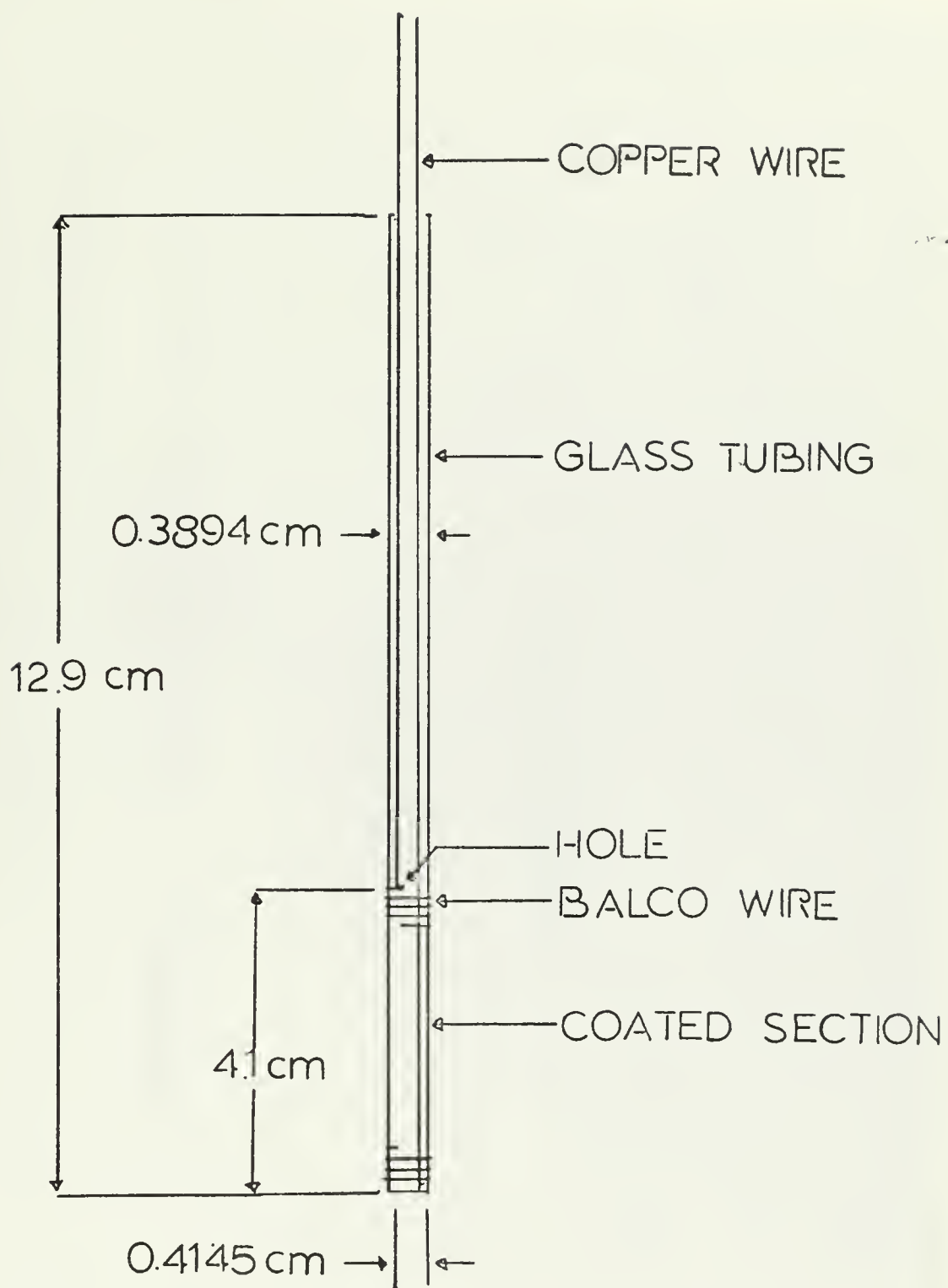


Figure 1. Construction of Probe.

HELWIG CARBON PRODUCTS, INC.
4350 N. 80TH STREET
MILWAUKEE, WISCONSIN 53210

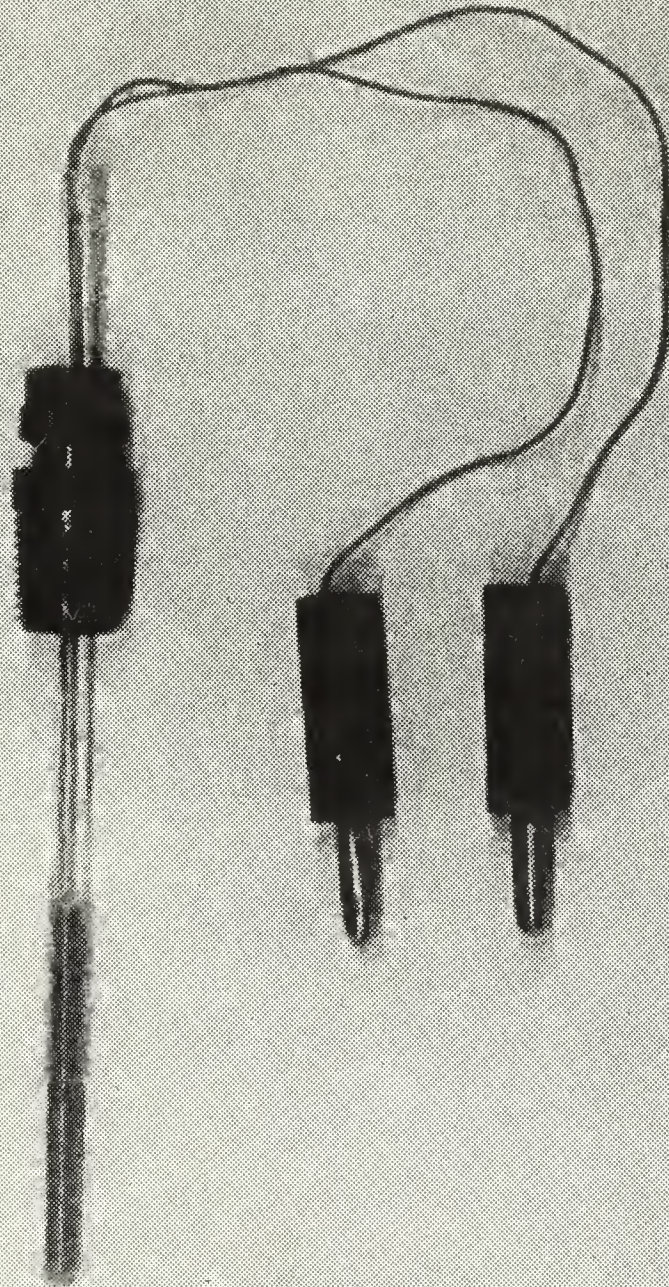


Figure 2. Completed Probe

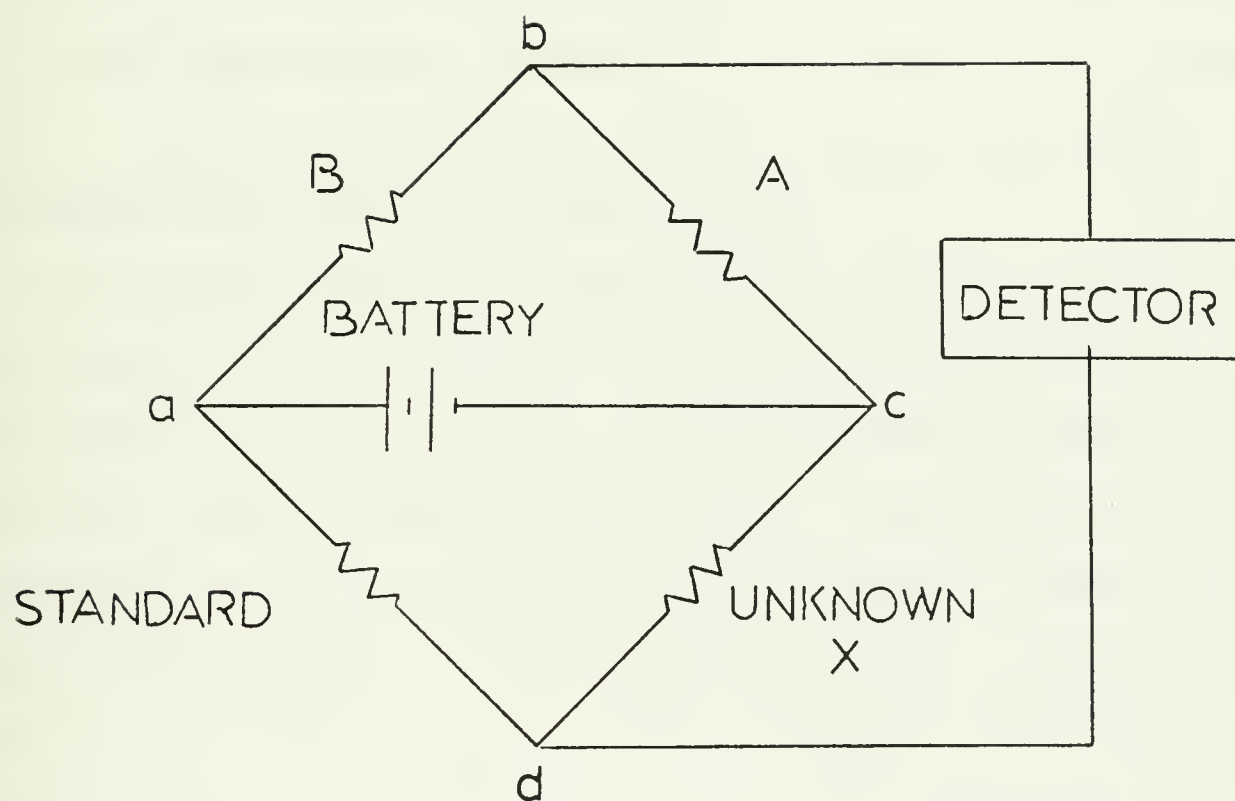


Figure 3. Wheatstone Bridge.

is in balance and the unknown resistance (X) is obtained by using the relationship:

$$X = \left(\frac{A}{B} \right) \times (\text{Standard}) \quad (4)$$

The probe was calibrated using a Rosemont variable temperature oil bath and commutating bridge. The calibration curve is shown in Figure 5. Because of the experimental apparatus, a probe temperature between 45°C and 50°C was desired. The reason for this choice will be discussed later. It should be noted, however, that in actual use, a probe temperature between 85°C to 95°C would be used.

As discussed earlier, the flow of current against a resistance causes heat to be generated. There is also a change in resistance with temperature. Since the temperature of the probe must be controlled precisely, it was necessary to ensure that the bridge resistances would not change as heat was generated in them. Therefore, 56.2 ohm resistors rated at five watts were used for resistances A and B. Referring to equation (4), it can be seen that since the ratio of A to B is one, the standard resistance will also be the resistance of the unknown (probe).

The standard resistance was wound using Evanohm wire. Evanohm is a commercial wire used in precision resistance standards and is an alloy of 75% nickel, 20% chromium, 2.5% aluminum and 2.5% copper. It has a low temperature coefficient of resistance over a wide range of temperatures [24]. The completed Evanohm standard had a resistance of 356.33 ohms which corresponded to a probe temperature of 48.5°C (see Figure 5).

The final probe circuit (see Figure 4) consisted of the two 56.2 ohm resistors, the Evanohm standard and the probe. A Lambda Model LP 413 FM regulated power supply was used to provide power to the probe. A Weston Model 1240 digital voltmeter was used as the detector.

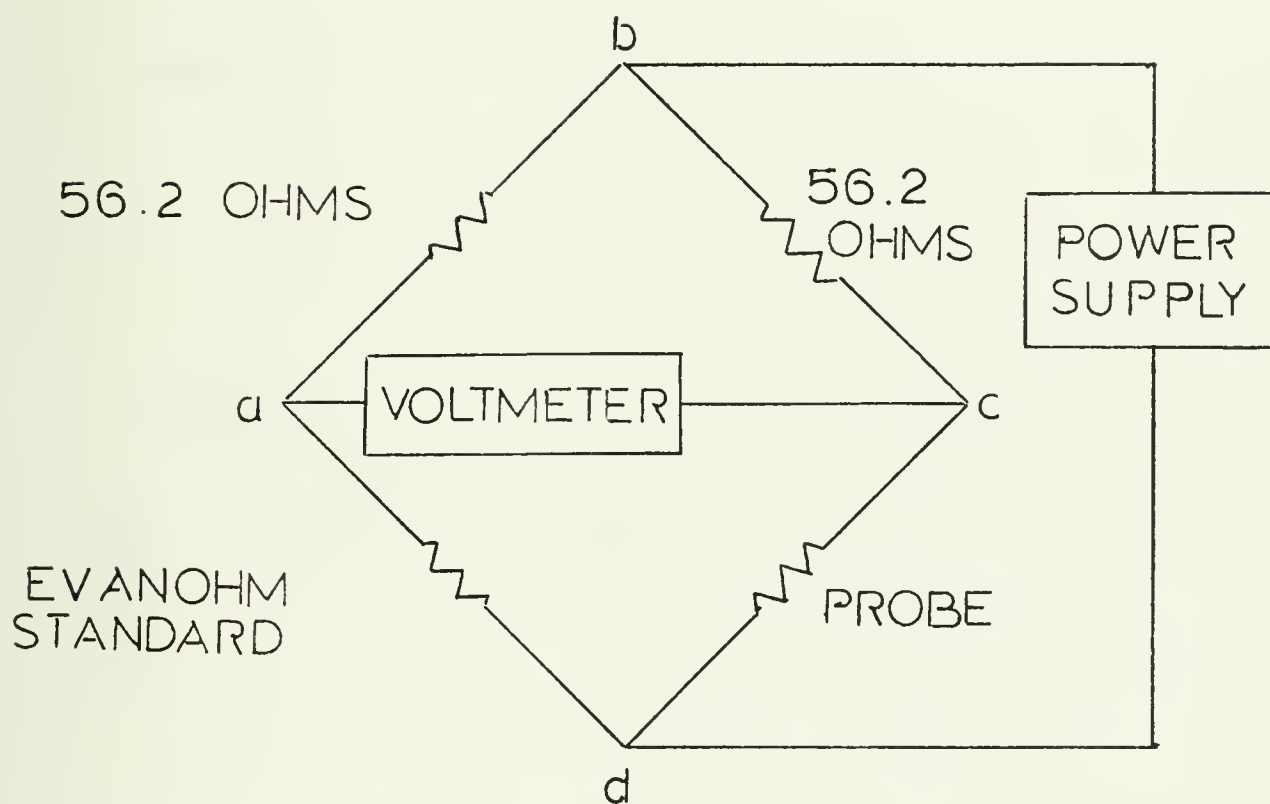


Figure 4. Temperature Control Circuit.

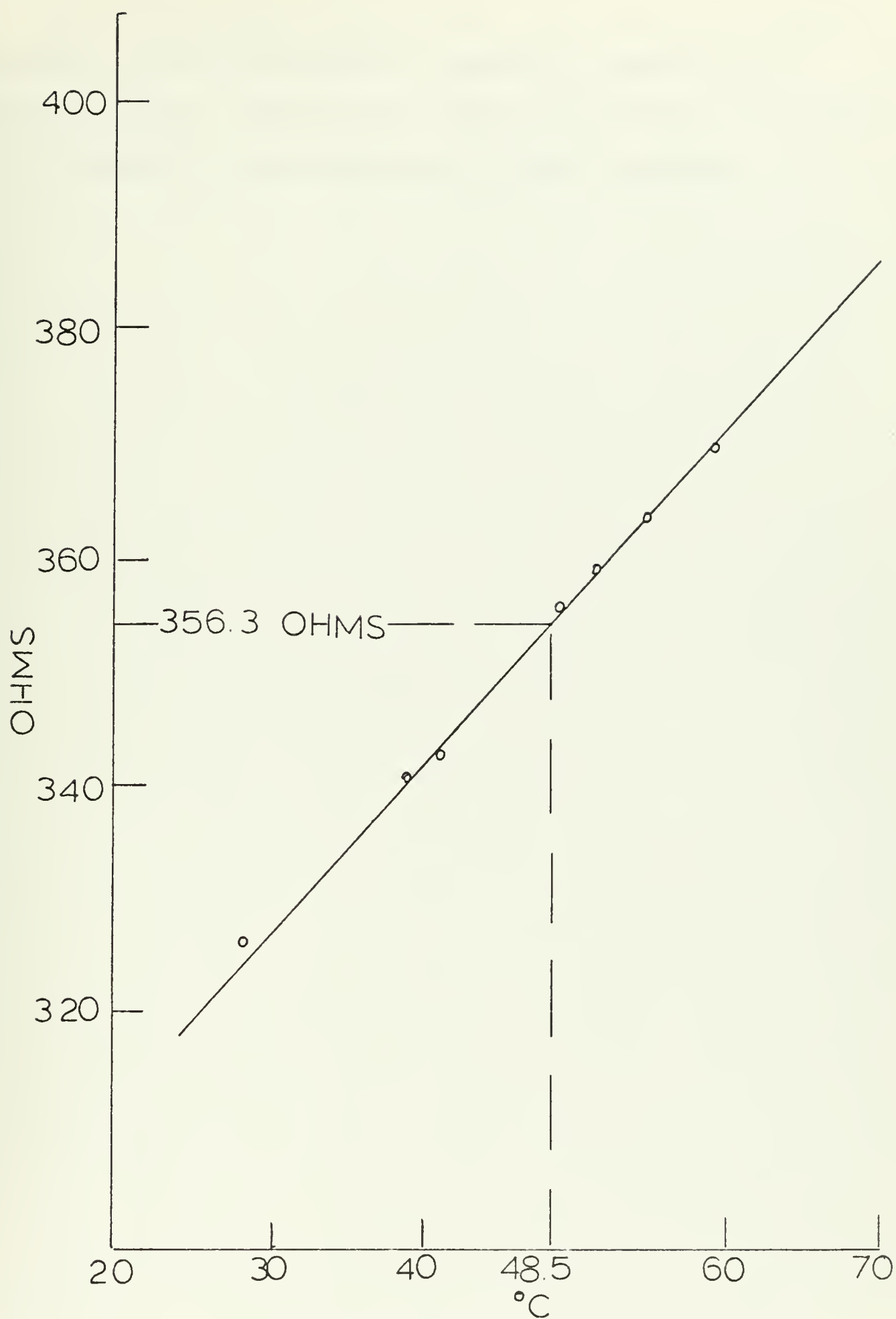


Figure 5. Calibration Curve.

Since the probe had a high temperature coefficient of resistance, the probe resistance was constantly changing as it generated heat. However, by manually regulating the Lambda power supply the bridge could be kept balanced and a probe temperature of 48.5°C maintained.

IV. EXPERIMENTAL APPARATUS

A. TEST MEDIUM

A region of nervous tissue is quite complex. However, to test the heating probe, a simplified medium that had the heat transfer characteristics of tissue was desired. Since the lesions produced by the heating probe are a result of thermal conduction, heat transfer by convection had to be negligible in the test medium. In addition, the medium had to be clear so that the region surrounding the probe could be seen.

Grayson [13] suggested that the water content is a major factor in determining the thermal conduction of animal tissue. Spells [22] investigated thermal conduction in both fluids and tissue and found there was a linear relationship between the conductivity and the water content of the tissue. The linear relationship was particularly close when the water content was above 50%.

Cooper and Trezek [7] obtained results that indicated the thermal properties of human tissue can be predicted within 5% by measuring the water content and assuming the remaining portion of the tissue is composed of equal amounts of fat and protein. They also found that the percentage of water in human tissue varied between 71% and 84%.

The above results indicate that an ideal test medium should have a high percentage of water. Gels would appear to be perfect. Gel consisting of gelatin mixed with an appropriate percentage of water would approximate tissue as a mixture of protein and water, and thermal properties close to those of human tissue could be expected. However, a characteristic of gels is that they melt at approximately 22°C. Since this would lead to convection effects, gel was not used as the test medium.

It was found, however, that agar-water solutions consisting of as little as 0.25% agar are clear, solidify at room temperature, and remain solid up to a temperature of approximately 85°C. In addition, the thermal properties of a 1%, or less, agar-water solution are almost identical with those of pure water, and within 10% of the thermal properties of most human tissues [7]. For these reasons, a mixture of 97.7% water and 0.3% Difco Bacto-Agar was chosen as the experimental test medium.

B. LIQUID CRYSTALS AND TEMPERATURE MEASUREMENT

Under appropriate conditions of temperature and pressure, matter can exist in a solid state, isotropic liquid state or gas state. The majority of organic and inorganic compounds are comprised of a regular, three-dimensional array of molecules or ions in the solid state, i.e., a crystal.

When the crystal lattice is heated, thermal agitation makes it impossible for the molecules to maintain a regular arrangement. At a given temperature, the crystal begins to melt and changes to a liquid. This change, known as the melting point, is usually very sharp and a characteristic of the compound. At still higher temperatures, the liquid boils and passes into the gas phase.

Near the turn of the century it was discovered that some compounds had a well defined melting point but the melt was opaque. The opacity disappeared when the temperature was increased to a definite limit, given a true isotropic liquid. Although this intermediate phase was fluid to some extent, it also exhibited some characteristics of a crystalline solid. This phase was called a mesophase and compounds exhibiting this phenomenon became known as liquid crystals [12].

There are three types of mesophase [12].

- (i) smectic - molecules have a parallel orientation and are in layers with their axes at right angles to the layers.
- (ii) nematic - molecules have a parallel orientation of their axes.
- (iii) cholesteric - molecules have a parallel orientation and are in layers with their axes in the plane of the layer.

The cholesteric mesophase is quite different from the smectic and nematic and possesses unique optical characteristics. Cholesteric liquid crystals having a certain structure exhibit dramatic changes in color with very small changes in temperature. This color-temperature relationship is constant and reappears everytime the liquid crystal passes through a particular temperature range.

Dowden [9] discusses the structure of cholesteric liquid crystals. These crystals are derived from cholesterol or other sterol systems and have a basically planar structure. The axial direction in each successive layer is displaced slightly from that in the previous layer giving a spiral trace. The thickness of each layer is about 3\AA and the pitch of the helix is about 5500\AA .

The property which is the basis of color behavior is circular dichroism. An incident beam of unpolarized light is split into two components having electrical vectors rotated in opposite directions. One component is transmitted and the other is scattered. The scattered light normally has a wavelength peak that occurs in the visible region of the spectrum.

Temperature changes disturb the intermolecular forces and cause a shift in the molecular structure. This changes the wavelength of the light that is scattered. Thus, cholesteric liquid crystals exhibit dramatic changes in color with very small changes in temperature.

Since the colors scattered by liquid crystals are unique for specific temperatures, the quantitative measurement of temperature is possible to an accuracy of less than 0.1°C [8].

Liquid crystals can be applied directly to a surface. However, a dark uniform layer is normally placed on the surface before the liquid crystals. This provides a standard surface texture, intensifies the resulting colors and isolates the crystals from surface contamination.

Liquid crystals have some application problems. Since they are viscous, applied film thicknesses can easily vary and result in non-reproducible thermal patterns. Direct exposure of the crystals to solvent vapors, oils, dirt and ultra-violet light can cause variations in their sensitivity. However, it is possible to encapsulate the liquid crystal in a tiny capsule (10 to 30 microns), thus shielding it from most of these detrimental effects [17].

Encapsulated crystals are available commercially in a variety of forms that cover a wide range of temperatures. Rochrome liquid crystal tapes manufactured by Hoffman-LaRoche Inc. were used. These crystals were coated on a mylar substratum with an absorptive black background. The overall thickness of the crystals and mylar was less than 0.01 inches.

The Rochrome crystals are calibrated with an accuracy of 0.1°C and have a response time of less than one second [18]. Parker [19] found that the response time of the encapsulated crystals depends on the crystal thickness. For a thickness of 0.0035 inches, response time was of the order of 200 to 300 milliseconds.

By placing the liquid crystal tape in the test medium, the temperature field around the probe could be seen and temperatures throughout the field accurately measured.

Rochrome liquid crystal tape lot no. AS-70-36 was used in the actual experiments. The color to temperature relationship of this tape was:

29.9°C - red

31.5°C - green

34.2°C - blue

During preliminary experiments with the liquid crystal tapes it was found that the water in the test medium caused the encapsulated crystals to separate from the mylar backing. To prevent this from happening, the tapes were given a thin coating of Varathane and the edges were sealed with a rubber adhesive.

C. TEST CELLS

Two test cells were used to study the three-dimensional temperature field surrounding the probe (see Figure 6). A circular container, five inches in diameter and four inches deep, was constructed of plexiglass and was used to visually observe the radial temperature field. A removable ring was fitted into the cell to support the liquid crystal tape (see Figure 7). The tape was attached to a thin sheet of mylar that was stretched across the ring. The probe was inserted through the bottom of the cell and was held in place by a bushing that allowed the height of the probe to be adjusted.

The second cell, a 4 5/8 x 5 1/2 x 6 inch rectangular container, also constructed of plexiglass, was used to observe the axial temperature field near the probe. The probe was inserted through the side of the container. A removable bracket was manufactured to hold the liquid crystal tape lengthwise along the probe (see Figure 7). Because of symmetry, the temperature field on only one side of the probe was measured.

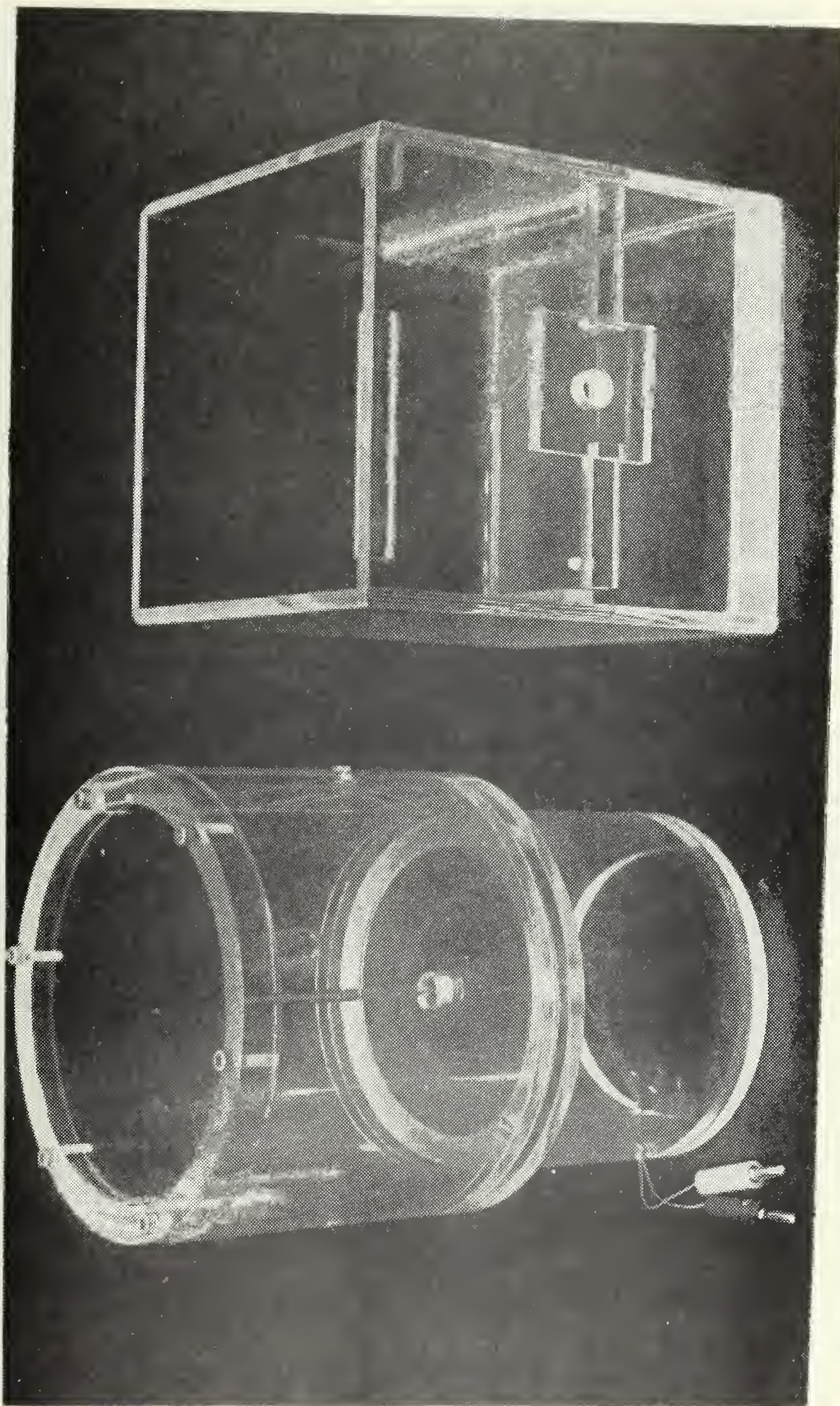


Figure 6. Test Cells

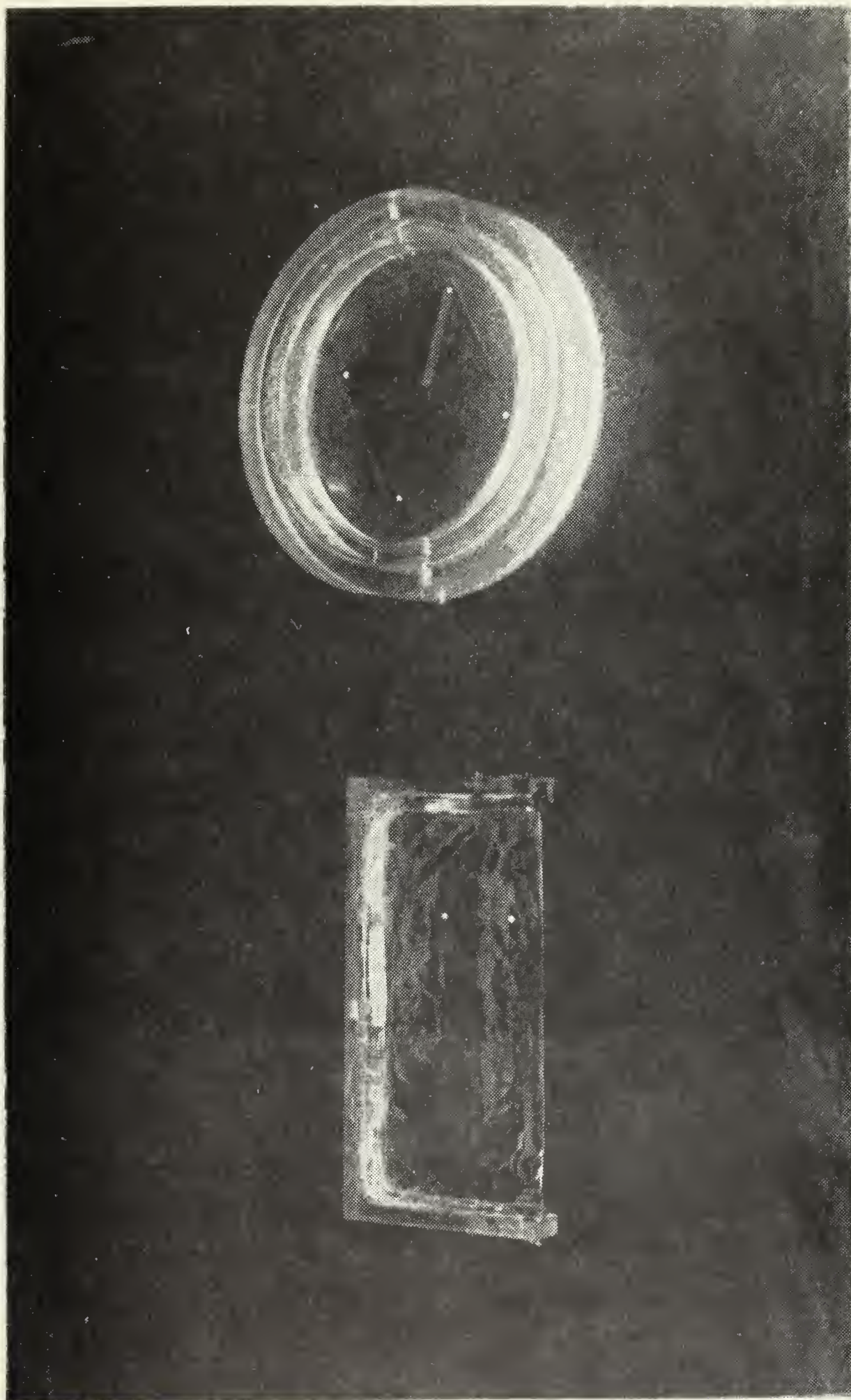


Figure 7. Removable Support Rings for Liquid Crystal Tape.

To ensure that the container walls would not disturb the temperature field around the probe, both containers were constructed so that their dimensions were large compared to the probe dimensions.

V. EXPERIMENTAL PROCEDURE

The test cells were filled with the 0.30% agar-97.79% water test medium for the experimental runs. The probe was positioned in the circular test cell so that there was an equal length of probe above and below the liquid crystal tape. Thus, the temperature field around the midpoint of the probe was measured. The probe was covered by the agar-water medium so that the top of the probe was at least five probe diameters below the surface.

All test runs were conducted at room temperature using Rochrome liquid crystal tape lot no. AS-70-36 to measure the temperature field around the probe. As mentioned earlier, this tape had the following temperature to color relationship:

29.9°C	-	red
31.5°C	-	green
34.2°C	-	blue

A narrow strip of Series 9 Rochrome tape was placed in the test medium to measure the medium's ambient temperature. The temperature to color relationship of the Series 9 tape was:

23.0°C	-	red
24.0°C	-	green
27.0°C	-	blue

The ambient room temperature, normally about 23.5°C, was used as a rough check of the temperature obtained from the Series 9 tape.

Before the containers were filled with the agar-water test medium, four reference marks, 4.57 centimeters apart, were placed on the corners of the tape. Figure 8 is a top view of the circular test

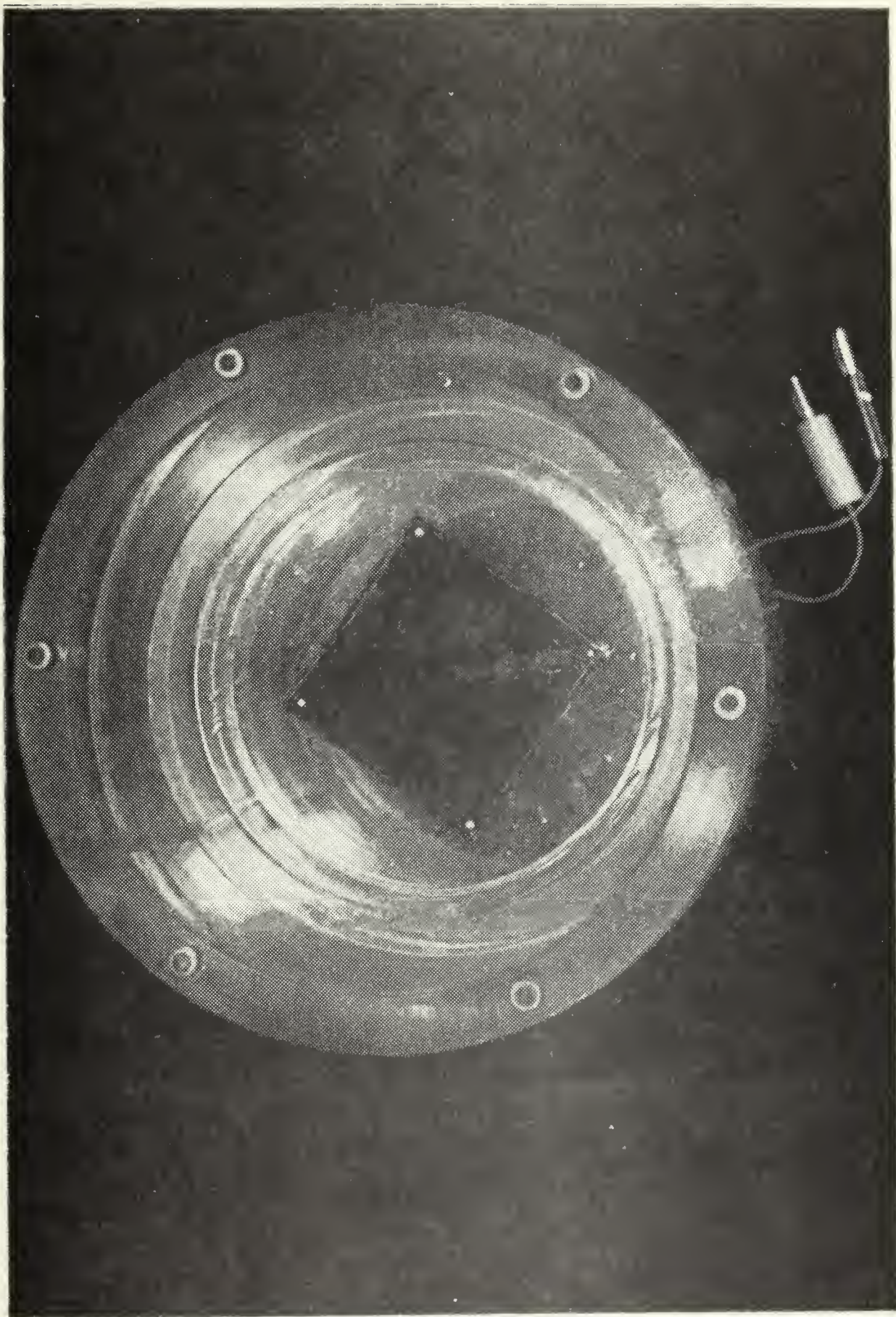


Figure 8. Top View of Circuit Test Cell.

cell showing the probe in place, the narrow strip of Series 9 tape, and the four reference marks.

The resistance of the probe was controlled manually by adjusting the Lambda power supply to maintain zero voltage on the detector.

Figure 9 is an overall view of the apparatus.

Photographs of the temperature field surrounding the probe were taken using a Graflex 4 x 5 Press camera fitted with a Polaroid Land film holder. Polaroid 4 x 5 Land film Type 57, 3000 speed was used.

Photographs were taken at various increments of time. The outer radius of the temperature field, corresponding to 29.9°C , and the reference marks were measured in each picture. Using the actual distance between the reference marks (4.57 cm) and the probe radius (0.2076 cm), the non-dimensional radius was calculated.

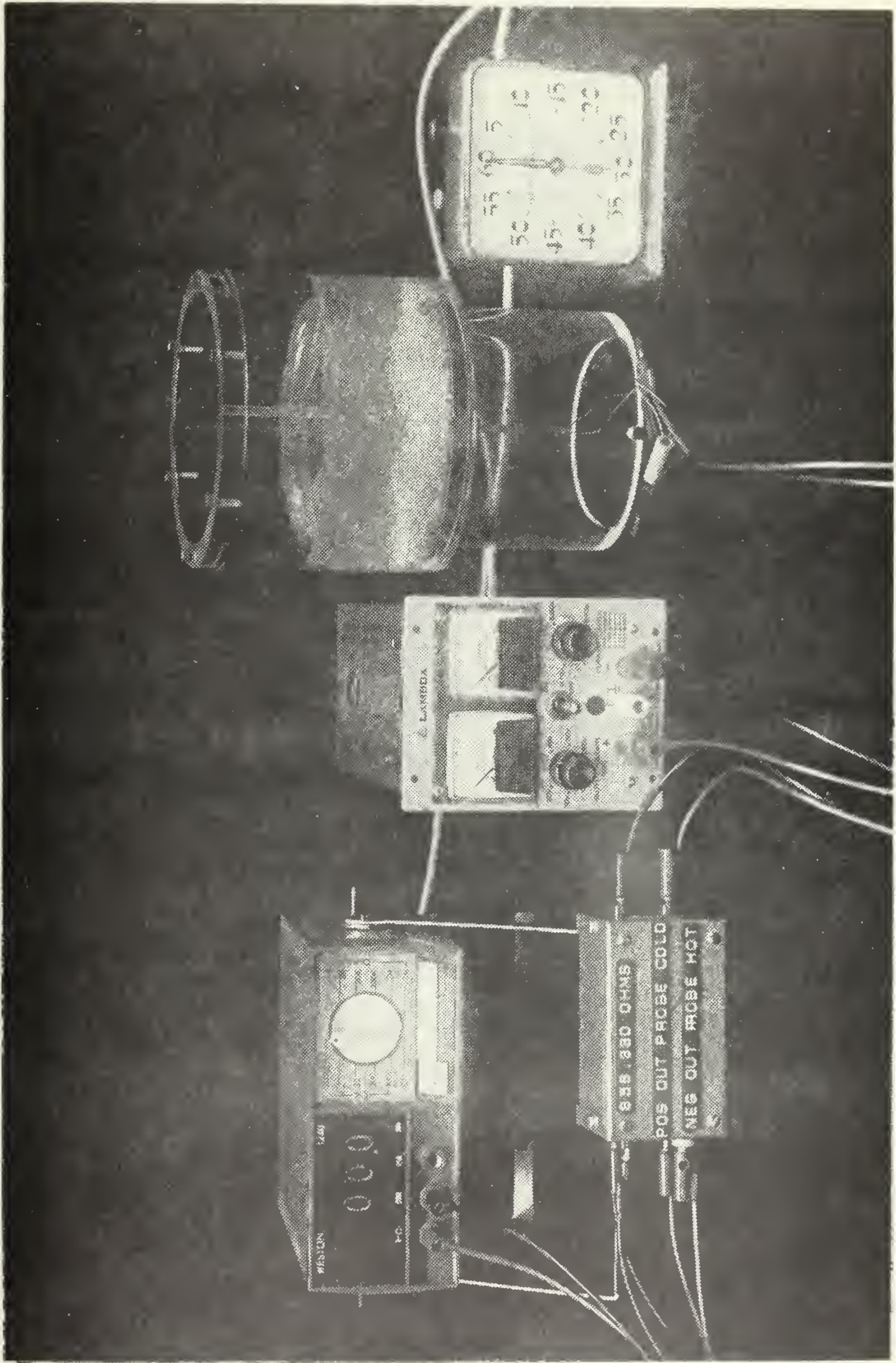


Figure 9. Overall View of Apparatus.

VI. THEORETICAL ANALYSIS

A. ONE-DIMENSIONAL MODEL

1. Metabolic and Blood Flow Effects Neglected

In order to simulate the heat transfer process in the region surrounding the probe, a one-dimensional heat transfer model must be developed. In this model it will be assumed that the tissue is an infinite homogenous medium with known conductivity, density and specific heat and that it is initially at a uniform temperature of T_0 . The probe is assumed to be a cylinder of infinite length and radius r_0 with a constant temperature of T_p (see Figure 10). Thus, the problem is to solve for the temperature distribution in a region bounded by a circular cylinder.

The general conduction equation is:

$$\frac{k}{r} \frac{\partial}{\partial r} \left(r \frac{\partial T}{\partial r} \right) = \rho c \frac{\partial T}{\partial t} \quad (5)$$

k = thermal conductivity

ρ = density

c = specific heat

$\alpha = \frac{k}{\rho c} = \text{thermal diffusivity}$

It is now convenient to introduce the following nondimensional variables:

$$R = \frac{r}{r_0} \text{ (distance)}$$

$$\tau = \frac{\alpha t}{r_0^2} \text{ (time)}$$

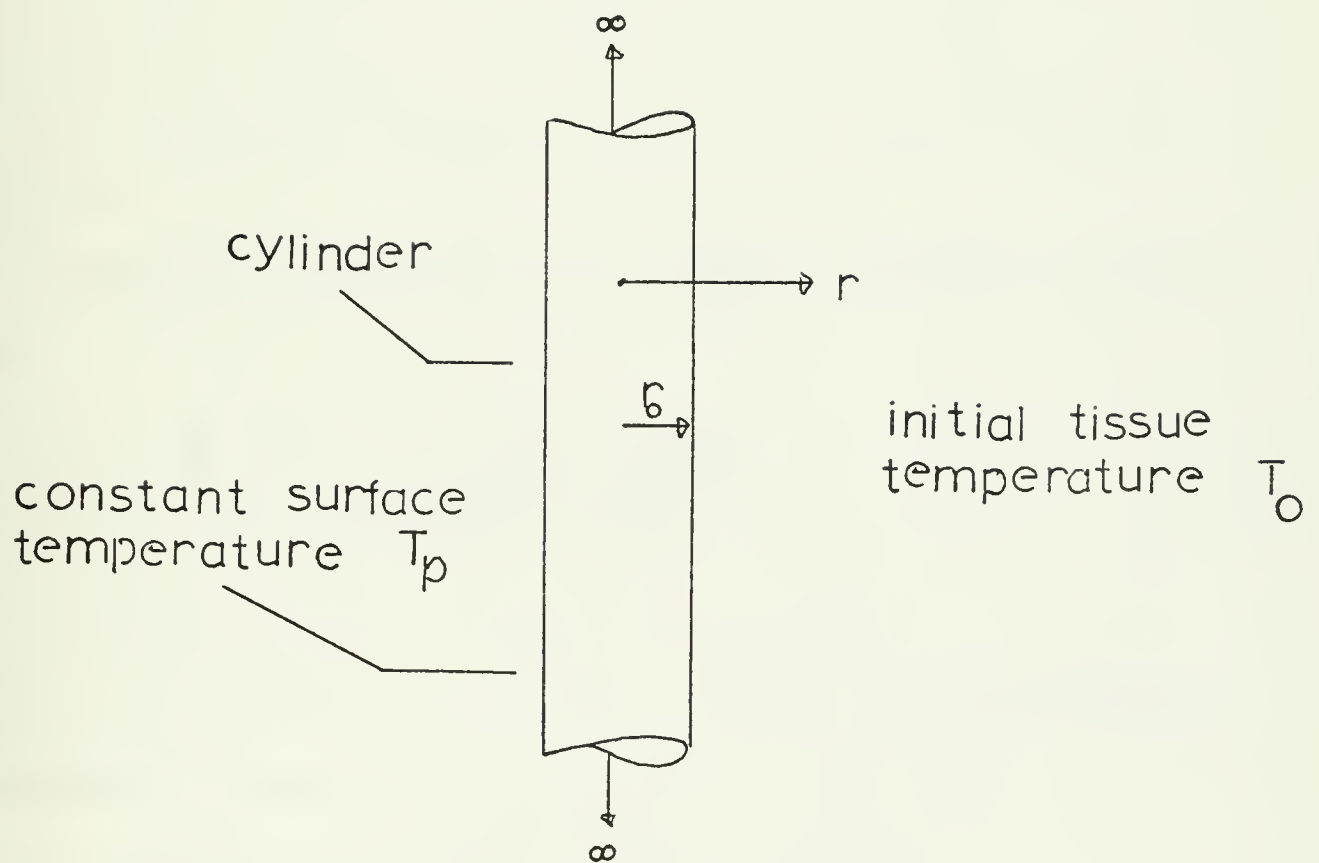


Figure 10. Mathematical Model of Probe.

$$\theta = \frac{T - T_0}{T_p - T_0} \quad (\text{temperature})$$

Substituting these variables into equation (5) yields,

$$\frac{1}{R} \frac{\partial \left(R \frac{\partial \theta}{\partial R} \right)}{\partial R} = \frac{\partial \theta}{\partial \tau} \quad (6)$$

The boundary conditions are:

- (a) at the probe surface ($r = a$, or $R = 1$), $T = T_p$ and $\theta = 1$.
- (b) at large distances from the probe the temperature of the tissue remains constant; that is, as $r \rightarrow \infty$, $T \rightarrow T_0$ or nondimensionally, as $R \rightarrow \infty$, $\theta \rightarrow 0$.

The initial condition is at time $t = 0$, $T = T_0$ or $\theta = 0$ for all locations.

Carslaw and Jaeger [5] give the closed form solution of equation (6):

$$\theta = 1 - \frac{2}{\pi} \int_0^\infty \frac{e^{-\tau u^2} C_0(u, Ru) du}{u [J_0^2(u) + Y_0^2(u)]} \quad (7)$$

$$C_0(u, Ru) = J_0(u) Y_0(Ru) - Y_0(u) J_0(Ru)$$

where, J_0 and Y_0 are Bessel functions. Equation (7) was evaluated numerically by Jaeger for various values of τ and R [15].

2. Metabolism and Blood Flow Effects Included

Pennes [20] was the first to account for metabolic and blood flow effects in the heat equation. Pennes suggests that the equation take the form:

$$\frac{k}{r} \frac{\partial \left(r \frac{\partial T}{\partial r} \right)}{\partial r} + m_b c_b (T_b - T) + S_m = \rho c \frac{\partial T}{\partial t} \quad (8)$$

where:

m_b = blood flow rate per unit volume

S_m = metabolic heat rate per unit volume

T_b = blood temperature

In this model, the effect of blood flow is treated as a perfect heat exchanger. That is, it is assumed that the blood enters a unit volume of tissue at the arterial temperature, T_b , and acquires the tissue temperature as it exits the volume.

If the metabolic heat generation rate is assumed to be constant, it can be combined with the blood flow term as:

$$m_b c_b (T_o - T)$$

where

$$T_o = T_b + \frac{S_m}{m_b c_b}$$

This corresponds to redefining the reference temperature. Cooper and Trezek [6] show that for brain tissue, T_o is on the order of 0.5°C higher than the arterial blood temperature, T_b .

Equation (8) may be normalized by defining a nondimensional "blood flow parameter":

$$\beta = \frac{m_b c_b r_o^2}{k} \quad (\text{blood flow term})$$

Substituting this variable along with R , τ and θ into equation (8) yields:

$$\frac{1}{R} \frac{\partial \left(R \frac{\partial \theta}{\partial \tau} \right)}{\partial R} - \beta \theta = \frac{\partial \theta}{\partial \tau} \quad (9)$$

The boundary conditions and initial condition are the same as were used for equation (6).

Equation (9) was solved with the use of Laplace Transformations and the following closed form solution was obtained:

$$\theta = \frac{K_0(\sqrt{\beta R})}{K_0(\sqrt{\beta})} - \frac{2}{\pi} e^{-\beta \tau} \int_0^{\infty} \frac{e^{-\tau u^2} C_0(u, Ru) du}{[u + \beta/u] [J_0^2(u) + Y_0^2(u)]} \quad (10)$$

$$C_0(u, Ru) = J_0(u) Y_0(uR) - J_0(uR) Y_0(u)$$

Equation (10) was solved numerically for various values of R and τ and for values of $\beta = 0.0, 0.1, 0.5$ and 1.0 and the results are tabulated in Tables II - XI. The reader is referred to Appendix A for details.

B. TWO-DIMENSIONAL MODEL

The one-dimensional model assumed that the probe was infinite in length. However, the probe consists of a constant temperature cylinder of finite length and a cylindrical insulated stem. The one-dimensional solution does not take end effects into account. Thus, it was desired to have a two-dimensional solution that would include these effects.

A digital computer program, by the code name of Trump [16], was used to determine the two-dimensional transient temperature field around the probe.

Since TRUMP obtains a solution in dimensional form, a nodal network (see Figure 11) had to be constructed for the geometric configuration of the probe. Due to symmetry, it was necessary to generate the field for only one half of the cross-sectional area. The dimensions of the network were chosen large enough so that the boundary conditions at $R = 30$ and $X = 24.0 r_0$ did not affect the temperature field during the transient period which was investigated. The network therefore simulated an "infinite" field.

The TRUMP solution gave values of θ at each node point for various values of nondimensional time. The results are given in Tables XII - XVI.

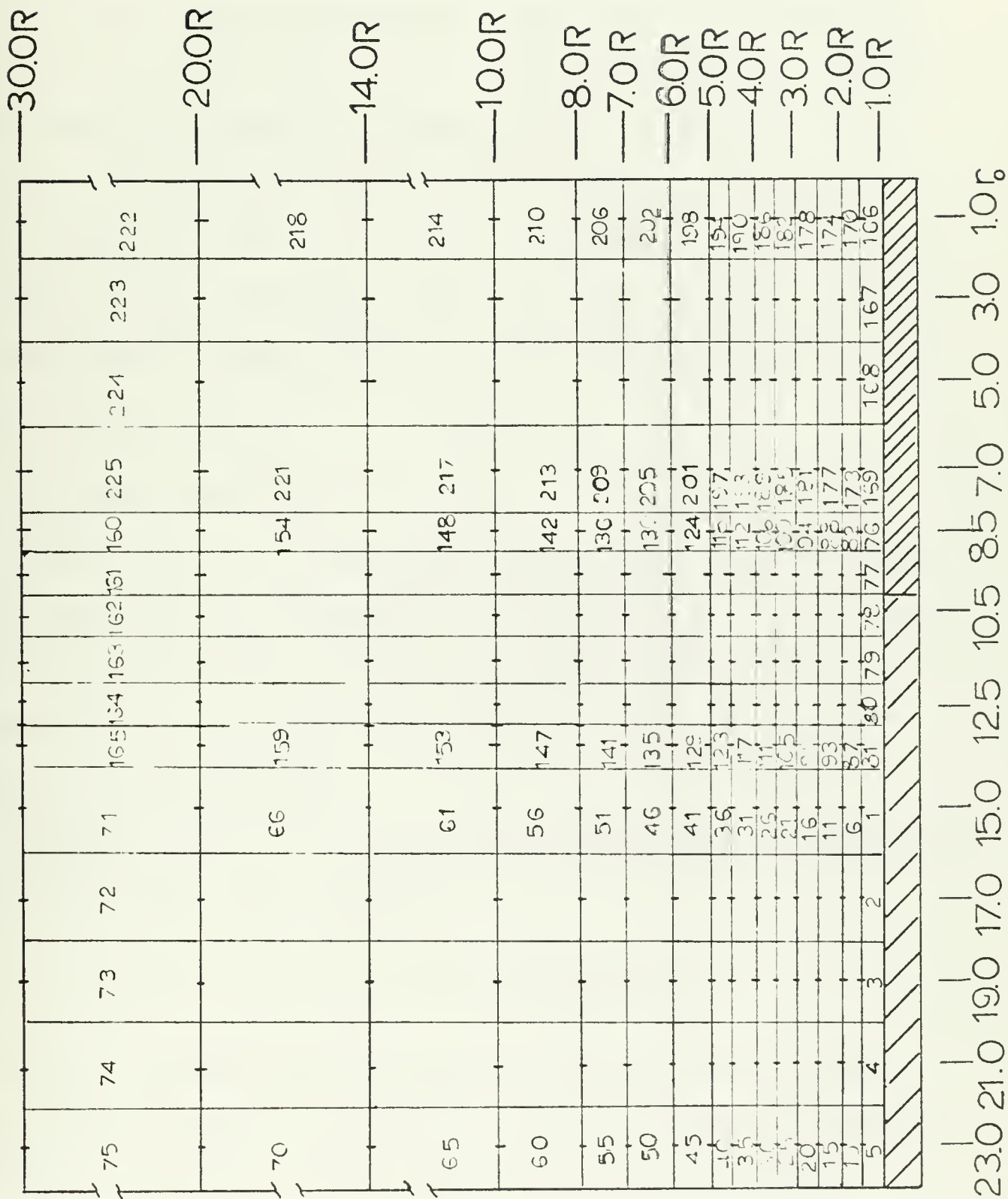


Figure 11. TRUMP Nodal Network.

VII. RESULTS

The preceding section gave details of the three models that were used; a one and two-dimensional model without blood flow and metabolic effects and a one-dimensional model including these effects. Numerical results for the one-dimensional models are given in Tables II-XI. Tables XII - XVI give the numerical results for the two-dimensional model. Values for θ are given at various nondimensional locations (R) and times (τ). The experimental results, differences between the one and two-dimensional models, and the relative effects of blood flow and time will now be discussed.

A. EXPERIMENTAL RESULTS

Figures 12, 13, 14, 15 and 16 are representative pictures of the radial temperature field surrounding the probe taken at $\tau = 0.0, 1.0, 3.0, 5.0$ and 10.0 . Figure 17, 18, 19, 20 and 21 depict the axial temperature field at $\tau = 0.0, 1.0, 3.0, 5.0$ and 10.0 . The latter pictures also show end effects.

It was convenient to use the following nondimensional variables in calculating the experimental results:

$$\theta_c = \frac{T_c - T_o}{T_p - T_o} \quad (\text{critical temperature})$$

where, T_c is the temperature corresponding to a given liquid crystal color. In the experimental runs, this color was red and corresponded to a temperature of 29.9°C . In a surgical application, T_c is the temperature at which tissue destruction begins.

$$R_c = \frac{r_c}{r_o} \quad (\text{radius of lesion})$$

The experimental data and results are given in Table XVII.

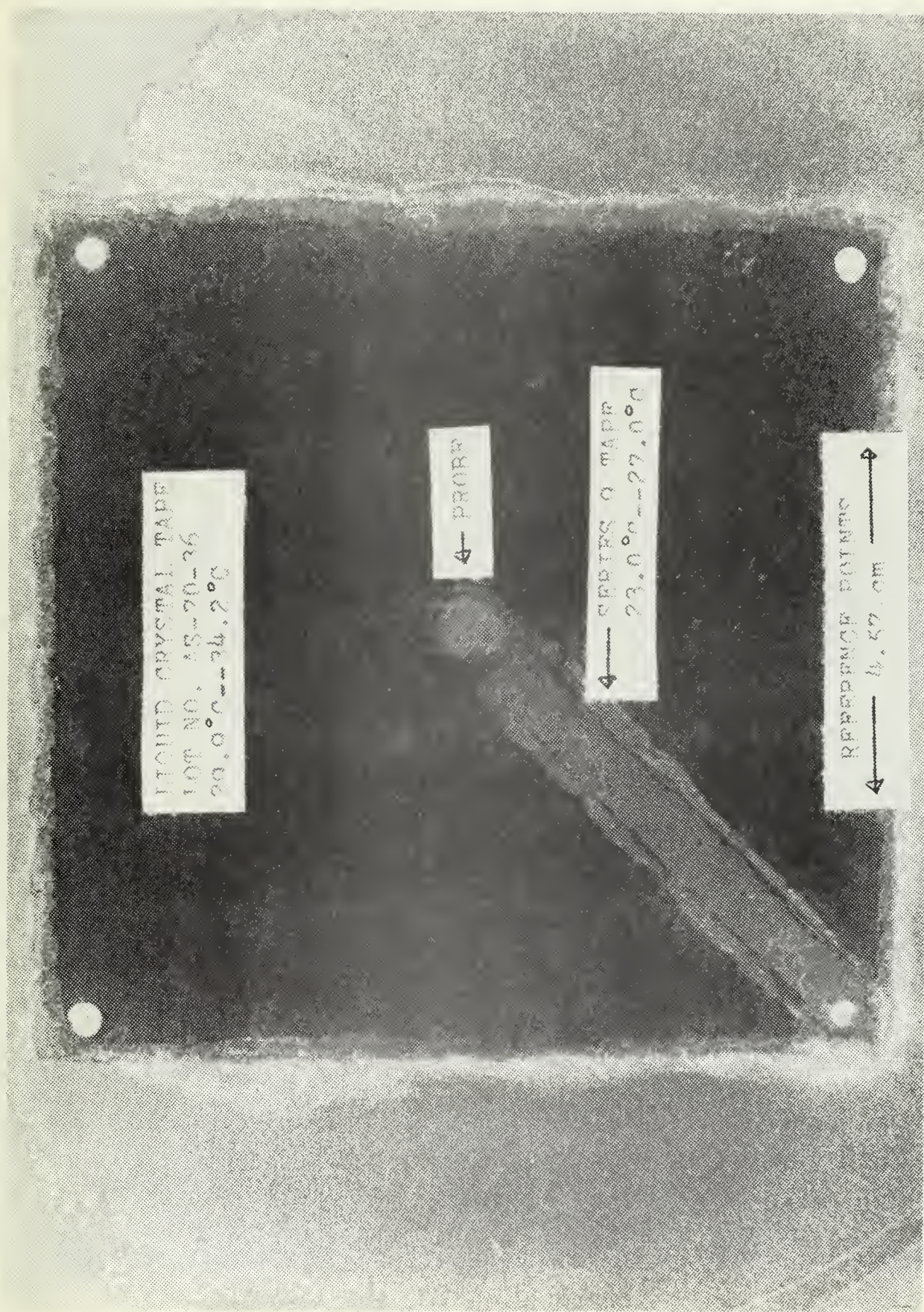


Figure 12. Radial Temperature Field for $\tau = 0.0$.

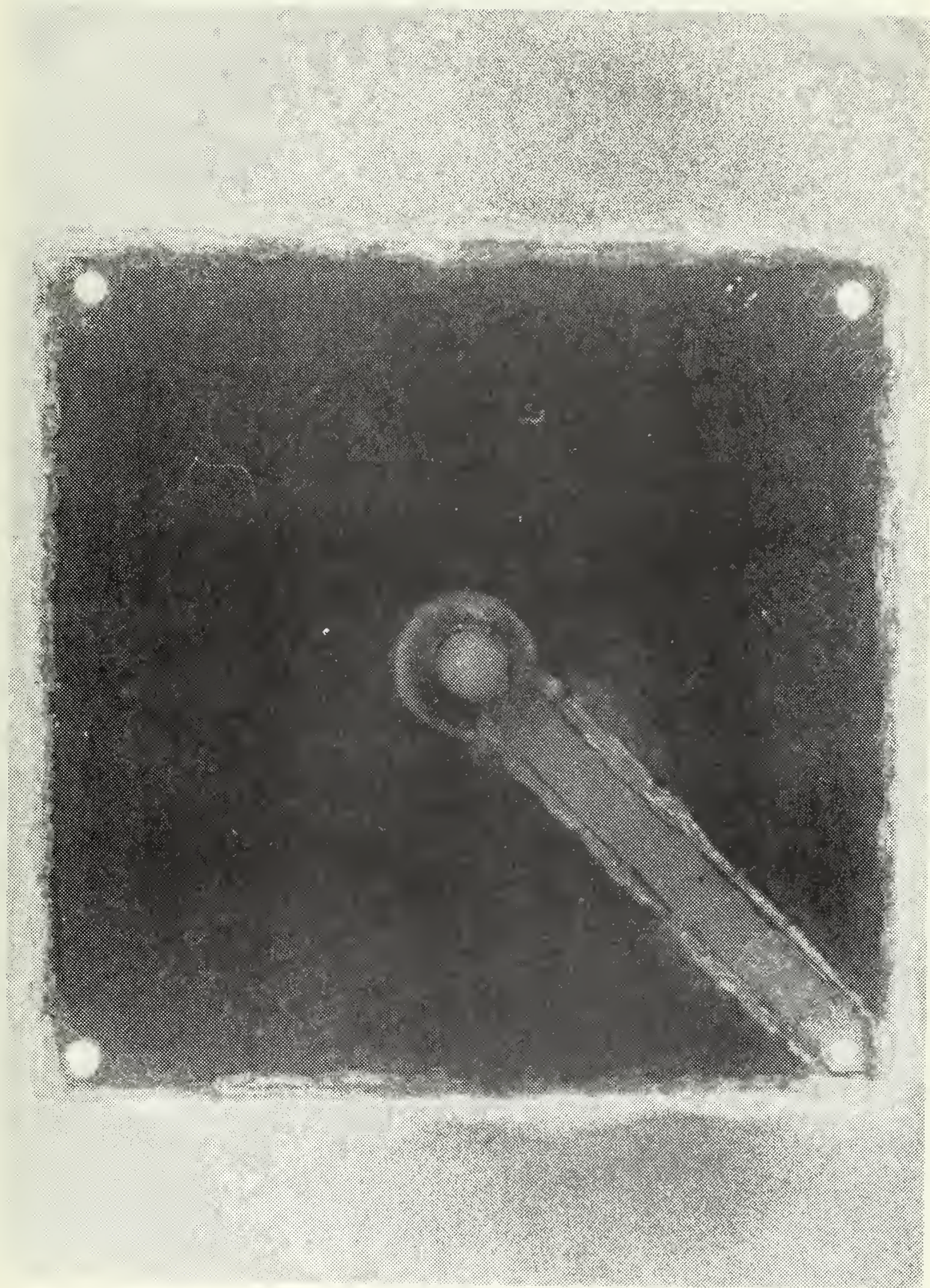


Figure 13. Radial Temperature Field for $\tau = 1.0$

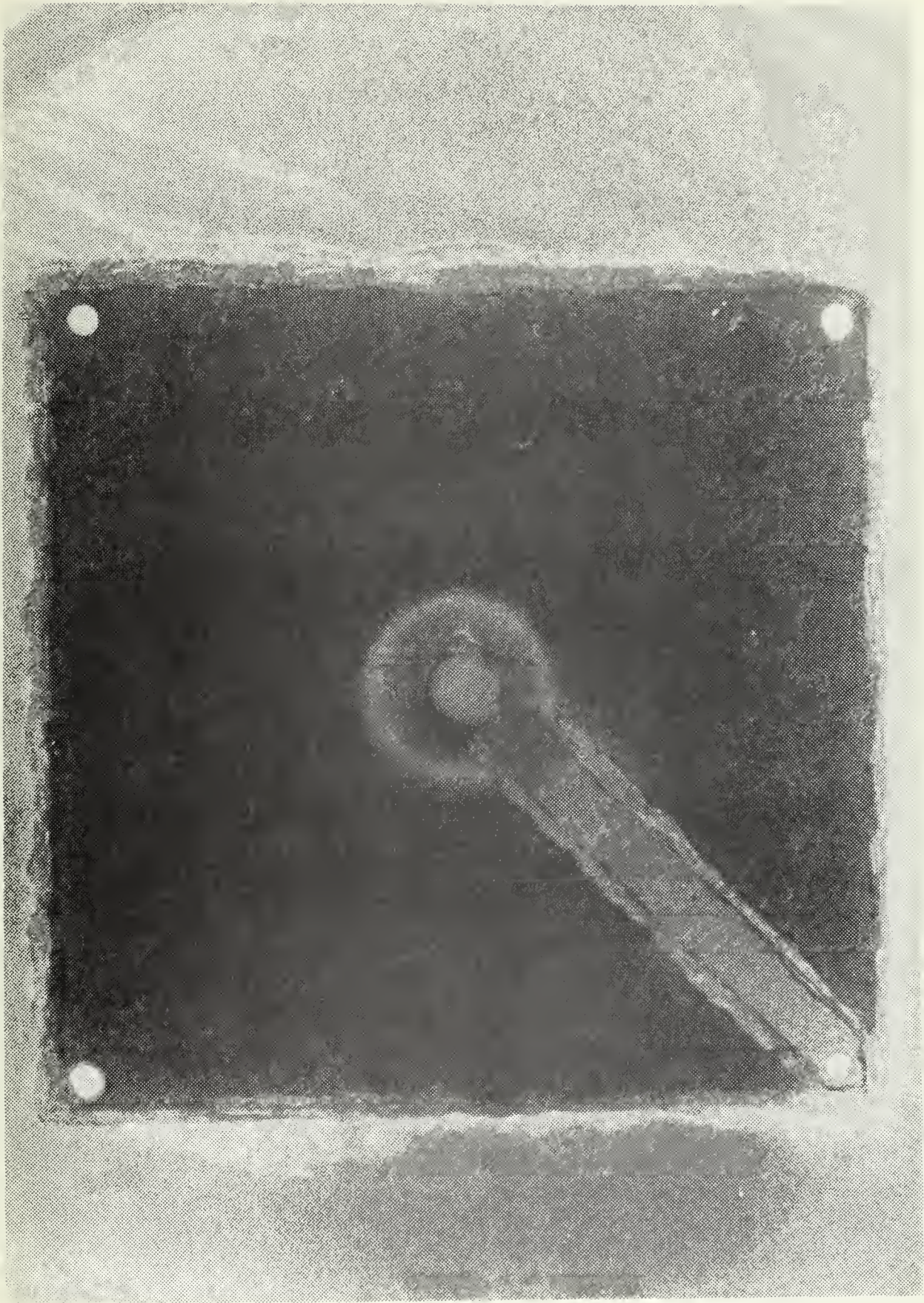


Figure 14. Radial Temperature Field for $\tau = 3.0$.

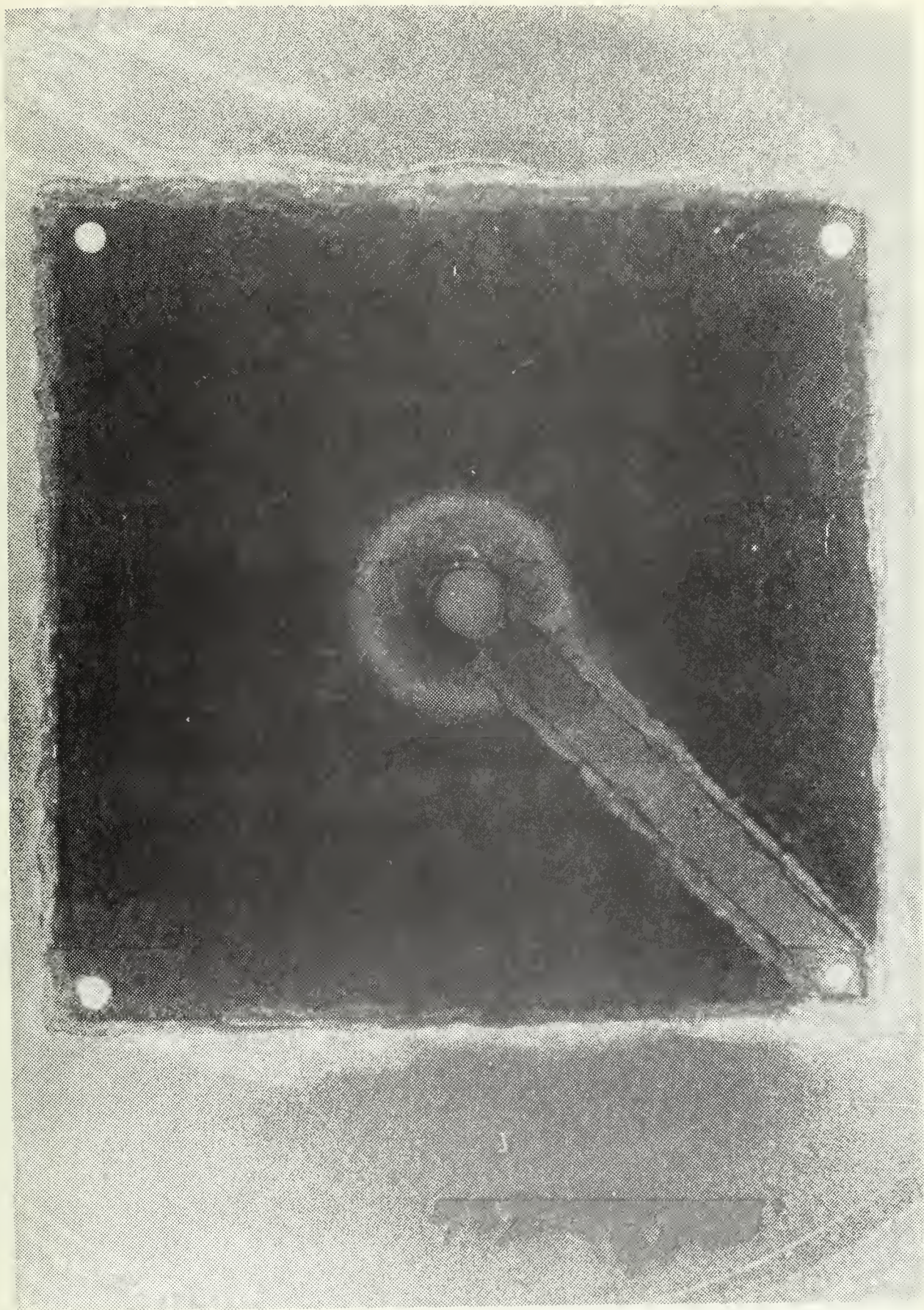


Figure 15. Radial Temperature Field for $\tau = 5.0$.

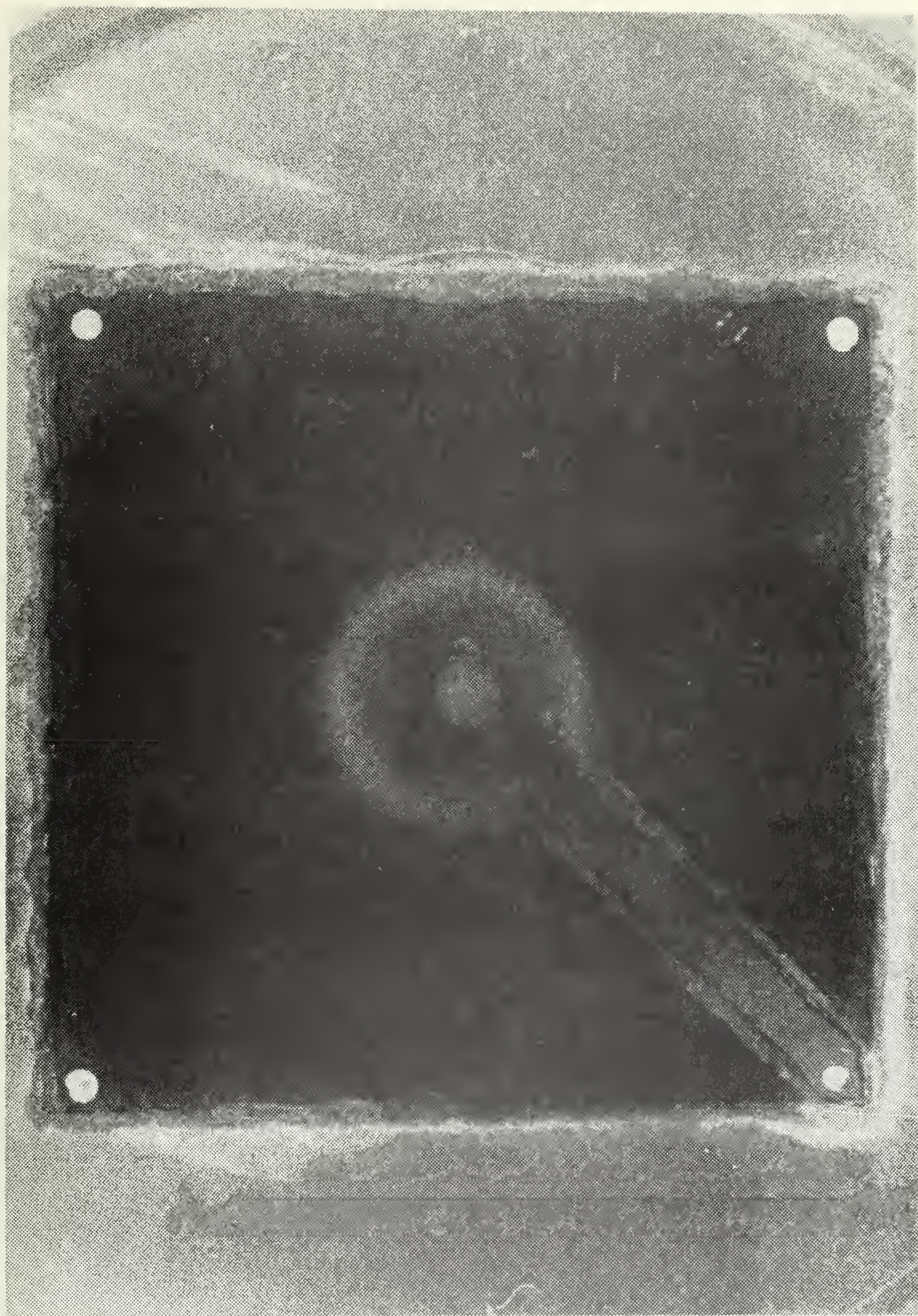


Figure 16. Radial Temperature Field for $\tau = 10.0$.



Figure 17. Axial Temperature Field for $\tau = 0.0$.



Figure 18. Axial Temperature Field for $\tau = 1.0$.



Figure 19. Axial Temperature Field for $\tau = 3.0$.

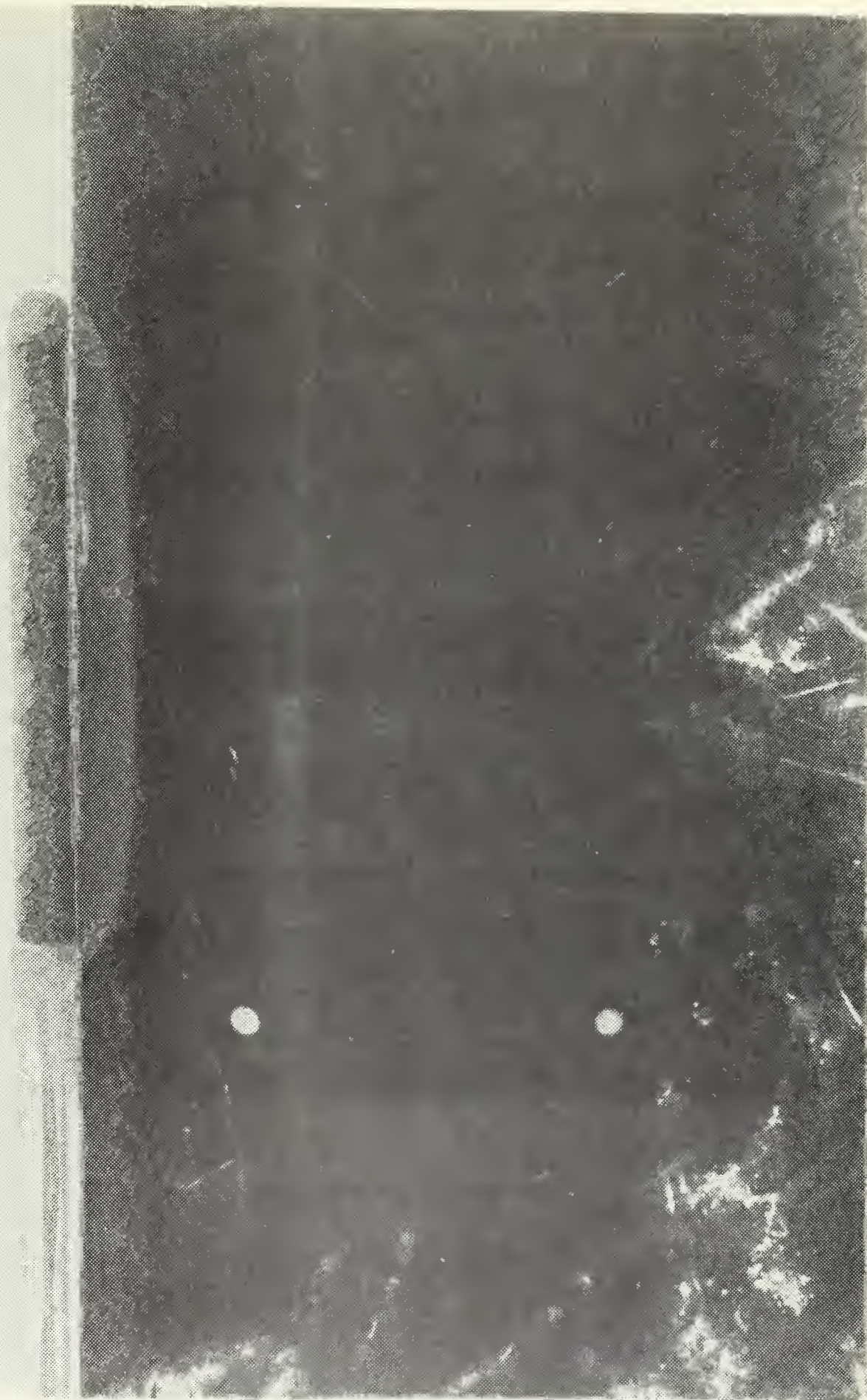


Figure 20. Axial Temperature Field for $\tau = 5.0$.



Figure 21. Axial Temperature Field for $\tau = 10.0$.

The experimental results were compared with the two-dimensional model. Figure 22 is a typical graph of the nondimensional time for a critical temperature, $\theta_c = 0.200$. The solid line represents the two-dimensional solution and the dashed lines represent the error bound. The reader is referred to Appendix B for details of the error analysis.

The experimental results fall within the error bounds except at short times. This is due to the fact that the analytical solutions were obtained assuming a step input. That is, it was assumed that the probe came to its final temperature immediately. Because of equipment limitations this was impossible to duplicate in the experimental runs and it took the probe approximately 15 seconds to reach its final temperature.

Figure 23 is a graph of the nondimensional lesion radius versus nondimensional time for a critical temperature of $\theta_c = 0.235$. The solid line represents the two-dimensional solution.

The axial temperature field is shown in Figure 24. Again, the solid lines represent the two-dimensional solution. Only one experimental run was conducted using this configuration. Although the experimental isotherms exhibit the same shape as the analytical isotherms, they are lagging in time. A great deal of difficulty was encountered in placing the liquid crystal sheet in a uniform plane next to the probe and, in fact, the edges of the sheet tended to sag after a short period in the agar-water solution. More work is needed on this particular aspect of the experiment since experimental errors are obviously large.

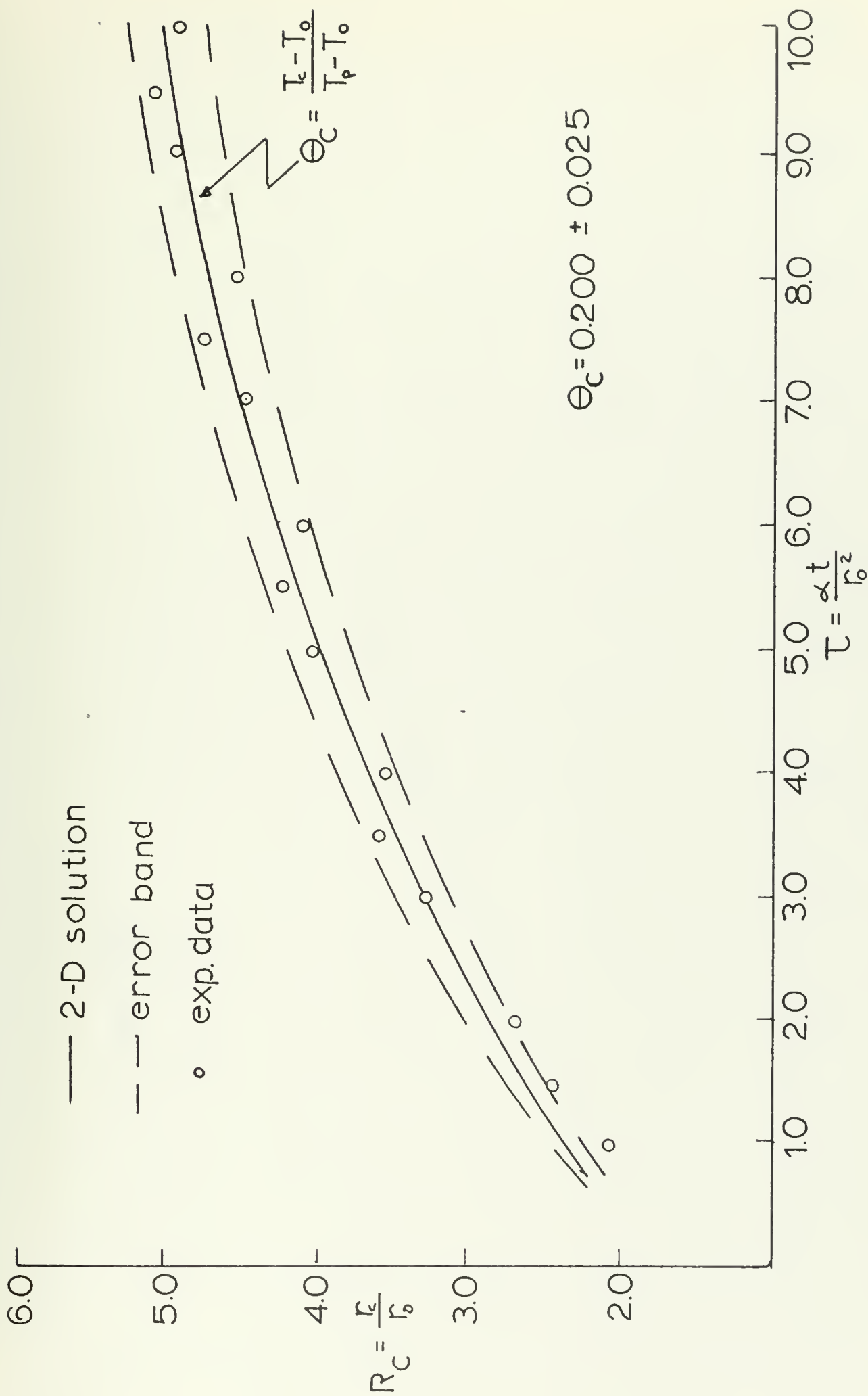


Figure 22. R_C vs τ for $\theta_C = 0.200$ and $\beta = 0.0$.

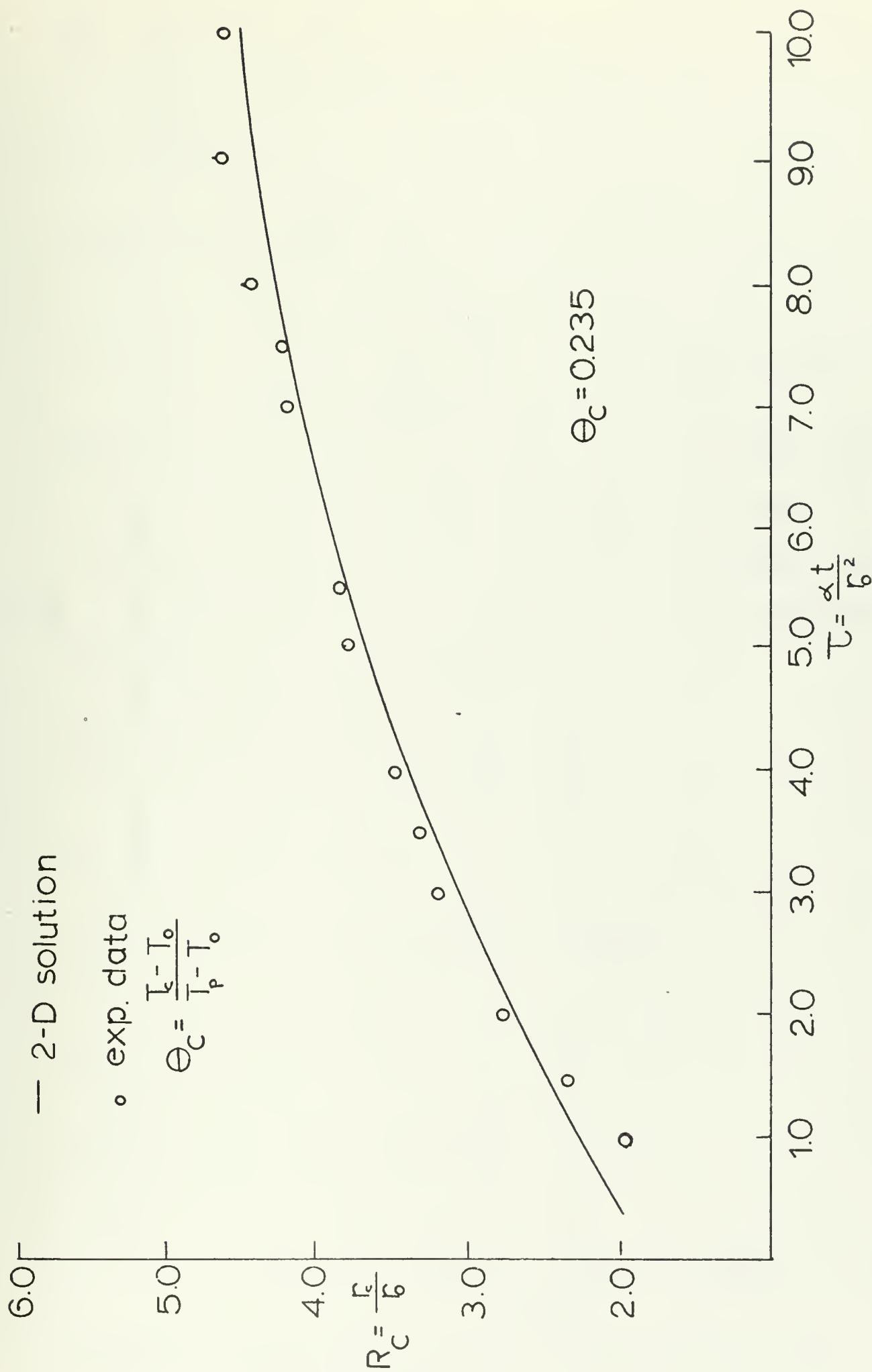


Figure 23. R_C vs τ for $\theta_c = 0.235$ and $\beta = 0.0$.

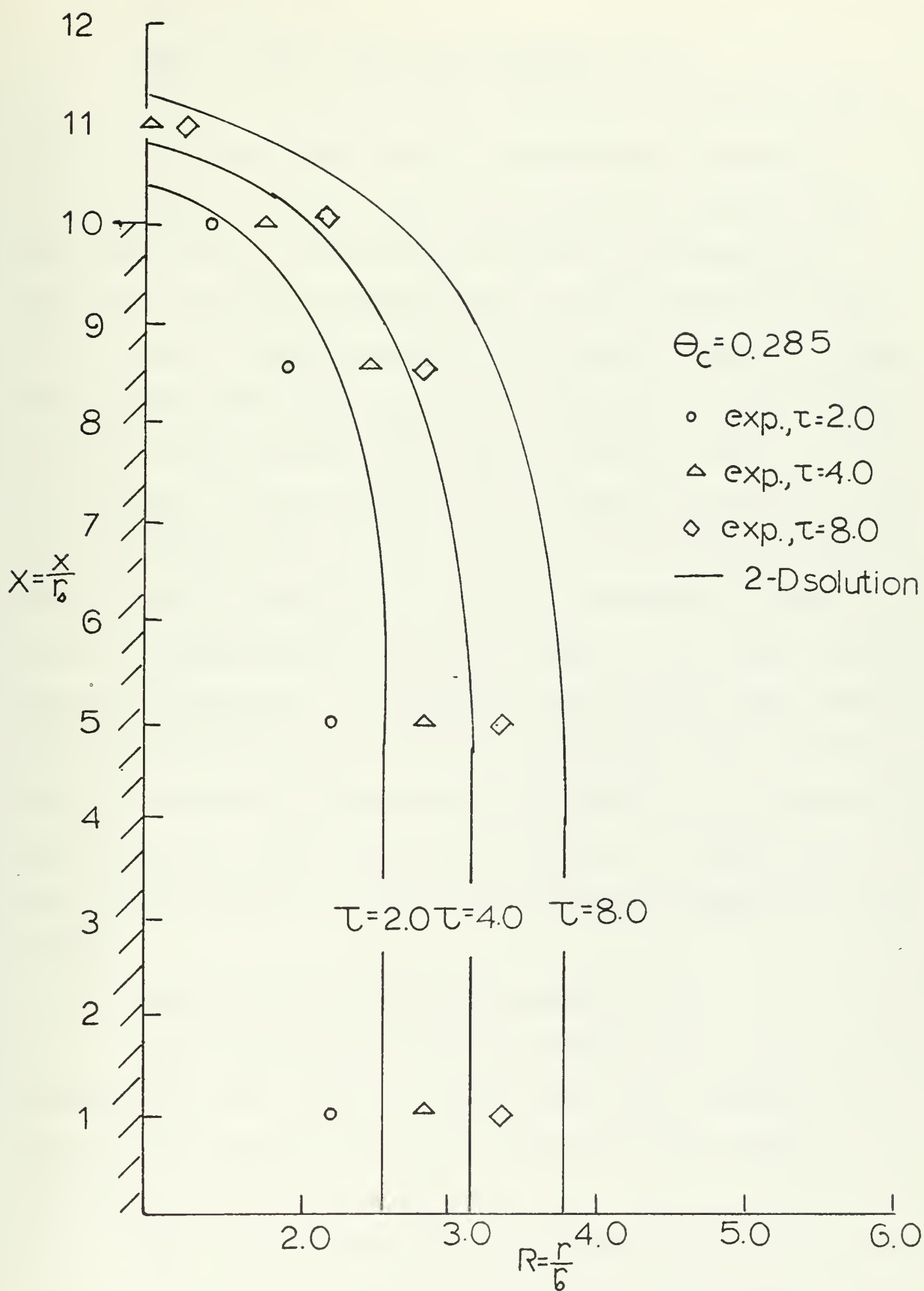


Figure 24. Axial Position (x) vs. R_c for Various Values of τ and $\theta_c = 0.285$.

B. ONE-DIMENSIONAL MODEL

1. Effect of Blood Flow on the Temperature Field

Figure 25 is a graph of the nondimensional temperature versus the radial location in the tissue for a nondimensional time equal to five (corresponds to a real time of approximately 150 seconds for the experimental probe). Four curves are presented: the dashed line represents no blood flow effect and the solid lines represent β 's of 0.1, 0.5 and 1.0. Note from the graph that blood flow tends to decrease the temperature field, resulting in a slightly smaller lesion. To gain a feeling for the magnitude of this effect, a typical value of β will be calculated. A typical value for $m_b c_b$ of blood flow in the brain is $0.01 \text{ cal/cm}^3/\text{sec}/^\circ\text{C}$ [21] and a typical value of the thermal conductivity of brain tissue is $0.0014 \text{ cal/cm}/^\circ\text{C}/\text{sec}$ [7]. Therefore, for brain tissue, β is approximately equal to $7 r_0^2$, where r_0 is the probe radius expressed in centimeters. The experimental heating probe had a radius of approximately 0.2 cm; thus, β would be of the order of 0.28. However, an actual probe would be approximately one fourth the size of the experimental probe and β would then be much less than 0.1. Figure 26 shows that values for blood flow in this range decreased the temperature only slightly.

2. Effect of Increased Time on Temperature Field

Figure 26 is a graph of the nondimensional temperature versus nondimensional time. One can see that at short times, the rate of lesion growth is large, but as time increases, the lesion growth decreases and approaches a steady size.

Figure 27 illustrates the effect of blood flow at various times. In this graph the temperature at a radius of 2.5 is plotted against time for $\beta = 0.0, 0.1, 0.5$ and 1.0 . At short times the blood flow effect

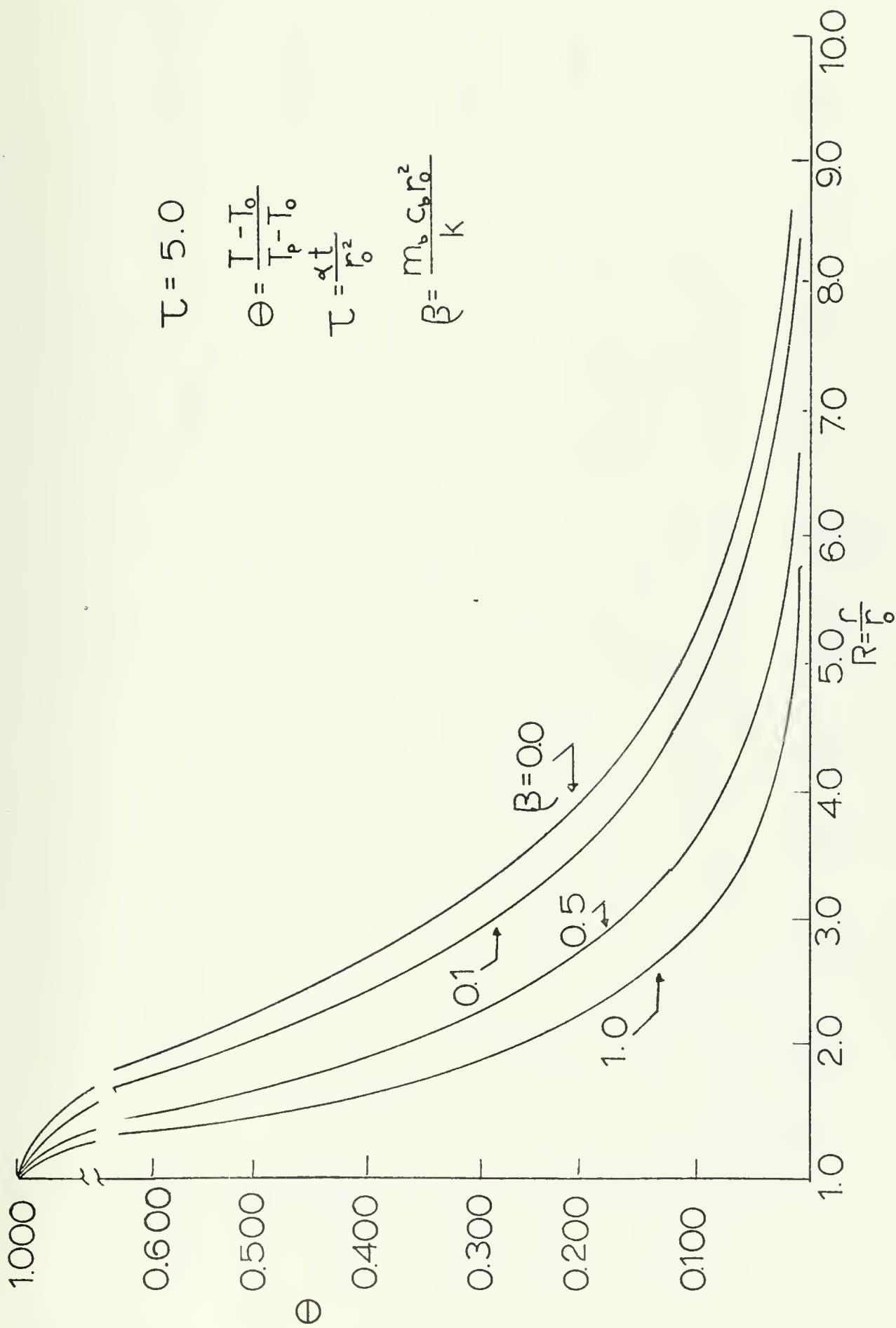


Figure 25. Θ vs. R for $\tau = 5.0$ and $\beta = 0.0, 0.1, 0.5$ and 1.0 .

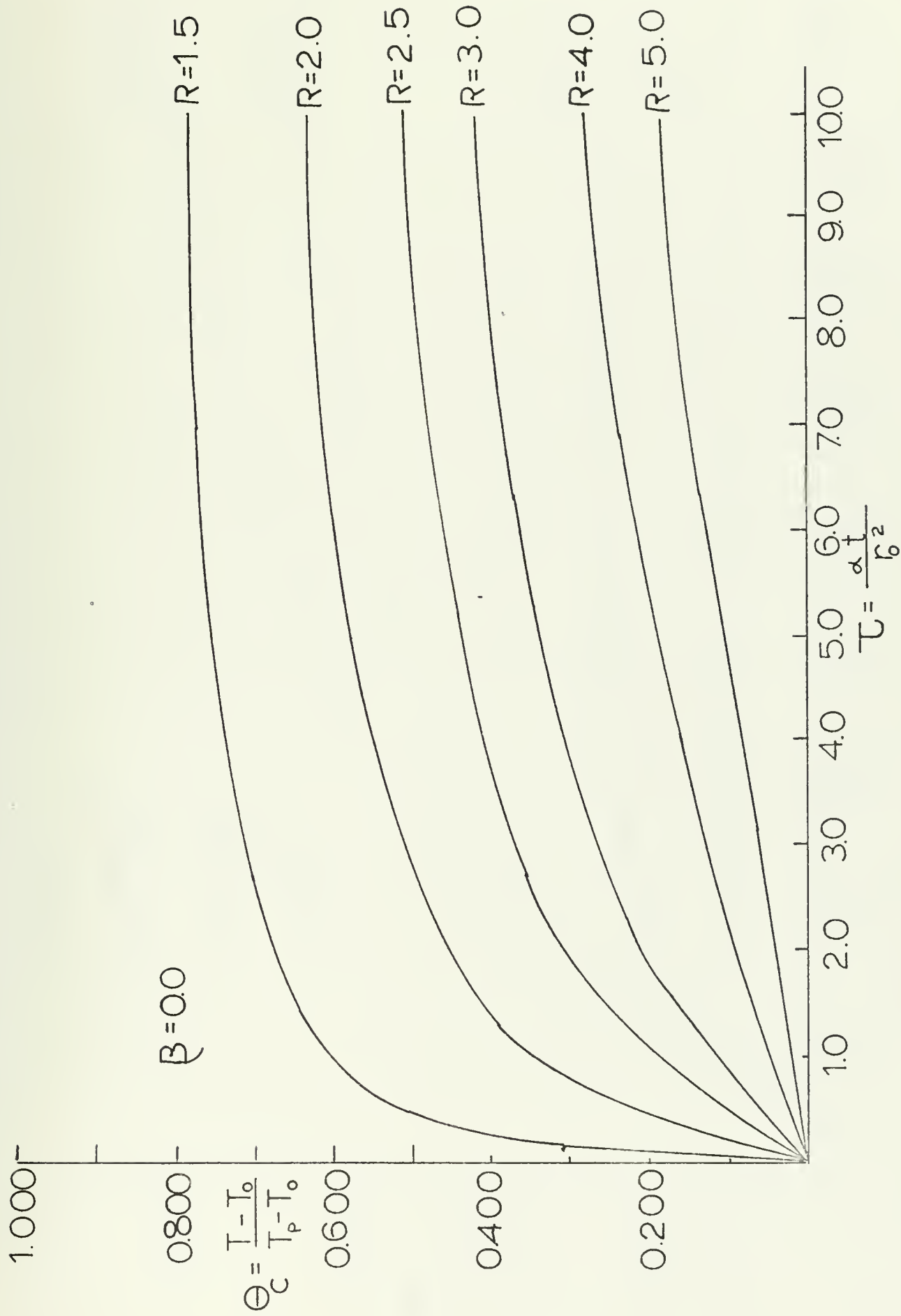


Figure 26. Θ vs τ for Various Values of R and $\beta = 0.0$.

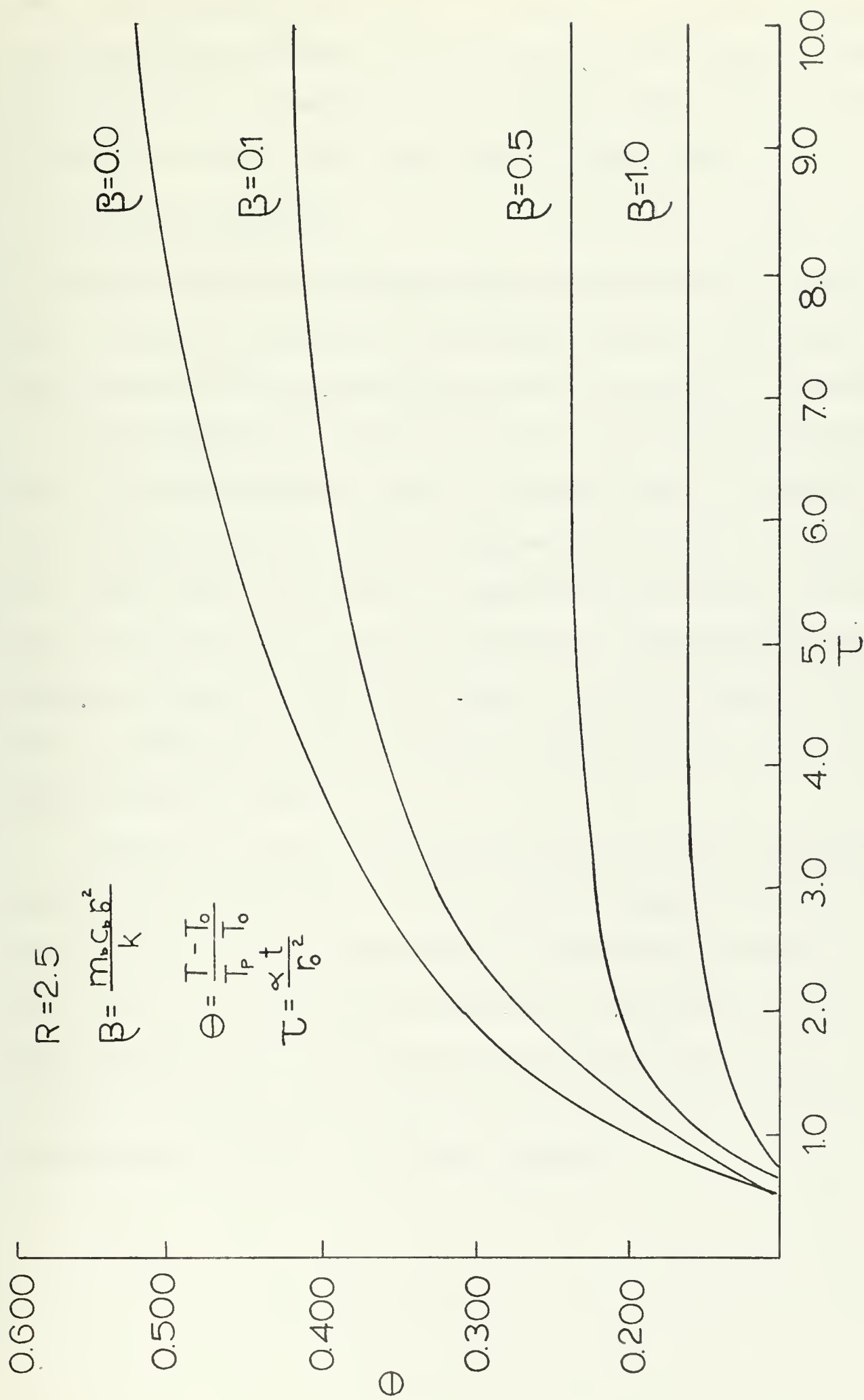


Figure 27. Θ vs τ for various values of β and $R = 2.5$.

seems to be negligible but as time is increased, the effect of blood flow becomes more noticeable. Since the probe radius enters the blood flow parameter as a squared term, the blood flow effect would become an important parameter for a larger probe at longer times.

C. TWO-DIMENSIONAL MODEL

Results for the two-dimensional model are tabulated in Tables XII - XVI. The results are given for various positions along the probe length, where the $X=0$ position corresponds to the midpoint of the probe.

The two-dimensional solution was used to compare the experimental results with the theoretical results. Figure 24 shows the isotherms along the probe length for various nondimensional times. By extending this graph it can be seen that the temperature field around a cylindrical probe has an elliptical shape. The dimensions of the ellipsoid can be changed by varying the length to diameter ratio of the probe. If this ratio is made small enough, the shape of the temperature field will approach that of a sphere.

Figure 28 is a graph of the axial position (X) versus the radial location in the tissue for a nondimensional time equal to five and $\theta_c = 0.300$. The solid lines represent the two-dimensional solution for an L/D of ten, and the dashed line represents the one-dimensional solution. Around the midpoint of the probe, the two solutions are in close agreement. However, as the distance from the mid-point increases, the one-dimensional solution is no longer accurate.

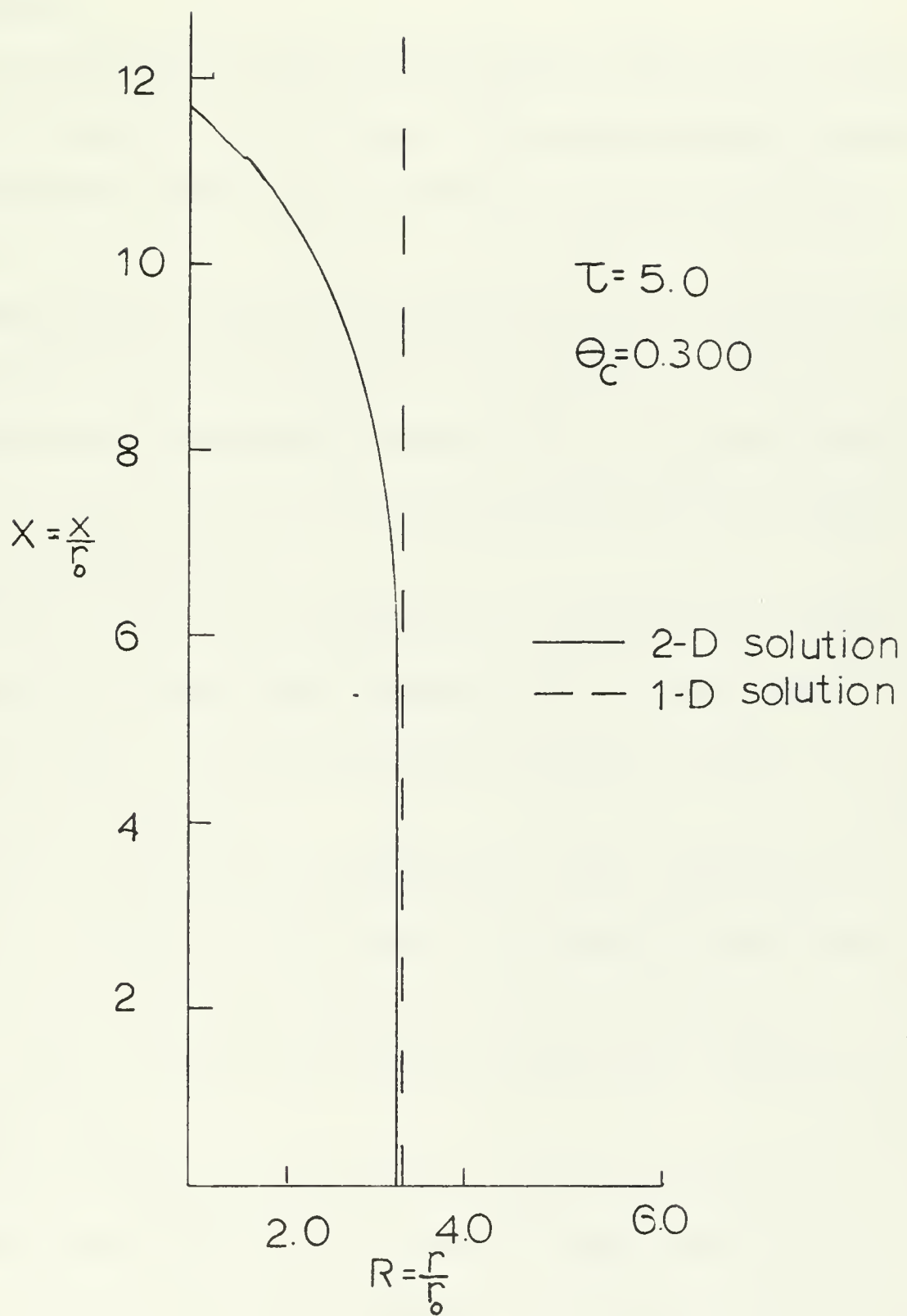


Figure 28. Axial Position (X) vs R for $\tau = 5.0$ and $\theta = 0.300$.

VIII. CONCLUSIONS AND RECOMMENDATIONS

A. CONCLUSIONS

Previous experimental methods used to predict lesion size and shape have generally reduced to trial and error. The usual procedure has been to produce lesions in animals, vary the time and current, and analyze the results.

The theoretical predictions of the temperature field obtained from the two-dimensional heat transfer model of the probe fall well within the error bounds of the experimental results. Thus, it appears possible to analytically predict the size of lesions produced with the constant temperature resistance probe.

Experimental isotherms are reproducible and exhibit sharp delimitation, particularly at short times. The probe itself is safe, easy to construct and simple. The temperature control circuit is small, accurate and easy to operate.

All results are presented in nondimensional form. However, it should be noted that both the experimental and theoretical models are simplified and the results have been verified only over a narrow temperature range and only for a cylindrical probe with a length to diameter ratio of ten.

The blood flow effect is found to be an important parameter in determining the temperature field in tissue if a large probe is used. For very small probes, the effect is marginal. Including the effect of blood tends to slightly decrease the temperature throughout the field and a steady state or equilibrium is reached at an earlier time than if blood flow is neglected. As time is increased, the effect of blood

flow becomes more predominant. Thus, if heat is applied for any substantial period of time, the effect of blood flow is felt more strongly.

B. RECOMMENDATIONS

It is recommended that additional experimental work be carried out with the heating probe over higher temperature ranges and with various probe dimensions and L/D ratios.

As mentioned previously, problems were encountered in attempting to place the liquid crystal tape uniformly along the axis of the probe. Accurate axial isotherms were therefore not obtained in the present set of experiments. Further investigation is needed on this aspect of the experiment.

It is also recommended that a technique for automatically controlling the probe surface temperature be developed. Two highly desirable features of such a control system would be: 1) an ability to select a range of probe surface temperatures, and 2) an ability to pre-select the duration of the heating period. These two features, together with the analytical model, will allow a more accurate prediction of lesion size.

APPENDIX A: ONE-DIMENSIONAL MODEL SOLUTION

Statement of Problem:

A cylindrical probe of radius r_0 is embedded in tissue which is initially at a uniform temperature T_0 . Within the tissue there is a volumetric heat generation due to metabolism of strength S_m . In addition, there is blood flow in the medium with a flowrate m_b , specific heat c_b and temperature T_b . Assume that the length to diameter ratio of the probe is large enough so that end effects may be neglected and assume the tissue is homogeneous and infinite in extent. The probe is at a constant temperature T_p . Also, assume that at an infinite distance from the probe, no temperature change occurs. Solve for the tissue temperature assuming constant properties and one dimensional radial heat flow. -

Notation:

<u>Symbol</u>	<u>Description</u>	<u>Typical Units</u>
α	Tissue thermal diffusivity	cm^2/sec
c	Tissue specific heat	$\text{cal}/\text{gm}/^\circ\text{C}$
c_b	Blood specific heat	$\text{cal}/\text{gm}/^\circ\text{C}$
k	Thermal conductivity of tissue	$\text{cal}/\text{cm}/\text{sec}/^\circ\text{C}$
m_b	Volumetric blood flowrate	$\text{gm}/\text{cm}^3/\text{sec}$
r	Radial location in tissue	cm
r_0	Probe radius	cm
S_m	Metabolic heat generation rate	$\text{cal}/\text{cm}^3/\text{sec}$
t	Time	sec
T	Tissue temperature	$^\circ\text{C}$

<u>Symbol</u>	<u>Description</u>	<u>Typical Units</u>
T_b	Arterial temperature	$^{\circ}\text{C}$
T_o	Initial tissue temperature	$^{\circ}\text{C}$
T_p	Probe temperature	$^{\circ}\text{C}$

Nondimensional Groups:

$$\theta = \frac{T - T_o}{T_p - T_o} \quad (\text{temperature})$$

$$R = \frac{r}{r_o} \quad (\text{distance})$$

$$\tau = \frac{\alpha t}{r_o^2} \quad (\text{time})$$

$$\beta = \frac{m_b c_b r_o^2}{k} \quad (\text{blood flow})$$

$$T_o = T_b + \frac{S_m}{m_b c_b} \quad (\text{initial temperature})$$

The general heat conduction equation in cylindrical coordinates is:

$$\frac{k}{r} \frac{\partial}{\partial r} \left(r \frac{\partial T}{\partial r} \right) + m_b c_b (T_b - T) + S_m = \rho c \frac{\partial T}{\partial t} \quad (\text{A.1})$$

Substituting the above nondimensional quantities into equation (A.1) yields:

$$\frac{1}{R} \frac{\partial}{\partial R} \left(R \frac{\partial \theta}{\partial R} \right) - \beta \theta = \frac{\partial \theta}{\partial \tau} \quad (\text{A.2})$$

Equation (A.2) must be solved in order to describe the temperature of the tissue as a function of time. In order to solve the problem, boundary conditions and initial conditions must be stated. They are as follows:

(a) at $r = r_0$, (at the probe surface), $T = T_p$ or, in nondimensional form at $R = 1$, $\theta = 1$,

(b) as $r \rightarrow \infty$, the medium remains unaffected as $r \rightarrow \infty$, $T \rightarrow T_0$ or, in nondimensional form as $R \rightarrow \infty$, $\theta \rightarrow 0$,

(c) at $t = 0$, $T = T_0$ or, in nondimensional form at $\tau = 0$, $\theta = 0$.

By using Laplace Transformations, a closed form solution to equation (A.2) can be obtained:

$$\theta = \frac{K_0 \sqrt{\beta R}}{K_0 \sqrt{\beta}} - \frac{2}{\pi} \int_0^\infty \frac{e^{-\tau u^2} C_0(u, Ru)}{\left(u + \frac{\beta}{u}\right) [Y_0^2(u) + Y_0^2(u)]} du \quad (A.3)$$

$$C_0 = J_0(u) Y_0(uR) - J_0(uR) Y_0(u)$$

If the blood flow term is neglected, equation (A.3) reduces to:

$$\theta = 1 - \frac{2}{\pi} \int_0^\infty \frac{e^{-\tau u^2} C_0(u, Ru) du}{u [J_0^2(u) + Y_0^2(u)]} \quad (A.4)$$

Equation (A.4) is the closed form solution given by Carslaw and Jaeger [5]. This integral has been solved by Jaeger [15].

Solution:

A finite increment technique was used to solve for the temperature field. Equation (A.3) was rewritten in the following form:

$$\theta = \frac{K_0 \left(\frac{\sqrt{\beta R}}{\sqrt{\beta}}\right)}{K_0 \left(\frac{\sqrt{\beta R}}{\sqrt{\beta}}\right)} - \frac{2}{\pi} \int_0^\infty q(u) du \quad (A.5)$$

$$q(u) = \frac{e^{-\tau u^2} C_0(u, Ru)}{\left(u + \frac{\beta}{u}\right) [J_0^2(u) + Y_0^2(u)]}$$

Assume an approximation to the integral can be derived by passing an interpolating function through several adjacent points and then

integrating the interpolating function. Simpson's Rule uses the parabola as an interpolatory function between u_{i-1} , u_i and u_{i+1} where the u_i are evenly spaced values of the interval (u_0, u_n) with a subinterval length $h = u_{i+1} - u_i$. Integrating the parabolic interpolating function gives:

$$\int_{u_{i-1}}^{u_{i+1}} q(u) du \approx \frac{h}{3} [Y_{i-1} + 4Y_i + Y_{i+1}] \quad (A.6)$$

where $Y_i = q(u_i)$

Expanding equation (A.6) over the entire interval yields,

$$\int_0^n q(u) du \approx \frac{h}{3} [Y_0 + 4Y_1 + 2Y_2 + \dots + 4Y_{n-1} + Y_n] \quad (A.7)$$

Computer programs 1, 2 and 3 were used to solve this problem for $\beta = 0.0$. Programs 4, 5, and 6 were used to solve for $\beta = 0.1$. To solve for other values of β only one card must be changed.

Because $q(u)$ is singular at $u = 0$, the lower limit of the integral was taken as 0.001. The error caused by this was assumed to be negligible. By varying the upper limit of the integral between 1.0 and 100.0, it was found that the solution coveredged at approximately 8.0. Therefore, an upper limit of 10.0 was used.

The Y Bessel functions involving the lower limit of the integral, 0.001, were solved using a separate program and calling the BESY subroutine. This was done to avoid underflow and reduce computer time.

The included programs solve the temperature field for times between 0.1 and 1.0 only. To change the time interval only one card must be changed.

Jaeger's results [15] were used as a check on the accuracy of the results obtained from Programs 1, 2 and 3 when $\beta = 0.0$. The greatest difference between the solutions was 0.001.

APPENDIX B: ERROR ANALYSIS OF EXPERIMENTAL RESULTS

Three nondimensional quantities were calculated in analyzing the experimental results.

$$\theta_c = \frac{T_c - T_o}{T_p - T_o} \text{ (critical temperature)}$$

$$R_c = \frac{r_c}{r_o} \text{ (critical radius)}$$

$$\tau = \frac{\alpha t}{r_o^2} \text{ (time)}$$

Ambrosius [1] gives the following equations for the resultant errors (R) in computations involving measurements:

(a) addition

$$(A \pm a) + (B \pm b) \\ R = \pm (a^2 + b^2)^{\frac{1}{2}} \quad (B.1)$$

(b) subtraction

$$(A \pm a) - (B \pm b) \\ R = \pm (a^2 + b^2)^{\frac{1}{2}} \quad (B.2)$$

(c) multiplication

$$(A \pm a) (B \pm b) \\ R = \pm [(Ab)^2 + (Ba)^2]^{\frac{1}{2}} \quad (B.3)$$

(d) division

$$(B \pm b) / (A \pm a) \\ R = \pm \left[\frac{(Ba/A)^2 + (b)^2}{(A)^2} \right]^{\frac{1}{2}} \quad (B.4)$$

where A and B are two measurements and an error of $\pm a$ is made in the measurement of A and an error of $\pm b$ is made in the measurement of B

The following errors were estimated for the variables in θ_c :

$$T_c = \pm 0.1^\circ\text{C}$$

$$T_o = \pm 0.3^\circ\text{C}$$

$$T_p = \pm 0.2^\circ\text{C}$$

An examination of θ_c along with equation (B.4) indicates that the largest error in θ_c occurs when T_o is the greatest, or when the quantity $T_c - T_o$ is the smallest. The highest value of T_o was in test run 10. The resultant errors will now be estimated using data from run 10.

$$T_o = 25.2^\circ\text{C} \pm 0.3^\circ\text{C}$$

$$T_c = 29.9^\circ\text{C} \pm 0.1^\circ\text{C}$$

$$T_p = 48.5^\circ\text{C} \pm 0.2^\circ\text{C}$$

$$T_c - T_o = 4.7^\circ\text{C}$$

$$T_p - T_o = 18.6^\circ\text{C}$$

Substituting these values into equation (B.2), the following errors are obtained:

$$T_c - T_o = \pm 0.32^\circ\text{C}$$

$$T_p - T_o = \pm 0.36^\circ\text{C}$$

From equation (B.4) the resultant error in θ_c is:

$$R = \pm 0.025$$

or, the percentage error in $\theta_c = 12.5\%$. This error would be reduced if a higher probe temperature (T_p) or a higher critical temperature (T_c) were used.

An analysis of the error in computing R_c and τ is more difficult since the variables in these quantities change with time. It was estimated that at short times the error in both R_c and τ could be of the order of 10%. However, this error decreases significantly as time is increased.

TABLE II

VALUES OF Θ FOR NONDIMENSIONAL TIME (τ) AND NONDIMENSIONAL LOCATION (R), ONE-DIMENSIONAL MODEL.

$\tau=0.1 \rightarrow 0.9$
 $R=1.0 \rightarrow 10.0$
 $\Theta=0.0$

τ	0.1	0.2	0.3	0.4	0.5	0.6	0.7	0.8	0.9
R									
1.0	1.000	1.000	1.000	1.000	1.000	1.000	1.000	1.000	1.000
1.2	0.601	0.691	0.733	0.758	0.776	0.789	0.800	0.808	0.815
1.4	0.316	0.450	0.519	0.562	0.592	0.615	0.634	0.648	0.661
1.6	0.143	0.274	0.352	0.405	0.443	0.472	0.496	0.515	0.532
1.8	0.055	0.156	0.229	0.282	0.323	0.356	0.382	0.405	0.424
2.0	0.018	0.082	0.142	0.190	0.230	0.263	0.290	0.313	0.333
2.2	0.005	0.039	0.083	0.124	0.159	0.189	0.216	0.239	0.259
2.4	0.001	0.017	0.046	0.077	0.107	0.134	0.158	0.179	0.199
2.6	0.000	0.007	0.024	0.047	0.070	0.092	0.113	0.132	0.150
2.8		0.002	0.012	0.027	0.044	0.062	0.079	0.096	0.111
3.0		0.001	0.006	0.015	0.027	0.040	0.054	0.068	0.081
3.2		0.000	0.002	0.008	0.016	0.025	0.036	0.047	0.058
3.4			0.001	0.004	0.009	0.016	0.024	0.032	0.041
3.6			0.000	0.002	0.005	0.009	0.015	0.021	0.029
3.8				0.001	0.002	0.005	0.009	0.014	0.019
4.0				0.000	0.001	0.003	0.006	0.009	0.013
5.0					0.000	0.000	0.000	0.001	0.001
6.0								0.000	0.000
7.0									
8.0									
9.0									
10.0									

TABLE III

VALUES OF Θ FOR NONDIMENSIONAL TIME (τ) AND NONDIMENSIONAL LOCATION (R), ONE-DIMENSIONAL MODEL.

$\tau = 1.0 \rightarrow 9.0$
 $R = 1.0 \rightarrow 10.0$
 $\beta = 0.0$

τ	1.0	2.0	3.0	4.0	5.0	6.0	7.0	8.0	9.0
R									
1.2	0.821	0.854	0.869	0.879	0.885	0.890	0.894	0.898	0.900
1.4	0.672	0.732	0.766	0.777	0.789	0.798	0.805	0.811	0.816
1.6	0.546	0.627	0.665	0.689	0.706	0.718	0.728	0.736	0.743
1.8	0.440	0.536	0.583	0.612	0.633	0.648	0.661	0.671	0.679
2.0	0.351	0.458	0.511	0.544	0.568	0.586	0.601	0.612	0.632
2.2	0.277	0.389	0.447	0.484	0.510	0.531	0.547	0.560	0.571
2.4	0.216	0.330	0.390	0.430	0.459	0.481	0.498	0.513	0.525
2.6	0.166	0.278	0.340	0.382	0.412	0.435	0.454	0.470	0.483
2.8	0.126	0.233	0.296	0.338	0.370	0.394	0.414	0.430	0.444
3.0	0.094	0.194	0.256	0.299	0.332	0.357	0.377	0.394	0.409
3.2	0.069	0.161	0.221	0.264	0.297	0.322	0.344	0.361	0.377
3.4	0.050	0.132	0.190	0.233	0.265	0.292	0.313	0.331	0.347
3.6	0.036	0.108	0.163	0.205	0.237	0.263	0.285	0.303	0.319
3.8	0.025	0.088	0.139	0.179	0.211	0.237	0.259	0.277	0.292
4.0	0.017	0.071	0.118	0.157	0.188	0.213	0.235	0.253	0.269
5.0	0.002	0.021	0.049	0.076	0.101	0.122	0.142	0.159	0.174
6.0	0.000	0.005	0.018	0.034	0.051	0.067	0.082	0.096	0.110
7.0		0.001	0.005	0.013	0.023	0.034	0.045	0.056	0.067
8.0		0.000	0.001	0.005	0.010	0.016	0.024	0.031	0.039
9.0			0.000	0.001	0.004	0.007	0.012	0.016	0.022
10.0				0.000	0.001	0.003	0.005	0.008	0.012

TABLE IV

VALUES OF Θ FOR NONDIMENSIONAL TIME(τ) AND
NONDIMENSIONAL LOCATION(R), ONE-DIMENSIONAL
MODEL.

$\tau = 10.0 \rightarrow 100.0$
 $R = 1.0 \rightarrow 10.0$
 $\Theta = 0.0$

τ	10.0	20.0	30.0	40.0	50.0	70.0	100.0
R							
1.0	1.000	1.000	1.000	1.000	1.000	1.000	1.000
1.2	0.903	0.916	0.922	0.926	0.929	0.933	0.937
1.4	0.820	0.845	0.857	0.864	0.869	0.877	0.884
1.6	0.749	0.783	0.800	0.810	0.818	0.828	0.838
1.8	0.687	0.729	0.750	0.763	0.772	0.785	0.797
2.0	0.631	0.681	0.705	0.720	0.731	0.746	0.760
2.2	0.581	0.637	0.664	0.682	0.694	0.711	0.728
2.4	0.536	0.597	0.628	0.647	0.660	0.679	0.698
2.6	0.494	0.561	0.594	0.615	0.629	0.650	0.670
2.8	0.457	0.529	0.563	0.595	0.601	0.623	0.644
3.0	0.422	0.497	0.534	0.557	0.574	0.598	0.621
3.2	0.390	0.468	0.507	0.532	0.550	0.575	0.598
3.4	0.360	0.441	0.482	0.508	0.526	0.553	0.578
3.6	0.333	0.416	0.458	0.485	0.505	0.532	0.558
3.8	0.307	0.392	0.436	0.464	0.484	0.512	0.539
4.0	0.283	0.370	0.415	0.444	0.465	0.494	0.522
5.0	0.188	0.277	0.325	0.358	0.381	0.414	0.446
6.0	0.122	0.207	0.256	0.290	0.315	0.350	0.385
7.0	0.077	0.153	0.201	0.235	0.260	0.297	0.334
8.0	0.047	0.112	0.157	0.190	0.216	0.253	0.291
9.0	0.027	0.081	0.122	0.153	0.178	0.215	0.254
10.0	0.015	0.057	0.094	0.123	0.147	0.183	0.222
20.0	0.000	0.001	0.003	0.009	0.016	0.031	0.053
30.0		0.000	0.000	0.000	0.001	0.003	0.010
40.0					0.000	0.000	0.002
50.0							0.000

TABLE V

VALUES OF Θ FOR NONDIMENSIONAL TIME (τ) AND NONDIMENSIONAL LOCATION (R), ONE-DIMENSIONAL MODEL.

$\tau = 0.1 \rightarrow 0.9$
 $R = 1.0 \rightarrow 10.0$
 $\Theta = 0.1$

τ	0.1	0.2	0.3	0.4	0.5	0.6	0.7	0.8	0.9
R									
1.0	1.000	1.000	1.000	1.000	1.000	1.000	1.000	1.000	1.000
1.2	0.599	0.688	0.729	0.754	0.770	0.783	0.793	0.800	0.807
1.4	0.314	0.447	0.514	0.555	0.584	0.606	0.623	0.637	0.649
1.6	0.142	0.272	0.348	0.398	0.435	0.463	0.485	0.503	0.518
1.8	0.055	0.154	0.225	0.277	0.316	0.347	0.372	0.392	0.410
2.0	0.018	0.081	0.139	0.186	0.224	0.255	0.281	0.302	0.321
2.2	0.005	0.039	0.082	0.121	0.155	0.183	0.208	0.229	0.248
2.4	0.001	0.017	0.046	0.076	0.104	0.129	0.151	0.171	0.189
2.6	0.000	0.007	0.024	0.045	0.067	0.089	0.108	0.126	0.142
2.8		0.003	0.012	0.026	0.043	0.059	0.076	0.091	0.105
3.0		0.001	0.006	0.014	0.026	0.039	0.052	0.064	0.077
3.2		0.000	0.002	0.008	0.015	0.025	0.035	0.045	0.055
3.4			0.001	0.004	0.009	0.015	0.023	0.031	0.039
3.6			0.000	0.002	0.005	0.009	0.014	0.020	0.027
3.8				0.001	0.003	0.005	0.009	0.013	0.018
4.0				0.000	0.001	0.003	0.005	0.009	0.012
5.0					0.000	0.000	0.000	0.001	0.001
6.0								0.000	0.000
7.0									
8.0									
9.0									
10.0									

TABLE VI

VALUES OF Θ FOR NONDIMENSIONAL TIME (τ) AND NONDIMENSIONAL LOCATION (R), ONE-DIMENSIONAL MODEL.

$\tau = 1.0 \rightarrow 9.0$
 $R = 1.0 \rightarrow 10.0$
 $\beta = 0.1$

τ	1.0	2.0	3.0	4.0	5.0	6.0	7.0	8.0	9.0
R									
1.0	1.0000	1.0000	1.0000	1.0000	1.0000	1.0000	1.0000	1.0000	1.0000
1.2	0.812	0.841	0.853	0.860	0.864	0.867	0.869	0.870	0.872
1.4	0.658	0.710	0.732	0.744	0.752	0.757	0.761	0.764	0.766
1.6	0.531	0.601	0.631	0.648	0.658	0.666	0.671	0.675	0.678
1.8	0.425	0.508	0.545	0.565	0.579	0.588	0.594	0.599	0.603
2.0	0.337	0.429	0.471	0.494	0.510	0.520	0.528	0.533	0.538
2.2	0.265	0.362	0.407	0.433	0.450	0.462	0.470	0.476	0.481
2.4	0.205	0.304	0.351	0.379	0.397	0.410	0.419	0.426	0.432
2.6	0.157	0.254	0.303	0.332	0.351	0.365	0.375	0.382	0.388
2.8	0.119	0.211	0.260	0.291	0.311	0.325	0.335	0.343	0.349
3.0	0.089	0.175	0.224	0.254	0.275	0.289	0.300	0.308	0.314
3.2	0.065	0.144	0.191	0.222	0.243	0.257	0.269	0.277	0.283
3.4	0.047	0.118	0.163	0.193	0.214	0.229	0.240	0.256	
3.6	0.034	0.096	0.139	0.168	0.189	0.204	0.215	0.224	0.231
3.8	0.024	0.077	0.118	0.146	0.168	0.181	0.193	0.201	0.208
4.0	0.016	0.062	0.099	0.126	0.146	0.161	0.172	0.181	0.188
5.0	0.002	0.019	0.040	0.059	0.075	0.088	0.098	0.106	0.112
6.0	0.000	0.005	0.014	0.026	0.036	0.046	0.054	0.061	0.066
7.0		0.001	0.005	0.010	0.017	0.023	0.029	0.034	0.038
8.0		0.000	0.001	0.004	0.007	0.011	0.015	0.018	0.021
9.0			0.000	0.001	0.003	0.005	0.007	0.009	0.012
10.0				0.000	0.001	0.002	0.003	0.005	0.006

TABLE VII

VALUES OF Θ FOR NONDIMENSIONAL TIME (τ) AND
NONDIMENSIONAL LOCATION (R), ONE-DIMENSIONAL
MODEL.

$\tau=10.0 \rightarrow 100.0$
 $R=1.0 \rightarrow 50.0$
 $\Theta=0.1$

τ	10.0	20.0	30.0	40.0	50.0	70.0	100.0
R							
1.0	1.000	1.000	1.000	1.000	1.000	1.000	1.000
1.2	0.872	0.876	0.876	0.876	0.876	0.877	0.877
1.4	0.768	0.774	0.775	0.775	0.775	0.775	0.775
1.6	0.680	0.689	0.690	0.690	0.691	0.691	0.691
1.8	0.605	0.616	0.618	0.618	0.618	0.618	0.618
2.0	0.541	0.553	0.556	0.556	0.556	0.556	0.556
2.2	0.485	0.499	0.501	0.502	0.502	0.502	0.502
2.4	0.436	0.451	0.454	0.454	0.455	0.455	0.455
2.6	0.392	0.409	0.412	0.413	0.413	0.413	0.413
2.8	0.354	0.371	0.375	0.375	0.375	0.376	0.376
3.0	0.319	0.338	0.341	0.342	0.342	0.342	0.342
3.2	0.288	0.308	0.311	0.312	0.312	0.313	0.313
3.4	0.261	0.281	0.285	0.286	0.286	0.286	0.286
3.6	0.236	0.257	0.261	0.261	0.262	0.262	0.262
3.8	0.214	0.235	0.239	0.240	0.240	0.240	0.240
4.0	0.193	0.215	0.219	0.220	0.220	0.220	0.220
5.0	0.118	0.140	0.144	0.145	0.145	0.145	0.145
6.0	0.071	0.092	0.096	0.097	0.097	0.098	0.098
7.0	0.042	0.061	0.065	0.066	0.066	0.066	0.066
8.0	0.024	0.040	0.044	0.045	0.045	0.045	0.045
9.0	0.014	0.026	0.030	0.031	0.031	0.031	0.031
10.0	0.007	0.017	0.020	0.021	0.022	0.022	0.022
20.0	0.000	0.000	0.000	0.001	0.001	0.001	0.001
30.0				0.000	0.000	0.000	0.000
40.0							
50.0							

TABLE VIII

VALUES OF Θ FOR NONDIMENSIONAL TIME (τ) AND NONDIMENSIONAL LOCATION (R), ONE-DIMENSIONAL MODEL.

$\tau=0.1 \rightarrow 0.9$
 $R=1.0 \rightarrow 10.0$
 $\Theta=0.5$

τ	0.1	0.2	0.3	0.4	0.5	0.6	0.7	0.8	0.9
R									
1.0	1.000	1.000	1.000	1.000	1.000	1.000	1.000	1.000	1.000
1.2	0.592	0.676	0.713	0.735	0.749	0.759	0.766	0.772	0.777
1.4	0.308	0.433	0.494	0.530	0.555	0.572	0.585	0.596	0.604
1.6	0.139	0.261	0.330	0.374	0.404	0.427	0.444	0.457	0.468
1.8	0.053	0.147	0.211	0.256	0.289	0.314	0.333	0.348	0.361
2.0	0.017	0.076	0.129	0.170	0.202	0.227	0.247	0.263	0.276
2.2	0.005	0.037	0.075	0.110	0.138	0.161	0.180	0.196	0.209
2.4	0.001	0.016	0.042	0.068	0.091	0.112	0.129	0.144	0.157
2.6	0.000	0.007	0.022	0.041	0.059	0.076	0.091	0.104	0.116
2.8		0.002	0.011	0.023	0.037	0.050	0.063	0.074	0.085
3.0		0.001	0.005	0.013	0.022	0.033	0.043	0.052	0.061
3.2		0.000	0.002	0.007	0.013	0.021	0.028	0.036	0.043
3.4			0.001	0.003	0.007	0.013	0.018	0.024	0.030
3.6			0.000	0.002	0.004	0.008	0.012	0.016	0.021
3.8				0.001	0.002	0.004	0.007	0.010	0.014
4.0				0.000	0.001	0.002	0.004	0.007	0.009
5.0					0.000	0.000	0.000	0.001	0.001
6.0								0.000	0.000
7.0									
8.0									
9.0									
10.0									

TABLE IX

VALUES OF Θ FOR NONDIMENSIONAL TIME (τ) AND NONDIMENSIONAL LOCATION (R), ONE-DIMENSIONAL MODEL.

$\tau = 1.0 \rightarrow 9.0$
 $R = 1.0 \rightarrow 10.0$
 $\beta = 0.5$

τ	1.0	2.0	3.0	4.0	5.0	6.0	7.0	8.0	9.0
R									
1.0	1.000	1.000	1.000	1.000	1.000	1.000	1.000	1.000	1.000
1.2	0.780	0.797	0.801	0.803	0.804	0.804	0.804	0.834	0.804
1.4	0.610	0.640	0.648	0.652	0.653	0.653	0.654	0.654	0.654
1.6	0.477	0.517	0.528	0.532	0.534	0.535	0.536	0.536	0.536
1.8	0.371	0.419	0.432	0.438	0.440	0.441	0.441	0.442	0.442
2.0	0.287	0.340	0.355	0.361	0.364	0.365	0.366	0.366	0.366
2.2	0.220	0.276	0.293	0.299	0.302	0.302	0.304	0.304	0.304
2.4	0.167	0.223	0.241	0.248	0.251	0.253	0.254	0.254	0.254
2.6	0.126	0.181	0.199	0.207	0.210	0.211	0.212	0.213	0.213
2.8	0.094	0.146	0.165	0.172	0.176	0.177	0.178	0.178	0.179
3.0	0.069	0.118	0.136	0.144	0.147	0.149	0.149	0.150	0.150
3.2	0.050	0.094	0.112	0.120	0.123	0.125	0.126	0.126	0.126
3.4	0.036	0.075	0.092	0.100	0.104	0.105	0.106	0.106	0.107
3.6	0.025	0.060	0.078	0.083	0.087	0.089	0.090	0.090	0.090
3.8	0.018	0.047	0.063	0.070	0.073	0.075	0.076	0.076	0.076
4.0	0.017	0.037	0.051	0.058	0.061	0.063	0.064	0.064	0.065
5.0	0.001	0.010	0.018	0.023	0.026	0.027	0.028	0.028	0.029
6.0	0.000	0.002	0.006	0.009	0.011	0.012	0.012	0.012	0.013
7.0		0.000	0.002	0.003	0.004	0.005	0.005	0.006	0.006
8.0			0.000	0.001	0.002	0.002	0.002	0.002	0.003
9.0				0.000	0.001	0.001	0.001	0.001	0.001
10.0					0.000	0.000	0.000	0.000	0.001

TABLE X

VALUES OF Θ FOR NONDIMENSIONAL TIME (τ) AND NONDIMENSIONAL LOCATION (R), ONE-DIMENSIONAL MODEL.

$\tau = 0.1 \rightarrow 0.9$
 $R = 1.0 \rightarrow 10.0$
 $\Theta = 1.0$

τ	0.1	0.2	0.3	0.4	0.5	0.6	0.7	0.8	0.9
R									
1.0	1.000	1.000	1.000	1.000	1.000	1.000	1.000	1.000	1.000
1.2	0.583	0.662	0.695	0.713	0.724	0.732	0.737	0.741	0.744
1.4	0.301	0.417	0.471	0.501	0.521	0.534	0.544	0.551	0.556
1.6	0.135	0.248	0.309	0.346	0.370	0.388	0.400	0.409	0.416
1.8	0.052	0.138	0.195	0.233	0.259	0.278	0.292	0.303	0.311
2.0	0.017	0.071	0.118	0.153	0.178	0.197	0.211	0.222	0.231
2.2	0.005	0.034	0.068	0.097	0.120	0.137	0.151	0.162	0.170
2.4	0.001	0.015	0.038	0.059	0.078	0.094	0.106	0.116	0.125
2.6	0.000	0.006	0.020	0.035	0.050	0.063	0.074	0.083	0.090
2.8		0.002	0.010	0.020	0.031	0.041	0.050	0.058	0.065
3.0		0.001	0.005	0.011	0.019	0.026	0.034	0.040	0.046
3.2		0.000	0.002	0.006	0.011	0.018	0.022	0.027	0.032
3.4			0.001	0.003	0.006	0.010	0.014	0.018	0.022
3.6			0.000	0.001	0.003	0.006	0.009	0.012	0.015
3.8				0.001	0.002	0.003	0.005	0.008	0.010
4.0				0.000	0.001	0.002	0.003	0.005	0.007
5.0					0.000	0.000	0.000	0.000	0.001
6.0									0.000
7.0									
8.0									
9.0									
10.0									

TABLE XI

VALUES OF Θ FOR NONDIMENSIONAL TIME (τ) AND NONDIMENSIONAL LOCATION (R), ONE-DIMENSIONAL MODEL.

$\tau=1.0$ 9.0
 $R=1.0$ 10.0
 $\Theta=1.0$

τ	1.0	2.0	3.0	4.0	5.0	6.0	7.0	8.0	9.0
R									
1.0	1.000	1.000	1.000	1.000	1.000	1.000	1.000	1.000	1.000
1.2	0.746	0.755	0.756	0.756	0.756	0.756	0.757	0.757	0.757
1.4	0.560	0.575	0.578	0.579	0.579	0.579	0.579	0.579	0.579
1.6	0.422	0.422	0.445	0.446	0.446	0.446	0.446	0.446	0.446
1.8	0.317	0.341	0.345	0.346	0.347	0.347	0.347	0.347	0.347
2.0	0.238	0.264	0.269	0.270	0.270	0.270	0.271	0.271	0.271
2.2	0.177	0.205	0.210	0.212	0.212	0.212	0.212	0.212	0.212
2.4	0.132	0.160	0.166	0.167	0.167	0.167	0.167	0.167	0.167
2.6	0.097	0.124	0.130	0.131	0.131	0.131	0.132	0.132	0.132
2.8	0.071	0.097	0.102	0.104	0.104	0.104	0.104	0.104	0.104
3.0	0.051	0.075	0.081	0.082	0.082	0.082	0.082	0.083	0.083
3.2	0.036	0.058	0.064	0.065	0.065	0.065	0.065	0.066	0.066
3.4	0.026	0.045	0.050	0.052	0.052	0.052	0.052	0.052	0.052
3.6	0.018	0.035	0.040	0.041	0.041	0.041	0.042	0.042	0.042
3.8	0.012	0.027	0.031	0.033	0.033	0.033	0.033	0.033	0.033
4.0	0.008	0.021	0.025	0.026	0.026	0.026	0.026	0.027	0.027
5.0	0.001	0.005	0.007	0.008	0.009	0.009	0.009	0.009	0.009
6.0	0.000	0.001	0.002	0.003	0.003	0.003	0.003	0.003	0.003
7.0		0.000	0.001	0.001	0.001	0.001	0.001	0.001	0.001
8.0			0.000	0.000	0.000	0.000	0.000	0.000	0.000
9.0									
10.0									

TABLE XII

VALUES OF Θ FOR NONDIMENSIONAL TIME (τ) AND NONDIMENSIONAL LOCATION (R), TWO-DIMENSIONAL MODEL (TRUMP SOLUTION)

$\tau=0.5 \rightarrow 50.0$
 $R=1.0 \rightarrow 30.0$
 $\Theta=0.0$
 $X=1R$

τ	0.5	1.0	3.0	5.0	10.0	20.0	50.0	100.0
R								
1.5	0.492	0.583	0.696	0.741	0.775	0.791	0.803	0.830
2.0	0.216	0.330	0.497	0.568	0.622	0.650	0.671	0.723
2.5	0.082	0.176	0.355	0.440	0.513	0.550	0.576	0.633
3.0	0.027	0.087	0.249	0.339	0.420	0.464	0.499	0.573
3.5	0.008	0.039	0.170	0.258	0.353	0.403	0.440	0.512
4.0	0.002	0.016	0.113	0.194	0.286	0.344	0.390	0.470
4.5	0.000	0.006	0.074	0.142	0.241	0.305	0.350	0.425
5.0		0.002	0.048	0.105	0.193	0.264	0.316	0.392
6.0		0.000	0.017	0.050	0.123	0.202	0.258	0.327
7.0			0.005	0.022	0.077	0.152	0.214	0.278
8.0			0.002	0.010	0.048	0.117	0.179	0.238
10.0			0.000	0.002	0.017	0.065	0.125	0.174
14.0				0.000	0.002	0.015	0.055	0.092
20.0					0.000	0.001	0.013	0.035
30.0						0.000	0.001	0.006

TABLE XIII

VALUES OF Θ FOR NONDIMENSIONAL TIME (τ) AND NONDIMENSIONAL LOCATION (R), TWO-DIMENSIONAL MODEL (TRUMP SOLUTION)

$R=1.0$ 30.0
 $\tau=0.5$ 50.0
 $\Theta=0.0$
 $X=5R$

τ	0.5	1.0	3.0	5.0	10.0	20.0	50.0	100.0
R								
1.5	0.491	0.582	0.695	0.739	0.770	0.786	0.796	0.819
2.0	0.216	0.330	0.496	0.566	0.617	0.643	0.661	0.699
2.5	0.083	0.176	0.354	0.438	0.506	0.539	0.563	0.611
3.0	0.028	0.087	0.247	0.337	0.413	0.453	0.486	0.541
3.5	0.008	0.040	0.170	0.256	0.343	0.388	0.424	0.485
4.0	0.002	0.016	0.112	0.192	0.280	0.332	0.374	0.437
4.5	0.000	0.008	0.073	0.072	0.141	0.232	0.290	0.332
5.0		0.003	0.047	0.103	0.188	0.251	0.297	0.361
6.0		0.000	0.017	0.049	0.119	0.188	0.239	0.300
7.0			0.005	0.021	0.073	0.141	0.196	0.253
8.0			0.002	0.009	0.045	0.107	0.163	0.217
10.0			0.000	0.002	0.015	0.057	0.112	0.158
14.0				0.000	0.001	0.013	0.047	0.084
20.0					0.000	0.001	0.011	0.032
30.0						0.000	0.001	0.006

TABLE XIV

VALUES OF Θ FOR NONDIMENSIONAL TIME(τ) AND NONDIMENSIONAL LOCATION(R), TWO-DIMENSIONAL MODEL (TRUMP SOLUTION)

$\tau=0.5 \rightarrow 50.0$
 $R=1.0 \rightarrow 30.0$
 $Q=0.0$
 $X=8.5R$

τ	0.5	1.0	3.0	5.0	10.0	20.0	50.0	100.0
R								
1.5	0.485	0.569	0.664	0.700	0.724	0.736	0.745	0.772
2.0	0.211	0.315	0.455	0.512	0.552	0.573	0.588	0.623
2.5	0.080	0.165	0.313	0.380	0.431	0.456	0.477	0.531
3.0	0.027	0.080	0.213	0.284	0.345	0.376	0.400	0.450
3.5	0.008	0.036	0.142	0.211	0.274	0.310	0.339	0.403
4.0	0.002	0.015	0.093	0.155	0.224	0.264	0.295	0.350
4.5	0.000	0.006	0.060	0.112	0.179	0.223	0.258	0.322
5.0		0.002	0.038	0.081	0.145	0.195	0.231	0.286
6.0		0.000	0.013	0.037	0.088	0.143	0.184	0.241
7.0			0.004	0.015	0.053	0.107	0.150	0.201
8.0			0.001	0.006	0.032	0.081	0.124	0.174
10.0			0.000	0.001	0.010	0.044	0.085	0.128
14.0				0.000	0.002	0.017	0.042	0.073
20.0					0.000	0.001	0.007	0.027
30.0						0.000	0.000	0.004

TABLE XV

VALUES OF Θ FOR NONDIMENSIONAL TIME (τ) AND NONDIMENSIONAL LOCATION (R), TWO-DIMENSIONAL MODEL (TRUMP SOLUTION)

$\tau = 0.5 \rightarrow 50.0$
 $R = 1.0 \rightarrow 30.0$
 $\phi = 0.0$
 $X = 11.5R$

τ	0.5	1.0	3.0	5.0	10.0	20.0	50.0	100.0
R								
1.5	0.010	0.029	0.094	0.137	0.183	0.223	0.241	0.293
2.0	0.006	0.022	0.083	0.124	0.172	0.214	0.231	0.277
2.5	0.003	0.014	0.066	0.106	0.153	0.193	0.214	0.266
3.0	0.001	0.008	0.050	0.086	0.134	0.178	0.197	0.245
4.0		0.002	0.024	0.051	0.095	0.142	0.165	0.212
4.5		0.001	0.016	0.037	0.075	0.125	0.150	0.199
5.0		0.000	0.010	0.027	0.064	0.111	0.138	0.184
6.0			0.004	0.012	0.040	0.084	0.118	0.160
7.0			0.001	0.005	0.024	0.055	0.098	0.140
8.0			0.000	0.002	0.014	0.049	0.083	0.123
10.0				0.000	0.004	0.027	0.058	0.095
14.0					0.000	0.007	0.027	0.061
20.0						0.001	0.004	0.022
30.0						0.000	0.000	0.003

TABLE XVI

VALUES OF Θ FOR NONDIMENSIONAL TIME (τ) AND NONDIMENSIONAL LOCATION (R), TWO-DIMENSIONAL MODEL (TRUMP SOLUTION)

$\tau = 0.5 \rightarrow 50.0$
 $R = 1.0 \rightarrow 30.0$
 $Q = 0.0$
 $X = 13.5R$

τ	0.5	1.0	3.0	5.0	10.0	20.0	50.0	100.0
R								
1.5	0.000	0.001	0.013	0.030	0.060	0.102	0.118	0.166
2.0		0.000	0.012	0.027	0.058	0.101	0.116	0.156
2.5			0.010	0.024	0.053	0.095	0.112	0.158
3.0			0.008	0.020	0.048	0.090	0.108	0.147
3.5			0.006	0.016	0.042	0.083	0.102	0.146
4.0			0.004	0.012	0.036	0.077	0.097	0.136
4.5			0.003	0.009	0.030	0.069	0.092	0.133
5.0			0.002	0.006	0.025	0.063	0.087	0.124
6.0			0.001	0.003	0.016	0.050	0.076	0.113
7.0			0.000	0.001	0.010	0.039	0.067	0.101
8.0				0.001	0.006	0.031	0.058	0.091
10.0				0.000	0.002	0.017	0.042	0.073
14.0					0.001	0.004	0.018	0.041
20.0					0.000	0.003	0.004	0.020
30.0						0.000	0.000	0.003

TABLE XVII. EXPERIMENTAL DATA

RUN NO.	τ	$r_p(\text{cm})$	$r_c(\text{cm})$	$T_o(^{\circ}\text{C})$	$T_c(^{\circ}\text{C})$	$T_p(^{\circ}\text{C})$	Θ_c	ref r_p (cm)	ref r_c (cm)	R
1	1.0	0.72	0.46	22.6	29.9	48.5	0.282	7.62	4.77	2.23
10-21-71	2.0	0.85	0.53	22.6	29.9	48.5	0.282	7.62	4.77	2.57
(radial)	4.0	1.00	0.63	22.6	29.9	48.5	0.282	7.62	4.77	3.03
X=1R	6.0	1.16	0.72	22.6	29.9	48.5	0.282	7.62	4.77	3.49
	8.0	1.24	0.78	22.6	29.9	48.5	0.282	7.62	4.77	3.76
	10.0	1.32	0.83	22.6	29.9	48.5	0.282	7.62	4.77	3.99
2	0.5	0.71	0.45	23.9	29.9	48.5	0.244	7.32	4.57	2.14
11-5-71	1.5	0.81	0.51	23.9	29.9	48.5	0.244	7.32	4.57	2.45
(radial)	3.0	0.97	0.60	23.9	29.9	48.5	0.244	7.32	4.57	2.91
X=1R	4.0	1.07	0.67	23.9	29.9	48.5	0.244	7.32	4.57	3.20
	5.0	1.13	0.71	23.9	29.9	48.5	0.244	7.32	4.57	3.40
	6.0	1.21	0.75	23.9	29.9	48.5	0.244	7.32	4.57	3.63
	7.0	1.26	0.78	23.9	29.9	48.5	0.244	7.32	4.57	3.78
3	2.0	0.99	0.62	23.0	29.9	48.5	0.271	7.34	4.57	2.97
11-8-71	4.0	1.17	0.73	23.0	29.9	48.5	0.271	7.34	4.57	3.50
(radial)	6.0	1.28	0.80	23.0	29.9	48.5	0.271	7.34	4.57	3.85
X=1R	8.0	1.40	0.87	23.0	29.9	48.5	0.271	7.34	4.57	4.20
	10.0	1.50	0.93	23.0	29.9	48.5	0.271	7.34	4.57	4.49
4	2.0	0.99	0.62	23.0	29.9	48.5	0.271	7.32	4.57	2.97
11-9-71	4.0	1.17	0.73	23.0	29.9	48.5	0.271	7.32	4.57	3.50
(radial)	6.0	1.32	0.83	23.0	29.9	48.5	0.271	7.32	4.57	3.91
X=1R	8.0	1.41	0.88	23.0	29.9	48.5	0.271	7.32	4.57	4.23
	10.0	1.50	0.93	23.0	29.9	48.5	0.271	7.32	4.57	4.49
5	2.0	0.91	0.59	24.0	29.9	48.5	0.240	7.11	4.57	2.82
11-19-71	4.0	1.12	0.72	24.0	29.9	48.5	0.240	7.11	4.57	3.46
(radial)										
X=1R										

TABLE XVII. EXPERIMENTAL DATA (Cont'd)

RUN NO	τ	$r_p(\text{cm})$	$r(\text{cm})$	$T_b(^{\circ}\text{C})$	$T_c(^{\circ}\text{C})$	$T_b(^{\circ}\text{C})$	Θ_c	$\text{ref}_p(\text{cm})$	$\text{ref}(\text{cm})$	R
6	2.0	0.91	0.59	23.6	29.9	48.5	0.253	7.11	4.57	2.83
11-20-71	6.0	1.28	0.83	23.6	29.9	48.5	0.253	7.11	4.57	3.98
(radial)	8.0	1.38	0.89	23.6	29.9	48.5	0.253	7.11	4.57	4.28
X=1R	10.0	1.48	0.95	23.6	29.9	48.5	0.253	7.11	4.57	4.56
7	2.0	0.86	0.53	24.2	29.9	48.5	0.235	6.83	4.57	2.79
11-21-71	4.0	1.09	0.73	24.2	29.9	48.5	0.235	6.83	4.57	3.51
(radial)	8.0	1.37	0.92	24.2	29.9	48.5	0.235	6.83	4.57	4.42
X=1R	10.0	1.42	0.95	24.2	29.9	48.5	0.235	6.83	4.57	4.59
8	1.0	0.61	0.41	24.2	29.9	48.5	0.235	6.83	4.57	1.97
11-21-71	3.0	0.99	0.66	24.2	29.9	48.5	0.235	6.83	4.57	3.20
(radial)	5.0	1.17	0.78	24.2	29.9	48.5	0.235	6.83	4.57	3.77
X=1R	7.0	1.32	0.88	24.2	29.9	48.5	0.235	6.83	4.57	4.26
	9.0	1.44	0.96	24.2	29.9	48.5	0.235	6.83	4.57	4.62
9	1.5	0.74	0.49	24.2	29.9	48.5	0.235	6.83	4.57	2.37
11-21-71	3.5	1.03	0.69	24.2	29.9	48.5	0.235	6.83	4.57	3.31
(radial)	5.5	1.18	0.79	24.2	29.9	48.5	0.235	6.83	4.57	3.82
X=1R	7.5	1.31	0.88	24.2	29.9	48.5	0.235	6.83	4.57	4.22
10	1.0	0.65	0.43	25.2	29.9	48.5	0.202	6.83	4.57	2.09
11-22-71	1.5	0.76	0.51	25.2	29.9	48.5	0.202	6.83	4.57	2.46
(radial)	2.0	0.84	0.56	25.2	29.9	48.5	0.202	6.83	4.57	2.70
X=1R	3.0	1.02	0.68	25.2	29.9	48.5	0.202	6.83	4.57	3.28
	3.5	1.14	0.76	25.2	29.9	48.5	0.202	6.83	4.57	3.68
	4.0	1.09	0.73	25.2	29.9	48.5	0.202	6.83	4.57	3.51
	5.0	1.26	0.84	25.2	29.9	48.5	0.202	6.83	4.57	4.05
	5.5	1.32	0.88	25.2	29.9	48.5	0.202	6.83	4.57	4.26
	6.0	1.24	0.83	25.2	29.9	48.5	0.202	6.83	4.57	4.01
	7.0	1.38	0.93	25.2	29.9	48.5	0.202	6.83	4.57	4.46

TABLE XVII. EXPERIMENTAL DATA (Cont'd)

RUN NO.	τ	$r_0(\text{cm})$	$r(\text{cm})$	$T_0(^{\circ}\text{C})$	$T_c(^{\circ}\text{C})$	$T_p(^{\circ}\text{C})$	Θ_c	$\text{ref}_p(\text{cm})$	$\text{ref}(\text{cm})$	R
10 (cont.)	7.5	1.47	0.99	25.2	29.9	48.5	0.202	6.83	4.57	4.75
	8.0	1.40	0.94	25.2	29.9	48.5	0.202	6.83	4.57	4.50
	9.0	1.52	1.02	25.2	29.9	48.5	0.202	6.83	4.57	4.91
	9.5	1.60	1.07	25.2	29.9	48.5	0.202	6.83	4.57	5.16
	10.0	1.52	1.02	25.2	29.9	48.5	0.202	6.83	4.57	4.91
11	2.0	0.71	0.46	22.5	29.9	48.5	0.285	3.40	2.21	2.23
11-28-71	4.0	0.91	0.59	22.5	29.9	48.5	0.285	3.40	2.21	2.86
(axial)	6.0	1.02	0.66	22.5	29.9	48.5	0.285	3.40	2.21	3.18
$X = 1R$	8.0	1.07	0.69	22.5	29.9	48.5	0.285	3.40	2.21	3.34
	10.0	1.12	0.73	22.5	29.9	48.5	0.285	3.40	2.21	3.50
$X = 8.5R$	2.0	0.61	0.40	22.5	29.9	48.5	0.285	3.40	2.21	1.91
	4.0	0.66	0.43	22.5	29.9	48.5	0.285	3.40	2.21	2.07
	6.0	0.81	0.53	22.5	29.9	48.5	0.285	3.40	2.21	2.54
	8.0	0.91	0.59	22.5	29.9	48.5	0.285	3.40	2.21	2.86
	10.0	0.97	0.63	22.5	29.9	48.5	0.285	3.40	2.21	3.02
$X = 10R$	2.0	0.51	0.33	22.5	29.9	48.5	0.285	3.40	2.21	1.59
	4.0	0.56	0.36	22.5	29.9	48.5	0.285	3.40	2.21	1.75
	6.0	0.66	0.43	22.5	29.9	48.5	0.285	3.40	2.21	2.07
	8.0	0.71	0.46	22.5	29.9	48.5	0.285	3.40	2.21	2.23
	10.0	0.76	0.49	22.5	29.9	48.5	0.285	3.40	2.21	2.39
$X = 11.5R$	2.0	0.33	0.20	22.5	29.9	48.5	0.285	3.40	2.21	1.00
	4.0	0.33	0.20	22.5	29.9	48.5	0.285	3.40	2.21	1.00
	6.0	0.33	0.20	22.5	29.9	48.5	0.285	3.40	2.21	1.00
	8.0	0.33	0.20	22.5	29.9	48.5	0.285	3.40	2.21	1.00
	10.0	0.41	0.26	22.5	29.9	48.5	0.285	3.40	2.21	1.27


```

COMPUTER PROGRAM 1.
EXTERNAL FUNC
DIMENSION AYORR(31)
A=LOWER LIMIT OF INTEGRAL
A=.001
B=UPPER LIMIT OF INTEGRAL
B=10.0
N=NUMBER OF INTERVALS
N=290
BETA=BLOOD FLOW TERM
BETA=0.0
INPUT Y BESSEL VALUES FOR A AND AR
AYORR(1)=-4.471416
AYORR(2)=-4.410739
AYORR(3)=-4.355347
AYORR(4)=-4.304389
AYORR(5)=-4.257210
AYORR(6)=-4.213287
AYORR(7)=-4.172200
AYORR(8)=-4.133606
AYORR(9)=-4.097217
AYORR(10)=-4.062797
AYORR(11)=-4.030141
AYORR(12)=-3.99080
AYORR(13)=-3.969463
AYORR(14)=-3.941165
AYORR(15)=-3.914070
AYORR(16)=-3.888082
AYORR(17)=-3.863112
AYORR(18)=-3.839086
AYORR(19)=-3.815933
AYORR(20)=-3.793592
AYORR(21)=-3.772010
AYORR(22)=-3.751135
AYORR(23)=-3.730922
AYORR(24)=-3.711331
AYORR(25)=-3.692327
AYORR(26)=-3.673872
AYORR(27)=-3.655937
AYORR(28)=-3.638493
AYORR(29)=-3.621515
AYORR(30)=-3.604978
AYORR(31)=-3.588861
TSUM=0.0
RSUM=0.0

```

```

START OUTER DO LOOP. TIME VARIES FROM 0.1 TO 1.0
DO 1000 I=1,10

```



```

C  VALUE  START  INNER DD LOOP.  RADIUS VARIES FROM 1.0 TO 4.0 FOR EACH
C  VALUE OF TIME.
C  DO 1100 K=1,31
C  R=RSUM+1.0
C  T=TSUM+0.1
C  AYO=-4.4714155
C  AYOR=AYOR(K)
C  EVALUATE INTEGRAL USING SIMPSON,S RULE.
C  SINT=SIMP(FUNC,A,B,N,T,R,BETA,AYO,AYOR)
C  COMBINE TERMS TO GET ANSWER.
C  PI=3.14159265
C  ANS=1.0-(2/PI)*((SINT)
C  WRITE(6,2000) T,R,ANS
C  FORMAT(10.1,T=,F5.1,F4.1,5X,'R=',F4.1,5X,'ANS=',F5.3)
C  RECALCULATE USING NEXT HIGHER VALUE OF R.
C  RSUM=RSUM+0.1
C  TSUM=TSUM+0.1
C  STOP
C  END
C  FUNCTION FUNC SUBPROGRAM
C
C  FUNCTION FUNC(U,T,RJOU,YOU,RJOUR,YOUR,RJOUS,YOUS,BETA)
C  FUNC=EXP(-T*U**2)*((RJOU*YOUR)-(RJOUR*YOU))/((U+BETA/U)*((YOUS+RJOU
C  2S))
C  RETURN
C  END
C  SIMPSON,S RULE SUBPROGRAM
C
C  FUNCTION SIMP(FUNC,A,B,N,T,R,BETA,AYO,AYOR)
C  FUNC=FUNCTION NAME
C  A=INITIAL VALUE OF U
C  B=FINAL VALUE OF U
C  N=NUMBER OF INTERVALS,EVEN.
C  EVALUATE INTEGRAL OF FUNC FROM U=A TO U=B USING N INTERVALS.
C  H=(B-A)/FLOAT(N)
C  D IS ACCURACY OF J BESSEL FUNCTION DESIRED.
C  D=.00001
C  CALCULATE BESSEL FUNCTIONS FOR LOWER LIMIT OF INTEGRAL, A=.001
C  CALL BESJ(A,0,AJO,D,IER)
C  AYOS=(AYO)**2
C  AJOS=(AJO)**2
C  AR=A*R
C  CALL BESJ(AR,0,AJOR,D,IER)
C  CALCULATE BESSEL FUNCTIONS OF UPPER LIMIT OF INTEGRAL, B.
C  CALL BESJ(B,0,BJO,D,IER)

```



```

C C      COMPUTE KO USING POLYNOMIAL APPROXIMATION
27  G0=A*(1.2533141-.1566642*T(1)+.08811128*T(2)-.09139095*T(3)
    2+.1344596*T(4)-.2299850*T(5)+.3792410*T(6)-.5247277*T(7)
    3+-.5575368*T(8)-.4262633*T(9)+.2184518*T(10)-.06680977*T(11)
    4+-.009189383*T(12))*C
    IF(N)20,28,29
28  BK=G0
    RETURN
C C C    COMPUTE K1 USING POLYNOMIAL APPROXIMATION
29  G1=A*(1.2533141+.4699927*T(1)-.1468583*T(2)+.1280427*T(3)
    2-.1736432*T(4)+.2847618*T(5)-.4594342*T(6)+.6283381*T(7)
    3-.6632295*T(8)+.5050239*T(9)-.2581304*T(10)+.07880001*T(11)
    4-.01082418*T(12))*C
    IF(N-1)20,30,31
30  BK=G1
    RETURN
C C C    FROM KO,K1 COMPUTE KN USING RECURRENCE RELATION
31  DO 35 J=2,N
    GJ=2.*(FLOAT(J)-1.)*G1/X+G0
    IF(GJ-1.0E70)33,33,32
32  GO TO 34
    IER=4
33  GO=G1
35  G1=GJ
34  BK=GJ
    RETURN
36  B=X/2.
    A=.5772157+ALOG(B)
    C=B*B
    IF(N-1)37,43,37
C C C    COMPUTE KO USING SERIES EXPANSION
37  G0=-A
    X2J=1.
    FACT=1.
    HJ=.0
    DO 40 J=1,6
    RJ=1./FLOAT(J)
    X2J=X2J*C
    FACT=FACT*RJ*RJ
    HJ=HJ+RJ
40  G0=G0+X2J*FACT*(HJ-A)
BESK 630
BESK 640
BESK 650
BESK 660
BESK 670
BESK 680
BESK 690
BESK 700
BESK 710
BESK 720
BESK 730
BESK 740
BESK 750
BESK 760
BESK 770
BESK 780
BESK 790
BESK 800
BESK 810
BESK 820
BESK 830
BESK 840
BESK 850
BESK 860
BESK 870
BESK 880
BESK 890
BESK 900
BESK 910
BESK 920
BESK 930
BESK 940
BESK 950
BESK 960
BESK 970
BESK 980
BESK 990
BESK 1000
BESK 1010
BESK 1020
BESK 1030
BESK 1040
BESK 1050
BESK 1060
BESK 1070
BESK 1080
BESK 1090
BESK 1100

```


C	SUBROUTINES AND FUNCTION SUBPROGRAMS REQUIRED	BESJ	290
C	NONE	BESJ	300
C		BESJ	310
C		BESJ	320
C	METHOD	BESJ	330
C	RECURRENCE RELATION TECHNIQUE DESCRIBED BY H. GOLDSTEIN AND	BESJ	340
C	R.M. THALER, 'RECURRENCE TECHNIQUES FOR THE CALCULATION OF	BESJ	350
C	BESSEL FUNCTIONS', M.T.A.C., V.13, PP.102-108 AND I.A. STEGUN	BESJ	360
C	AND M. ABRAMOWITZ, 'GENERATION OF BESSEL FUNCTIONS ON HIGH	BESJ	370
C	SPEED COMPUTERS', M.T.A.C., V.11, 1957, PP.255-257	BESJ	380
C	BESJ	390
C		BESJ	400
C		BESJ	410
C		BESJ	420
C		BESJ	430
C		BESJ	440
C		BESJ	450
C		BESJ	460
C		BESJ	470
C		BESJ	480
C		BESJ	490
C		BESJ	500
C		BESJ	510
C		BESJ	520
C		BESJ	530
C		BESJ	540
C		BESJ	550
C		BESJ	560
C		BESJ	570
C		BESJ	580
C		BESJ	590
C		BESJ	600
C		BESJ	610
C		BESJ	620
C		BESJ	630
C		BESJ	640
C		BESJ	650
C		BESJ	660
C		BESJ	670
C		BESJ	680
C		BESJ	690
C		BESJ	700
C		BESJ	710
C		BESJ	720
C		BESJ	730
C		BESJ	740

C	SUBROUTINE BESJ(X,N,BJ,D,IER)
	BJ=.0
10	IF(N)10,20,20
	IER=1
	RETURN
20	IF(X)30,30,31
30	IER=2
	RETURN
31	IF(X-15.)32,32,34
32	NTEST=20.+10.*X-X** 2/3
	GO TO 36
34	NTEST=90.+X/2.
36	IF(N-NTEST)40,38,38
38	IER=4
	RETURN
40	IER=0
	N1=N+1
	BPREV=.0
C	COMPUTE STARTING VALUE OF M
	IF(X-5.)50,60,60
50	MA=X+6.
	GO TO 70
60	MA=1.4*X+60./X
70	MB=N+IFIX(X)/4+2
	MZERO=MAX0(MA,MB)
C	SET UPPER LIMIT OF M
	MMAX=NTEST
100	DO 190 M=MZERO,MMAX,3


```

1  +.0001064741)*T2-.0006390400)*T2+.03740084
A=2.0/SQRT(X)
B=A*T1
C=X-.7853982
Y0=A*P0*SIN(C)+B*Q0*COS(C)
Y1=-A*P1*COS(C)+B*Q1*SIN(C)
GO TO 90
C      COMPUTE Y0 AND Y1 FOR X LESS THAN OR EQUAL TO 4
C
C
40  XX=X/2.
    X2=XX*XX
    T=ALOG(XX)+.5772157
    SUM=0.
    TERM=T
    Y0=T
    DO 70 L=1,15
    IF(L-1)50,60,50
50  SUM=SUM+1./FLOAT(L-1)
60  FL=L
    TS=T-SUM
    TERM=(TERM*(-X2)/FL**2)*(1.-1./(FL*TS))
70  Y0=Y0+TERM
    TERM = XX*(T-.5)
    SUM=0.
    Y1=TERM
    DO 80 L=2,16
    SUM=SUM+1./FLOAT(L-1)
    FL=L
    FL1=FL-1.
    TS=T-SUM
    TERM=(TERM*(-X2)/(FL1*FL))*((TS-.5/FL)/(TS+.5/FL1))
80  Y1=Y1+TERM
    PI2=.6366198
    Y0=PI2*Y0
    Y1=-PI2/X+PI2*Y1
C      CHECK IF ONLY Y0 OR Y1 IS DESIRED
C
C
90  IF(N-1)100,100,130
C      RETURN EITHER Y0 OR Y1 AS REQUIRED
C
C
100 IF(N)110,120,110
110 BY=Y1
    GO TO 170
120 BY=Y0
    GO TO 170

```

BESY 640
 BESY 650
 BESY 660
 BESY 670
 BESY 680
 BESY 690
 BESY 700
 BESY 710
 BESY 720
 BESY 730
 BESY 740
 BESY 750
 BESY 760
 BESY 770
 BESY 780
 BESY 790
 BESY 800
 BESY 810
 BESY 820
 BESY 830
 BESY 840
 BESY 850
 BESY 860
 BESY 870
 BESY 880
 BESY 890
 BESY 900
 BESY 910
 BESY 920
 BESY 930
 BESY 940
 BESY 950
 BESY 960
 BESY 970
 BESY 980
 BESY 990
 BESY1000
 BESY1010
 BESY1020
 BESY1030
 BESY1040
 BESY1050
 BESY1060
 BESY1070
 BESY1080
 BESY1090
 BESY1100
 BESY1110


```

C
C
C      PERFORM RECURRENCE OPERATIONS TO FIND YN(X)
130  YA=Y0
      YB=Y1
      K=1
140  T=FLOAT(2*K)/X
      YC=T*YB-YA
      IF (ABS(YC)-1.0E70)145,145,141
141  IER=3
      RETURN
145  K=K+1
150  IF (K-N)150,160,150
      YA=YB
      YB=YC
      GO TO 140
160  BY=YC
170  RETURN
180  IER=1
      RETURN
190  IER=2
      RETURN
      END

```

```

BESSY11120
BESSY11130
BESSY11140
BESSY11150
BESSY11160
BESSY11170
BESSY11180
BESSY11190
BESSY11200
BESSY11210
BESSY11220
BESSY11230
BESSY11240
BESSY11250
BESSY11260
BESSY11270
BESSY11280
BESSY11290
BESSY11300
BESSY11310
BESSY11320
BESSY11330
BESSY11340

```



```

COMPUTER PROGRAM 2.

EXTERNAL FUNC
DIMENSION AYORR(5)
A=LOWER LIMIT OF INTEGRAL
A=.001
B=UPPER LIMIT OF INTEGRAL
B=10.0
N=NUMBER OF INTERVALS
N=290
BETA=BLOOD FLOW TERM
BETA=0.0
INPUT Y BESSEL VALUES FOR A AND AR
DIMENSION AYORR(7)
AYORR(1)=3.588861
AYORR(2)=-3.446794
AYORR(3)=-3.330711
AYORR(4)=-3.232564
AYORR(5)=-3.147543
AYORR(6)=-3.072545
AYORR(7)=-3.005455
START OUTER DO LOOP.    TIME VARIES FROM 0.1 TO 1.0
TSUM=0.0
DO 1000 I=1,10
  RSUM=0.0
  START INNER DO LOOP.  RADIUS VARIES FROM 4.0 TO 10.0 FOR EACH
  VALUE OF TIME.
  DO 1100 K=1,7
    R=RSUM+4.0
    T=TSUM+0.1
    AY0=-4.4714155
    AYOR=AYORR(K)
    EVALUATE INTEGRAL USING SIMPSON,S RULE.
    SINT=SIMP(FUNC,A,B,N,T,R,BETA,AO,AYOR)
    COMBINE TERMS TO GET ANSWER.
    PI=3.14159265
    ANS=1.0-(2/PI)*(SINT)
    WRITE(6,2000) T,R,ANS
  2000 FORMAT(' ',T=,F5.1,5X,'R=',F4.1,5X,'ANS=',F5.3)
  RECALCULATE USING NEXT HIGHER VALUE OF R.
  1100 RSUM=RSUM+1.0
  RECALCULATE FOR NEXT VALUE OF T.
  1000 TSUM=TSUM+0.1
  STOP
END
FUNCTION FUNC SUBPROGRAM

```



```

FUNCTION FUNC(U,T,RJOU,YOU,RJOUR,YOUR,RJOUS,YOUS,BETA)
FUNC=EXP(-T*U**2)*((RJOU*YOUR)-(RJOUR*YOU))/((U+BETA/U)*(YOUS+RJOU
2S))
RETURN
END
C SIMPSON,S RULE SUBPROGRAM

C
C FUNCTION SIMP(FUNC,A,B,N,T,R,BETA,AYO,AYOR)
C FUNC=FUNCTION NAME
C A=INITIAL VALUE OF U
C B=FINAL VALUE OF U
C N=NUMBER OF INTERVALS,EVEN.
C EVALUATE INTEGRAL OF FUNC FROM U=A TO U=B USING N INTERVALS.
C 9005 H=(B-A)/FLOAT(N)
C D IS ACCURACY OF J BESSEL FUNCTION DESIRED.
C D=.0001
C CALCULATE BESSEL FUNCTIONS FOR LOWER LIMIT OF INTEGRAL, A=.001
C CALL BESJ(A,O,AJO,D,IER)
C AYOS=(AYO)**2
C AJOS=(AJO)**2
C 9001 AR=A*R
C CALL BESJ(AR,O,AJOR,D,IER)
C CALCULATE BESSEL FUNCTIONS OF UPPER LIMIT OF INTEGRAL, B.
C 9003 BJOS=(BJO)**2
C BYOS=(BYO)**2
C BR=B*R
C CALL BESJ(BR,O,BJOR,D,IER)
C CALL BESY(BR,O,BYOR,IER)
C 9004 EVNSUM=0.0
C ODDSUM=0.0
C ENDSUM=FUNC(A,T,AJO,AYO,AJOR,AYOR,AJOS,AYOS,BETA)+FUNC(B,T,BJO,BYO
2,BJOR,BYOR,BJOS,BYOS,BETA)
C M=N-1
C J=1
C DO 1500 I=1,M
C X=A+H*FLOAT(I)
C CALCULATE BESSEL FUNCTIONS FOR X.
C CALL BESJ(X,O,XJO,D,IER)
C CALL BESY(X,O,XYO,IER)
C XJOS=(XJO)**2
C XYOS=(XYO)**2
C XR=X*R
C CALL BESJ(XR,O,XJOR,D,IER)
C CALL BESY(XR,O,XYOR,IER)
C GO TO (1001,1002),J

```



```

1001 ODDSUM=ODDSUM+FUNC(X,T,XJO,XYO,XJOR,XYOR,XJOS,XYOS,BETA)
      J=2
      GO TO 1500
1002 EVNSUM=EVNSUM+FUNC(X,T,XJO,XYO,XJOR,XYOR,XJOS,XYOS,BETA)
      J=1
1500 CONTINUE
1600 SIMP=(H/3.)*(ENDSUM+4.0*ODDSUM+2.0*EVNSUM)
      RETURN
      END

```



```

COMPUTER PROGRAM 3.
EXTERNAL FUNC
DIMENSION AYORR(5)
A=LOWER LIMIT OF INTEGRAL
A=.001
B=UPPER LIMIT OF INTEGRAL
B=10.0
N=NUMBER OF INTERVALS
N=290
BETA=BLOOD FLOW TERM
BETA=0.0
INPUT Y BESSEL VALUES FOR A AND AR
AYORR(1)=-3.005456
AYORR(2)=-2.563955
AYORR(3)=-2.305486
AYORR(4)=-2.121901
AYORR(5)=-1.979311
START OUTER DO LOOP.    TIME VARIES FROM 0.1 TO 1.0
TSUM=0.0
DO 1000 I=1,10
  RSUM=0.0
  START INNER DO LOOP.  RADIUS VARIES FROM 10.0 TO 50.0 FOR EACH
  VALUE OF TIME.
  DO 1100 K=1,5
    R=RSUM+10.0
    T=TSUM+0.1
    AY0=-4.4714155
    AYOP=AYORR(K)
    EVALUATE INTEGRAL USING SIMPSON'S RULE.
    SINT=SIMP(FUNC,A,B,N,T,R,BETA,AYO,AYOR)
    COMBINE TERMS TO GET ANSWER.
    PI=3.14159265
    ANS=1.0-(2/PI)*((SINT)
    WRITE(6,2000) T,R,ANS
    FORMAT(10.1,10.1,10.1,F5.1,F5.1,5X,'R=',F4.1,5X,'ANS=',F5.3)
    2000 RECALCULATE USING NEXT HIGHER VALUE OF R.
    RSUM=RSUM+10.0
    1100 RECALCULATE FOR NEXT VALUE OF T.
    TSUM=TSUM+0.1
    1000 STOP
  END
FUNCTION FUNC SUBPROGRAM

```



```

FUNCTION FUNC(U,T,RJOU,YOU,RJOUR,YOUR,RJOURS,YOUS,BETA)
FUNC=EXP(-T*U**2)*((RJOU*YOUR)-(RJOUR*YOU))/((U+BETA/U))*(YOUS+RJOU
2S))
RETURN
END
C SIMPSON,S RULE SUBPROGRAM

C
C FUNCTION SIMP(FUNC,A,B,N,T,R,BETA,AJO,AYO,AYOR)
C FUNC=FUNCTION NAME
C A=INITIAL VALUE OF U
C B=FINAL VALUE OF U
C N=NUMBER OF INTERVALS,EVEN.
C EVALUATE INTEGRAL OF FUNC FROM U=A TO U=B USING N INTERVALS.
9005 H=(B-A)/FLOAT(N)
C D IS ACCURACY OF J BESSEL FUNCTION DESIRED.
C D=.00001
C CALCULATE BESSEL FUNCTIONS FOR LOWER LIMIT OF INTEGRAL, A=.001
C CALL BESJ(A,0,AJO,D,IER)
C AYOS=(AYO)**2
C AJOS=(AJO)**2
9001 AR=A*R
C CALL BESJ(AR,0,AJOR,D,IER)
C CALCULATE BESSEL FUNCTIONS OF UPPER LIMIT OF INTEGRAL, B.
9003 CALL BESJ(B,0,BJO,D,IER)
C CALL BESY(B,0,BYO,IER)
C BJOS=(BJO)**2
C BYOS=(BYO)**2
C BR=B*R
C CALL BESJ(BR,0,BJOR,D,IER)
C CALL BESY(BR,0,BYOR,IER)
C EVNSUM=0.0
C ODDSUM=0.0
C ENDSUM=FUNC(A,T,AJO,AYO,AJOR,AYOR,AJOS,AYOS,BETA)+FUNC(B,T,BJO,BYO
2,M=1
C J=1
C DO 1500 I=1,M
C X=A+H*FLOAT(I)
C CALCULATE BESSEL FUNCTIONS FOR X.
C CALL BESJ(X,0,XJO,D,IER)
C CALL BESY(X,0,XYO,IER)
C XJOS=(XJO)**2
C XYOS=(XYO)**2
C XR=X*R
C CALL BESJ(XR,0,XJOR,D,IER)
C CALL BESY(XR,0,XYOR,IER)
C GO TO (1001,1002),J

```



```

1001 ODDSUM=ODDSUM+FUNC(X,T,XJ0,XY0,XJ0R,XY0R,XJ0S,XY0S,BETA)
      J=2
      GO TO 1500
1002 EVNSUM=EVNSUM+FUNC(X,T,XJ0,XY0,XJ0R,XY0R,XJ0S,XY0S,BETA)
      J=1
1500 CONTINUE
1600 SIMP=(H/3.)*(ENDSUM+4.0*ODDSUM+2.0*EVNSUM)
      RETURN
      END

```


COMPUTER PROGRAM 4.

```

EXTERNAL FUNC
DIMENSION AYORR(31)
A=LOWER LIMIT OF INTEGRAL
A=.001
B=UPPER LIMIT OF INTEGRAL
B=10.0
N=NUMBER OF INTERVALS
N=290
BETA=BLOOD FLOW TERM
BETA=.1
INPUT Y BESSEL VALUES FOR A AND AR
AYORR(1)=-4.471416
AYORR(2)=-4.410739
AYORR(3)=-4.355347
AYORR(4)=-4.304389
AYORR(5)=-4.257210
AYORR(6)=-4.213287
AYORR(7)=-4.172200
AYORR(8)=-4.133606
AYORR(9)=-4.097217
AYORR(10)=-4.062797
AYORR(11)=-4.030141
AYORR(12)=-3.99080
AYORR(13)=-3.969463
AYORR(14)=-3.941165
AYORR(15)=-3.914070
AYORR(16)=-3.888082
AYORR(17)=-3.863112
AYORR(18)=-3.839086
AYORR(19)=-3.815933
AYORR(20)=-3.793592
AYORR(21)=-3.772010
AYORR(22)=-3.751135
AYORR(23)=-3.730922
AYORR(24)=-3.711331
AYORR(25)=-3.692327
AYORR(26)=-3.673872
AYORR(27)=-3.655937
AYORR(28)=-3.638493
AYORR(29)=-3.621515
AYORR(30)=-3.604978
AYORR(31)=-3.588861
TSUM=0.0
RSUM=0.0

```

```

START OUTER DO LOOP. TIME VARIES FROM 0.1 TO 1.0
DO 1000 I=1,10

```



```

C      VALUE      START INNER DO LOOP.  RADIUS VARIES FROM 1.0 TO 4.0 FOR EACH
C      OF TIME.
DO 1100 K=1,31
R=RSUM+1.0
T=TSUM+0.1
AYO=-4.4714155
AYOR=AYORR(K)
EVALUATE INTEGRAL USING SIMPSON,S RULE.
SINT=SIMP(FUNC,A,B,N,T,R,BETA,AYO,AYOR)
CALCULATE REMAINING TERMS IN THE EQUATION.
W=SQR(T*(BETA))
CALL BESK(W,O,BKW,IER)
RKOB=BKW
X=W*R
CALL BESK(X,O,BKX,IER)
RKOBX=BKX
COMBINE TERMS TO GET ANSWER.
PI=3.14159265
ANS=(RKOBX/RKOB)-(2/PI)*SINT*EXP(-BETA*T)
WRITE(6,2000) T,R,ANS
FORMAT(1,' ',T=,F5.1,5X,'R=',F4.1,5X,'ANS=',F5.3)
2000 RECALCULATE USING NEXT HIGHER VALUE OF R.
1100 RSUM=RSUM+0.1
C      RECALCULATE FOR NEXT VALUE OF T.
1000 TSUM=TSUM+0.1
STOP
END
C      FUNCTION FUNC SUBPROGRAM

FUNCTION FUNC(U,T,RJOU,YOU,RJOUR,YOUR,RJOUS,YOUS,BETA)
FUNC=EXP(-T*U**2)*((RJOU*YOUR)-(RJOUR*YOU))/((U+BETA/U)*((YOUS+RJOU
2S))
RETURN
END
C      SIMPSON,S RULE SUBPROGRAM

FUNCTION SIMP(FUNC,A,B,N,T,R,BETA,AYO,AYOR)
FUNC=FUNCTION NAME
A=INITIAL VALUE OF U
B=FINAL VALUE OF U
N=NUMBER OF INTERVALS,EVEN.
EVALUATE INTEGRAL OF FUNC FROM U=A TO U=B USING N INTERVALS.
H=(B-A)/FLOAT(N)
D IS ACCURACY OF J BESSEL FUNCTION DESIRED.
D=.00001
C      CALCULATE BESSEL FUNCTIONS FOR LOWER LIMIT OF INTEGRAL, A=.001

```



```

          CALL BESJ(A,0,AJO,D,IER)
          AYOS=(AYO)**2
          AJOS=(AJO)**2
          AR=A*R
          CALL BESJ(AR,0,AJOR,D,IER)
          CALCULATE BESSEL FUNCTIONS OF UPPER LIMIT OF INTEGRAL, B.
          CALL BESJ(B,0,BJO,D,IER)
          CALL BESY(B,0,BYO,IER)
          BJOS=(BJO)**2
          BYOS=(BYO)**2
          BR=B*R
          CALL BESJ(BR,0,BJOR,D,IER)
          CALL BESY(BR,0,BYOR,IER)
          EVNSUM=0.0
          ODDSUM=0.0
          ENDSUM=FUNC(A,T,AJO,AYO,AJOR,AYOR,AJOS,AYOS,BETA)+FUNC(B,T,BJO,BYO
2,BJOR,BYOR,BJOS,BYOS,BETA)
          M=N-1
          J=1
          DO 1500 I=1,M
            X=A+H*FLOAT(I)
            CALCULATE BESSEL FUNCTIONS FOR X.
            CALL BESJ(X,0,XJO,D,IER)
            CALL BESY(X,0,XYO,IER)
            XJOS=(XJO)**2
            XYOS=(XYO)**2
            XR=X*R
            CALL BESJ(XR,0,XJOR,D,IER)
            CALL BESY(XR,0,XYOR,IER)
            GO TO (1001,1002),J
            ODDSUM=ODDSUM+FUNC(X,T,XJO,XYO,XJOR,XYOR,XJOS,XYOS,BETA)
1001      J=2
            GO TO 1500
            EVNSUM=EVNSUM+FUNC(X,T,XJO,XYO,XJOR,XYOR,XJOS,XYOS,BETA)
1002      J=1
1500      CONTINUE
1600      SIMP=(H/3.)*(ENDSUM+4.0*ODDSUM+2.0*EVNSUM)
          RETURN
          END

```



```

COMPUTER PROGRAM 5.

EXTERNAL FUNC
DIMENSION AYORR(5)
A=LOWER LIMIT OF INTEGRAL
A=.001
B=UPPER LIMIT OF INTEGRAL
B=10.0
N=NUMBER OF INTERVALS
N=290
BETA=BLOOD FLOW TERM
BETA=.1
INPUT Y BESSEL VALUES FOR A AND AR
DIMENSION AYORR(7)
AYORR(1)=-3.588861
AYORR(2)=-3.446794
AYORR(3)=-3.330711
AYORR(4)=-3.232564
AYORR(5)=-3.147543
AYORR(6)=-3.072545
AYORR(7)=-3.005455
START OUTER DO LOOP.      TIME VARIES FROM 0.1 TO 1.0
TSUM=0.0
DO 1000 I=1,10
  RSUM=0.0
  START INNER DO LOOP.    RADIUS VARIES FROM 4.0 TO 10.0 FOR EACH
  VALUE OF TIME.
  DO 1100 K=1,7
    R=TSUM+4.0
    T=TSUM+0.1
    AY0=-4.4714155
    AYOR=AYORR(K)
    EVALUATE INTEGRAL USING SIMPSON'S RULE.
    SINT=SIMP(FUNC,A,B,N,T,R,BETA,AY0,AYOR)
    CALCULATE REMAINING TERMS IN THE EQUATION.
    W=SQRT(BETA)
    CALL BESK(W,0,BKW,IER)
    RKOB=BKW
    X=W*R
    CALL BESK(X,0,BKX,IER)
    RKOBR=BKX
    COMBINE TERMS TO GET ANSWER.
    PI=3.14159265
    ANS=(RKOBR/RKOB)-((2/PI)*SINT*EXP(-BETA*T))
    WRITE(6,2000) T,R,ANS
    FORMAT(10.1,10.1,F5.1,F4.1,5X,'ANS=',F5.3)
  2000 RECALCULATE USING NEXT HIGHER VALUE OF R.
  1100 RSUM=RSUM+1.0

```



```

C 1000 RECALCULATE FOR NEXT VALUE OF T.
      TSUM=TSUM+O.1
      STOP
      END
C      FUNCTION FUNC SUBPROGRAM

      FUNCTION FUNC(U,T,RJOU,YOU,RJOUR,YOUR,RJOUS,YOUS,BETA)
      FUNC=EXP(-T*U**2)*((RJOU*YOUR)-(RJOUR*YOU))/((U+BETA/U))*((YOUS+RJOU
2S))
      RETURN
      END
C      SIMPSON,S RULE SUBPROGRAM

      FUNCTION SIMP(FUNC,A,B,N,T,R,BETA,AYO,AYOR)
      FUNC=FUNCTION NAME
      A=INITIAL VALUE OF U
      B=FINAL VALUE OF U
      N=NUMBER OF INTERVALS,EVEN.
      EVALUATE INTEGRAL OF FUNC FROM U=A TO U=B USING N INTERVALS.
      H=(B-A)/FLOAT(N)
      D IS ACCURACY OF J BESSEL FUNCTION DESIRED.
      D=.00001
      CALCULATE BESSEL FUNCTIONS FOR LOWER LIMIT OF INTEGRAL, A=.001
      CALL BESJ(A,O,AJO,D,IER)
      AYOS=(AYO)**2
      AJOS=(AJO)**2
      AR=A*R
      CALL BESJ(AR,O,AJOR,D,IER)
      CALCULATE BESSEL FUNCTIONS OF UPPER LIMIT OF INTEGRAL, B.
      CALL BESJ(B,O,BJO,D,IER)
      CALL BESY(B,O,BYO,IER)
      BJOS=(BJO)**2
      BYOS=(BYO)**2
      BR=B*R
      CALL BESJ(BR,O,BJOR,D,IER)
      CALL BESY(BR,O,BYOR,IER)
      EVNSUM=0.0
      ODDSUM=0.0
      ENDSUM=FUNC(A,T,AJO,AYO,AJOR,AYOR,AJOS,AYOS,BETA)+FUNC(B,T,BJO,BYO
2,BJOR,BYOR,BJOS,BYOS,BETA)
      M=N-1
      J=1
      DO 1500 I=1,M
      X=A+H*FLOAT(I)
      CALCULATE BESSEL FUNCTIONS FOR X.
      CALL BESJ(X,O,XJO,D,IER)

```



```

CALL BESY(X,0,XY0,IER)
XJOS=(XJ0)**2
XYOS=(XY0)**2
XR=X*R
CALL BESJ(XR,0,XJOR,D,IER)
CALL BESY(XR,0,XYOR,IER)
GO TO (1001,1002),J
1001 ODDSUM=ODDSUM+FUNC(X,T,XJ0,XY0,XJOR,XYOR,XJOS,XYOS,BETA)
      J=2
      GO TO 1500
1002 EVNSUM=EVNSUM+FUNC(X,T,XJ0,XY0,XJOR,XYOR,XJOS,XYOS,BETA)
      J=1
1500 CONTINUE
1600 SIMP=(H/3.)*(ENDSUM+4.0*ODDSUM+2.0*EVNSUM)
      RETURN
      END

```


COMPUTER PROGRAM 6.

```

EXTERNAL FUNC
DIMENSION AYORR(5)
A=LOWER LIMIT OF INTEGRAL
A=.001
B=UPPER LIMIT OF INTEGRAL
B=10.0
N=NUMBER OF INTERVALS
N=290
BETA=BLOOD FLOW TERM
BETA=.1
INPUT Y BESSEL VALUES FOR A AND AR
AYORR(1)=-3.005456
AYORR(2)=-2.563955
AYORR(3)=-2.305486
AYORR(4)=-2.121901
AYORR(5)=-1.979311
START OUTER DO LOOP. TIME VARIES FROM 0.1 TO 1.0
TSUM=0.0
DO 1000 I=1,10
  RSUM=0.0
  START INNER DO LOOP. RADIUS VARIES FROM 10.0 TO 50.0 FOR EACH
  VALUE OF TIME.
  DO 1100 K=1,5
    R=RSUM+10.0
    T=TSUM+0.1
    AYO=-4.4714155
    AYOR=AYORR(K)
    EVALUATE INTEGRAL USING SIMPSON'S RULE.
    SINT=SIMP(FUNC,A,B,N,T,R,BETA,AYO,AYOR)
    CALCULATE REMAINING TERMS IN THE EQUATION.
    W=SQRT(BETA)
    CALL BESK(W,0,BKW,IER)
    RKOB=BKW
    X=W*R
    CALL BESK(X,0,BKX,IER)
    RKOB=BKX
    COMBINE TERMS TO GET ANSWER.
    PI=3.14159265
    ANS=(RKOB/RKOB)-((2/PI)*SINT*EXP(-BETA*T))
    WRITE(6,2000) T,R,ANS
    FORMAT(10.1,10.1,F5.1,F5.1,F4.1,F5.3)
  2000 RECALCULATE USING NEXT HIGHER VALUE OF R.
  1100 RSUM=RSUM+10.0
  1000 RECALCULATE FOR NEXT VALUE OF T.
  TSUM=TSUM+0.1
  STOP

```



```

C
END
FUNCTION FUNC SUBPROGRAM

FUNCTION FUNC(U,T,RJOU,YOU,RJOUR,YOUR,RJOUS,YOUS,BETA)
FUNC=EXP(-T*U**2)*((RJOU*YOUR)-(RJOUR*YOU))/((U+BETA/U))*((YOUS+RJOU
2S))
RETURN
END
C
SIMPSON,S RULE SUBPROGRAM

FUNCTION SIMP(FUNC,A,B,N,T,R,BETA,AYO,AYOR)
FUNC=FUNCTION NAME
A=INITIAL VALUE OF U
B=FINAL VALUE OF U
N=NUMBER OF INTERVALS,EVEN, FROM U=A TO U=B USING N INTERVALS.
EVALUATE INTEGRAL OF FUNC FROM U=A TO U=B USING N INTERVALS.
9005 H=(B-A)/FLOAT(N)
C D IS ACCURACY OF J BESSEL FUNCTION DESIRED.
D=.0001
C CALCULATE BESSEL FUNCTIONS FOR LOWER LIMIT OF INTEGRAL, A=.001
CALL BESJ(A,0,AJO,D,IER)
AYOS=(AYO)**2
AJOS=(AJO)**2
9001 AR=A*R
CALL BESJ(AR,0,AJOR,D,IER)
C CALCULATE BESSEL FUNCTIONS OF UPPER LIMIT OF INTEGRAL, B.
9003 CALL BESJ(B,0,BJO,D,IER)
CALL BESY(B,0,BYO,IER)
BJOS=(BJO)**2
BYOS=(BYO)**2
BR=B*R
9004 CALL BESJ(BR,0,BJOR,D,IER)
CALL BESY(BR,0,BYOR,IER)
EVNSUM=0.0
ODDSUM=0.0
ENDSUM=FUNC(A,T,AJO,AYO,AJOR,AYOR,AJOS,AYOS,BETA)+FUNC(B,T,BJO,BYO
2,BJOR,BYOR,BJOS,BYOS,BETA)
M=N-1
J=1
DO 1500 I=1,M
X=A+H*FLOAT(I)
C CALCULATE BESSEL FUNCTIONS FOR X.
CALL BESJ(X,0,XJO,D,IER)
CALL BESY(X,0,XYO,IER)
XJOS=(XJO)**2
XYOS=(XYO)**2

```



```

XR=X*R
CALL BESJ(XR,0,XJOR,D,IER)
CALL BESY(XR,0,XYOR,IER)
GO TO (1001,1002),J
1001 ODDSUM=ODDSUM+FUNC(X,T,XJO,XYO,XJOR,XYOR,XJOS,XYOS,BETA)
      J=2
      GO TO 1500
1002 EVNSUM=EVNSUM+FUNC(X,T,XJO,XYO,XJOR,XYOR,XJOS,XYOS,BETA)
      J=1
1500 CONTINUE
1600 SIMP=(H/3.)*(ENDSUM+4.0*ODDSUM+2.0*EVNSUM)
      RETURN
      END

```


BIBLIOGRAPHY

1. Ambrosius, E.E., Fellows, R.D. and Brickman, A.D., Mechanical Measurement and Instrumentation, Ronald Press, 1966.
2. Aronow, S., "The Use of Radio-Frequency Power in Making Lesions in the Brain," J. Neurosurg., p. 431-438, May 1960.
3. Brodkey, J.S., Miyazaki, Y., Ervin, F.R. and Mark, V.H., "Reversible Heat with Radiofrequency Current," J. Neurosurg., v. 21, p. 49-53, 1964
4. Carpenter, M., and Whittier, J.R., "Study of Methods for Producing Experimental Lesions of the Central Nervous System with Special Reference to Stereotaxic Technique," J. of Comp. Neurology, v. 97, p. 73-117, 1952.
5. Carslaw, H.S., and Jaeger, J.C., Conduction of Heat in Solids, 2d ed., p. 327-338, Oxford Press, 1959.
6. Cooper, T.E., and Trezek, G.J., "Analytical Prediction of the Temperature Field Emanating From a Cryogenic Surgical Cannula," Cryobiology, v. 7, no. 2-3, p. 79-93.
7. Cooper, T.E., and Trezek, G.J., "Correlation of Thermal Properties of Some Human Tissue with Water Content", Aerospace Med., v. 42, p. 24-27, January 1971.
8. Daves, F., "Liquid Crystals: A new Tool for NDT," Research/Development, p. 24-27, June 1967.
9. Dowden, W.A., "Cholesteric Liquid Crystals," Non-Destructive Testing, p. 99-102, November 1967.
10. Gengler, P.L., Heat Transfer Analysis of a Radio-frequency Brain Probe, M.S. Thesis, Naval Postgraduate School, Monterey, California, 1971.
11. Gildenberg, P.L., "Studies in Stereencephalotomy X", Confinia Neurologica, v. 20, p. 53-65, 1960.
12. Gray, G.W., Molecular Structure and the Properties of Liquid Crystals, Academic Press, 1962.
13. Grayson, J., "Internal Calorimetry in the Determination of Thermal Conductivity and Blood Flow", J. Physiol., v. 118, p. 54-72, 1952.
14. Herrero, S., "Radio-Frequency-Current and Direct Current Lesions in the Ventromedial Hypothalamus," Am. J. Physiol., v. 217, no. 2, p. 403-410, August 1969.

15. Jaeger, J.C., "Numerical Values of the Temperature in Radial Heat Flow," J. Math. Phys., v. 34, p. 316-321, 1956.
16. Lawrence Radiation Lab, TRUMP: A Computer Program for Transient and Steady-State Temperature Distributions in Multi-dimensional Systems, Edwards, A.L., July, 1969.
17. National Cash Register Company, Encapsulated Liquid Crystals.
18. Naval Postgraduate School, M.E. Laboratory II Report, Liquid Crystals, by J.R. Fitts and others, December 1971.
19. Parker, R., Lawrence Livermore Laboratory, Personal conversation, 22 October 1971.
20. Pennes, H.H., "Analysis of Tissue and Arterial Blood Temperature in the Resting Human Forearm," J. Appl. Physiol., v. 1, no. 2, p. 93-122, August 1948.
21. Perl, W., "Heat and Matter Distribution in Body Tissue and the Determination of Tissue Blood Flow by Local Clearance Methods," J. Theoret. Biol., v. 2, p. 201-235, 1962.
22. Spells, K.E., "The Conductivities of Some Biological Fluids," Phys. Med. Biol. p. 139-1953, 1960.
23. Watkins, E.S., "Heat Gains in Brain During Electrocoagulative Lesions," J. Neurosurg., v. 23, p. 319-328, 1965.
24. Wilbur B. Driver Company, A Guide to Fine Wire Resistance Alloys for Electronic Applications.

INITIAL DISTRIBUTION LIST

	No. Copies
1. Defense Documentation Center Cameron Station Alexandria, Virginia 22314	2
2. Library, Code 0212 Naval Postgraduate School Monterey, California 93940	2
3. Mechanical Engineering Department Library, Code 59 Naval Postgraduate School Monterey, California 93940	1
4. Assistant Professor T.E. Cooper, Code 59Cg Department of Mechanical Engineering Naval Postgraduate School Monterey, California 93940	3
5. LCDR Jon P. Groff 207 Dunecrest Avenue Monterey, California 93940	1
6. Thesis Office, Attn: M. Burton Naval Postgraduate School Monterey, California 93940	1

DOCUMENT CONTROL DATA - R & D

(Security classification of title, body of abstract and indexing annotation must be entered when the overall report is classified)

1 ORIGINATING ACTIVITY (Corporate author) Naval Postgraduate School Monterey, California 93940		2a. REPORT SECURITY CLASSIFICATION Unclassified	
		2b. GROUP	
3 REPORT TITLE Design and Analysis of a Resistively Heater Surgical Probe			
4 DESCRIPTIVE NOTES (Type of report and, inclusive dates) Master's Thesis; December 1971			
5 AUTHOR(S) (First name, middle initial, last name) Jon Philip Groff			
6 REPORT DATE December 1971		7a. TOTAL NO. OF PAGES 124	7b. NO. OF REFS 24
8a. CONTRACT OR GRANT NO.		9a. ORIGINATOR'S REPORT NUMBER(S)	
b. PROJECT NO			
c.		9b. OTHER REPORT NO(S) (Any other numbers that may be assigned this report)	
d.			
10 DISTRIBUTION STATEMENT Approved for public release; distribution unlimited.			
11. SUPPLEMENTARY NOTES		12. SPONSORING MILITARY ACTIVITY Naval Postgraduate School Monterey, California 93940	
13. ABSTRACT This thesis examines the use of heat for producing clinical lesions in tissue and presents the design and analysis of a resistively heated surgical probe. The probe temperature is accurately maintained and measured by using a Wheatstone bridge. The probe was embedded in an agar-water test medium and the temperature field emanating from the probe was measured using liquid crystal tapes. The experimental results compare within approximately 10% of a two-dimensional numerical solution. A one-dimensional theoretical model is developed and results are presented to show the relative effects of metabolism and blood flow on the temperature field.			

KEY WORDS	LINK A		LINK B		LINK C	
	ROLE	WT	ROLE	WT	ROLE	WT
Surgical Probe						
Resistance Heating						
Nervous Tissue						
Liquid Crystals						
Heat Transfer						
Blood Flow						



29 JUL 72

BINDERY
20583

Thesis

133150

G852 Groff

c.1

Design and analysis
of a resistively heat-
ed surgical probe.

29 JUL 72

29 JUL 72

20583

Thesis

133150

G852 Groff

c.1

Design and analysis
of a resistively heat-
ed surgical probe.

thesG852

Design and analysis of a resistively hea



3 2768 002 13954 5

DUDLEY KNOX LIBRARY